Enzyme-responsive supramolecular assemblies for controlled release

A thesis submitted to the University of Strathclyde for the degree of Doctor of Philosophy in the Faculty of Pure and Applied Chemistry

2012

Pier Francesco Caponi

Declaration

This thesis is the result of the author's original research. It has been composed by the author and has not been previously submitted for examination which has led to the award of a degree.

Copyright

Abstract

The use of "smart materials" is increasing due to the variety of stimuli to which the materials can be tailored to respond. In particular, enzyme responsive materials are of great interest for drug delivery applications due to the high biocompatibility and numerous advantages offered by enzymes. The number of publications in this area shows the increasing interest of the scientific community towards possible applications of enzyme responsive materials. In this thesis a new approach towards drug delivery is documented and explored through the synthesis and the study of self assembly behaviour of a new class of enzyme responsive polymers.

Through an innovative, yet straight forward, one step-synthetic approach, we functionalised poly(2-isopropyl-2-oxazoline), a thermally responsive polymer, with enzyme substrates attached to fluorenylmethyloxy carbonyl moieties, creating the first example of temperature/phosphatase responsive polymer. The interactions developed after enzyme catalysis not only led to self assembly, but also affected the dimensions of the colloidal aggregates formed below and above the phase transition temperature of the polymer. Moreover, due to the presence of fluorenyl groups we were able to study the self assembly behaviour of the functionalised polymers gaining insight on the self assembly mechanisms.

To have a deeper understanding of the self assembly mechanism and the role that interactions, e.g. π-π, hydrophobic, ionic, play during the process, a small library of amino acid functionalised polymers was synthesized. The polymers contained in the library were studied both singularly and as mixed populations. Through the study of self assembly behaviour of single populations, we found that ionic interactions have an important role in disrupting the formation of aggregates and, as expected, the presence of planar/hydrophobic groups facilitates it. By mixing two polymer populations, we

were able to create multicomponent systems that would vary their sizes depending on enzyme catalysis/temperature and the amino acids forming the nanostructures. Moreover, the aggregates formed by two populations are still enzyme accessible, *i.e.* the enzyme can access the core of the particles and trigger dis-assembly, which is particularly important for applications in the drug delivery field.

Finally, to prove the versatility of peptidic based materials, we exploited the self assembly properties of fluorenylmethoxycarbonyl-dipeptides to create hydrogels that can actively trap pheromones, often volatile and sensible substances, to afford a controllable and tuneable release over time. The peptide used for the study was chosen due to its capacity to self-assembly into micelles before enzymatic catalysis and form hydrogels after dephosphorylation. The tailored design allowed us not only to achieve controlled release, but also to improve the handling and storing process of volatile pheromones. Thanks to the number of variables that could be modified to create different systems with particular characteristics, e.g. different peptide-based hydrogels, peptide concentration, this innovative method shows potential to find application as a pest control/crop protecting agent in the agricultural industry.

Acknowledgements

I would like to thank my supervisor, Rein, for giving me the opportunity to undertake my PhD in such an interesting and stimulating field, for continuous support and encouragement to make experiences that helped me to grow not only from a professional point of view. A special thank goes to Prof. Winnik who taught me a number of techniques and skills that have been fundamental through the course of my PhD and to Dr. Tony Hooper for the collaboration that led to the results reported in the last chapter of the thesis.

The last three years would have not been the same without all the colleagues that made the working hours -and not only- much more enjoyable. Special acknowledgment goes to the people that started this adventure with me, Jan, Lou and Meghan, and that have been there until the end.

Friends played a very important role during my Scottish experience, without them I would not have lasted very long in the rainy Glaswegian weather. With many of them I just spent few months while others have been there for the all the duration of my studies, sharing with me unforgettable experiences.

Last but not least, the biggest thank goes to my parents, “i Bofy”, for being there through all the stages of my life, always showing trust and support in all the decisions I have made so far. Without them, nothing I have accomplished and achieved, would have been possible.

List of content

List of Figures

List of tables

List of schemes

List of abbreviations

ACN	Acetonitrile
AFM	Atomic force spectroscopy
Ala	Alanine
AQ	6-Aminoquinoline
Arg	Arginine
Asn	Asparagine
Asp	Aspartic acid
ATP	Adenosine-5'-triphosphate
Boc	*Tert*-butyloxycarbonyl
CROP	Cationic ring opening polymerisation
Cys	Cysteine
DCM	Dichloromethane
DIC	*N,N*-Diisopropylcarbodiimide
DIPEA	*N,N*-Diisopropylethylamine
DMF	*N,N*-Dimethylformamide
DLS	Dynamic light scattering
ERM	Enzyme responsive material
EPR	Enhanced permeation and retention
FDA	Food and drug administration
Fmoc	9-Fluorenylmethyloxycarbonyl
Glu	Glutamic acid
Gly	Glycine
GOx	Glucose oxidase
HBTU	*O*-(Benzotriazol-1-yl)-*N,N,N′,N′*-tetramethyluronium hexafluorophosphate
His	Histidine
HPLC	High performance liquid chromatography
Ile	Isoleucine

LCST	Lower critical solution temperature
Leu	Leucine
Lys	Lysine
MALDI-TOF	Matrix-assisted laser desorption/ionisation-time of flight
Met	Methionine
MMP	Matrix metallo protease
Naph	Naphtalene
NHE	Human neutrophil elastase
NHS	*N*-Hydroxysuccinimide
OEG	Oligo(ethylene glycol)
PBH	Peptide-based hydrogel
PEG	Poly(ethylene glycol)
PEGA	Poly(ethylene glycol)-co-acrylamide
PEG-b-PLKC	Methoxy-poly(ethylene glycol)-block-poly(L-lysine hydrochloride)
Phe	Phenylalanine
PiPrOx	Poly(2-isopropyl-2-oxazoline)
PLA-b-PEG	Poly(lactide)-block-poly(ethylene glycol)
PLA-b-PNIPAM	Poly(lactide)-block-poly(N-isopropylacrylamide)
Pro	Proline
***p*Tyr**	Phosphorylated tyrosine
Ser	Serine
SN	Silica nanocontainers
TFA	Trifluoroacetic acid
THF	Tetrahydrofuran
Thr	Threonine
Tyr	Tyrosine
Val	Valine

1. Enzyme-responsive drug delivery systems*

1.1 Introduction

Enzyme responsive materials (ERMs) belong to a field which is generating increasing interest to pursue the concept of a "magic bullet",[1] a theory first described more than 100 years ago by Dr. Ehrlich, who discovered the first effective syphilis treatment and was awarded the Nobel Prize. This concept relies on the ability to target only (micro-) organisms that participate in, or cause, a disease without affecting the host. Nowadays this concept has evolved in the need to target certain kinds of tissues, *i.e.* cancer, whilst leaving healthy tissue unaffected. Thanks to progresses in crystallisation techniques, molecular modelling, and protein engineering a number of classes of enzymes have been discovered to play crucial roles in human body biochemistry. Their disregulation, e.g. hypo/hyperexpression, can lead to the development of a range of disease state. These findings make enzymes highly suitable targets to achieve a selective, effective and localized drug delivery release. Table 1.1 shows a number of examples of enzymes, whose disregulation can lead to development of a disease. Indeed, a number of these enzymes are used as markers for diagnosis.

Moreover, signal amplification is an important and unique property achievable by exploiting enzymatic catalysis where each enzyme molecule can turnover many substrate molecules (typical turnover=10^6 min^{-1}). This is the case of ERMs, where enzymes can trigger a large number of incorporated substrate molecules, that lead to macroscopic change in physical/chemical properties of the system. It is then no surprise that enzymatic mechanisms are important in controlled release and a number of approaches have been developed over the last decades.

* Published as: P.F. Caponi, R.V. Ulijn, Chapter 9 "*Enzyme-responsive drug delivery systems*" in "*Smart materials for drug delivery*", eds. C. Alvarez-Lorenzo and A. Concheiro, **2013**, Royal Society of Chemistry – Smart Materials Series, RSC Publishing, *printing*.

1.1.1 Exploiting enzymes in drug delivery

There is significant precedent for exploitation of enzymes in drug delivery, only in the last decade resulting in an increase in research activity in ERMs. We will firstly summarise other areas where enzymes have been exploited or targeted, these areas are discussed briefly below and compared with the ERM approach.

1.1.1.1 Enzyme inhibitors

In order to target selectively a malfunctioning or harmfully overexpressed enzyme the most direct and intuitive approach is to synthesize drug molecules which are able to bind and inhibit a specific enzyme (*i.e.* synthetic enzyme inhibitors). For example, kinases are known to be over-expressed and to play a crucial role in the development of tumors. Many examples of kinase inhibitors can be found in drug treatments that have been recently commercialized. E.g. Imatinib Mesylate (Gleevec®) and Dasatinib (Sprycel®) are ABL kinase inhibitors and are FDA (Food and Drug Administration) approved for use against certain kinds of tumors and leukemia. Studies are currently ongoing to use these drugs in different malignancies.[2]

Another well-known example that shows the efficacy of targeting enzymes using synthetic inhibitors relates to acquired immune deficiency syndrome (AIDS). Since the human immunodeficiency virus (HIV) was reported at the beginning of the 80's,[3] no treatment has shown good efficacy until HIV protease inhibitors were discovered and used to treat AIDS in the mid 90's.[4] The mode of action of this class of drugs is focused on prevention of the correct production of viral proteins that are responsible for the spread of the infection to new cells. These therapies have significantly contributed in increasing the life expectancy and quality of life for patients.[5]

One drawback of this very effective approach is related to the toxicology profiles and pharmacokinetics of new drugs and the long clinical trials that the new molecules have to pass before being approved.

Enzyme name	Family	Role	Linked diseases	Enzyme malfunction	Ref.
Urokinase	Serine-protease	Participation in thrombolysis and extracellular matrix degradation	Vascular diseases, cancer malignity	Anomalous activation	6
Prostatic cancer specific antigen (kallikrein-3)	Serine-protease	Sperm liquefaction	Prostate cancer	Hyperexpression	7
Deubiquitase	Protease	Protein degradation/ trafficking/ localization	Tumors, cancers	Enzyme mutation	8
Plasmodium falciparum amidase (PfA-M1)	Amino-peptidase	Hemoglobin digestion	Malaria	Expression by bacteria	9
Nox	Oxidase	Signal transduction, immune functions, hormone biosynthesis	Genome damages, apoptosis	Overexpression	10
Protein kinase	Phospho-transferase	Cell signaling, signal transduction	Alzheimer's syndrome, tumors, cancers	Antagonistic disregulation, hyperexpression	11
Acid lipase	Esterase	Fatty acids metabolism	Fatty liver, Wolman diseases	Deficiency	12
Phosphatases	Esterase	Cell signaling, signal transduction, bone formation	Alzheimer's syndrome, tumors, cancers, osteoporosis	Antagonistic disregualtion	12, 13

Table 1.1 Examples of diseases that can be generated or detected by disregulation of enzyme activity.

1.1.1.2 Prodrugs

An alternative approach that exploits (disease specific) enzymes is the concept of prodrugs. A prodrug consists of a drug molecule which is modified with an enzyme cleavable moiety, which is cleaved upon enzymatic catalysis, restoring the pharmaceutical activity of the molecule in the vicinity of the enzyme expression site. This approach is very useful to increase characteristics of already existing drugs, e.g. bioavailability, pharmacokinetics, but implicates the chemical modification of the drug molecule. Many prodrugs are currently used, examples can be found in an excellent review published by Rautio *et al*.[14] One example of enzyme triggered prodrug to target cancer tissues has been reported in 1999[15] and is currently undergoing clinical trials.[16] The authors synthesized a *N*-(2-hydroxypropyl)methacrylamide copolymer and coupled doxorubicin, an anti-cancer drug, to it *via* a peptide linker. The polymer is internalized by pinocytosis and the peptide linker is cleaved by lysozomes releasing the drug.

As seen in the example above, the polymer component of a drug delivery system has an important effect on the properties and characteristics of the whole system. Most examples that we report regarding use of polymers for biological applications involve the use of poly(ethylene glycol) (PEG). PEG is the most used polymer for drug delivery purposes, due to high biocompatibility and low side effects. PEG is not the only polymer used for this kind of applications since it presents some aspects that are not fully understood, e.g. suspects of complement activation.[17] Alternatives, such as poly(acrylamide) or poly(amino acid), are available and new bio-compatible polymers are always object of study. Please refer to an excellent review that has been published recently regarding PEG and other polymers suitable for drug delivery purposes.[17]

A more sophisticated prodrug method which is worth mentioning is the so-called antibody directed enzyme prodrug therapy which is used to increase drug selectivity against tumours. In this approach, monoclonal antibodies for specific tumour receptors are linked to enzymes, e.g. carboxypeptidase.[18] When the concentration of antibodies is

considerably higher in tumour tissues compared to healthy tissues, a prodrug is injected and activated by the enzymes, achieving cytotoxicity only against tumour cells.[19] This two-step strategy has been proven to be effective and is currently undergoing clinical trials. However, this technique shows limitations such as the antigenicity of monoclonal antibodies and the difficulties to effectively control the concentration and the pharmacokinetics of the drug in the body. Similar techniques have been developed using different carrier to achieve selectivity, such as viral/gene-directed enzyme prodrug therapy[20] or polymer directed enzyme prodrug.[21]

1.1.1.3 Enzyme Responsive Materials

The ERM approach is based on responsive polymers able to act as a carrier and release the payload only upon the catalytic action of enzymes. An ERM can be defined as a system which undergoes macroscopic changes of physical/chemical properties upon the catalytic action of an enzyme.

This strategy, on which this chapter will focus, does not always require modifications of existing drugs, as they may be physically, not chemically, entrapped, and it has the potential to lower the toxicity of treatments currently used. The interactions that lead to the change in properties of an enzyme-responsive material can be either based on covalent interactions, e.g. chemical cross-linked hydrogels, or formed by a combination of weak interactions, such as electrostatic interactions, hydrogen bonding, hydrophobic interactions, van der Waals forces, steric interactions and π-π interactions, forming a supramolecular assembly. Despite the efforts in developing ERMs for drug delivery applications, there are not yet any examples of ERMs which are currently undergoing clinical trial.

Table 1.2 summarises the main advantages of the different drug delivery approaches treated in this introduction.

Targeting mode	System characteristics			
	Selectivity	Drug biocompatibility	Controlled release	Amplification
Enzyme inhibition	✓	✘	✘	✘
Prodrug	✓	✓	✘	✘
ERM	✓	✓	✓	✓

Table 1.2 Main advantages (✓)/disadvantages (✘) of the drug delivery systems described. While enzyme inhibition and prodrugs show some limits, ERMs have the potentiality to overcome these drawbacks.

1.1.2 Factors to consider with design of ERMs for drug delivery

1.1.2.1 Particle size

Depending on the enzyme locale we can define two classes of targets for ERM i) Extracellular enzymes, *i.e.* exploiting enzymes that are expressed on cell surface or secreted by target cells; ii) Intracellular enzymes, *i.e.* enzymes that are not secreted and are only present inside cells. In the first case, since the enzyme is expressed on the cell surface or secreted, the size of the system is not a primary concern. In the second case, the ERM has to be designed in order to have particular characteristics which allow it to enter the cell. In this case, not only the size matters but even the overall charge,[22] shape and surface chemistry[23] has to be taken into account, e.g. if the cellular uptake involves channel proteins or charged pores.

Particle size is of particular importance in target delivery via intravenous administration (IV). One of the most used mechanisms to achieve passive targeting of tumour tissue is the so called enhanced permeation and retention (EPR).[24] This concept relies on the lack of organisation of cancer cells that makes the pores on the blood vessels less tight, allowing bulkier particles to pass through. Moreover, tumoural tissues have a poor lymphatic system which does not drain efficiently, permitting accumulation of relevant concentrations of conjugated drugs. Greish published a comprehensive review about the relation between particle size and accumulation in tumour tissue.[25] The ideal drug carrier administrated through IV should have a size which is bigger than the renal threshold, which is around 10 nm, and smaller than 100 nm to avoid liver capture and, hence, excretion. Moreover, knowing that carriers with a particle size which is less than 100 nm can be enclosed into endocytes, it is clear that the preferable size is between 10 and 100 nm.[26]

Alternative routes to IV administration are available, such as oral administration and depot-systems. For oral administration the enzyme sensitive part must be protected against the harsh conditions present along the gastro intestinal tract, e.g. acid pH present in the stomach. For such purposes, pH responsive polymers, which are able to protect the payload in the stomach but to expose the enzyme responsive part in basic conditions, are particularly suitable. Depot systems provide a long and sustained release of drug from a single application, e.g. intramuscular injection, and a slow release of the loaded molecules. This approach can be exploited designing networks or carriers that are slowly degraded under *in vivo* conditions and assure a sustained and controlled drug release.

Different approaches to selectively target enzymes through ERM will be treated in this chapter.

The response mechanism of ERMs is composed of at least two parts: an enzyme sensitive component, that usually is a substrate or substrate mimic of the enzyme, and a second component that is responsible for changes of interactions inside the material, which can lead to a macroscopic transition. We have categorised the ERMs, according to

the physical and chemical properties of the release system, in three groups: hydrogels, micelles and nanocontainers (Fig 1.1).

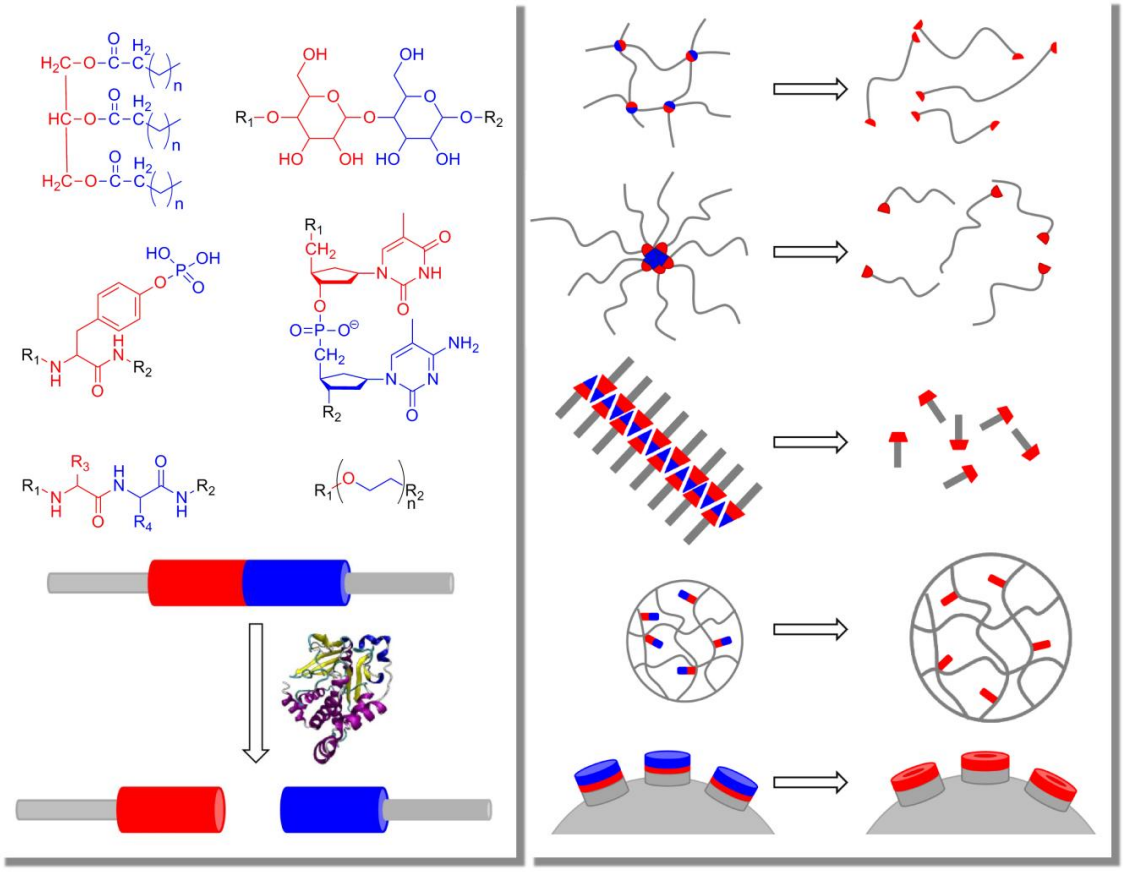

Figure 1.1 Left. Schematic description of the enzyme sensitive part which compose ERMs and examples of molecules which are used as enzyme substrates. Right. Examples of enzyme-responsive systems used to trigger drug release that are presented in this chapter. (Top to bottom) 1. Degradable hydrogel; 2. Disruptive micelle; 3. Supramolecular hydrogel ; 4. Triggered swelling hydrogel; 5. Silica nanocontainer.

1.2 Enzyme-responsive hydrogels

One of the firsts to recognize the unique properties of gels was Thomas Graham in 1861, a Scottish chemist who is considered the pioneer of studies on colloids.[27] When the liquid content is water, they are commonly defined as hydrogels, adding the Greek suffix hydro-, due to their high content of water (up to 99% w/w).

Hydrogels are elastic, three dimensional structures, constituted of two phases, a network of molecules that defines the properties of the structure and an aqueous phase which is trapped inside it. The nature of the building blocks that constitute the network greatly influences the properties of the gel, e.g. hydrophobicity or the presence of polar functional groups on the molecules define the amount of water that the hydrogel will incorporate.[28]

Hydrogels are highly suitable for drug delivery applications due to several characteristics: i) they provide a semiwet environment, ideal for biological interactions, ii) they can be designed to change physical properties, resulting in swelling or dissolution, iii) a wide range of molecules can be used to form hydrogels, from polymers to natural occurring building blocks, iv) they allow small molecules to diffuse freely, while larger (macro) molecules are restricted in mobility.[29]

Hydrogels can be formed either by chemical cross-linking of insoluble monomers (*chemical hydrogels*) or by molecules that self-assemble through non-covalent interactions (*physical hydrogels*).[30] Both types can be tailored in order to achieve a number of different particle sizes, from nano- to centimetre, and potential administration can vary from IV to intramuscular depot systems.

Even if it does not fulfil the definition of ERM (this system does not respond directly to the catalytic action of enzymes but to concentrations of glucose) we briefly mention the work of Kost and co-workers,[31] as it is a pioneering example that shows how the versatility of enzymes combined with responsive hydrogels can be used for drug

delivery purposes. They reported the controlled release of insulin based on both crosslinked and non-crosslinked poly(2-hydroxyethylmethacrylate-co-*N*,*N*-dimethylaminoethyl methacrylate) hydrogels. The authors trapped inside the hydrogels glucose oxidase (GOx), catalase and insulin and, simulating *in vivo* conditions, demonstrated the release of insulin varying glucose concentration. GOxs converted the glucose, diffusing in the hydrogels, into gluconic acid causing the swelling of the hydrogel and the consequent release of insulin, while catalases were included to provide oxygen to the oxidation reaction. It was found that the release of insulin was glucose concentration dependant and that the non-crosslinked hydrogels had a better release profile. This concept, first reported in 1985, [32] is still actively researched today.[33]

1.2.1 Chemically crosslinked hydrogels

Many strategies have been reported for chemical cross-linking, such as radical polymerization, high energy irradiation or chemical reaction with complementary groups.[34] Also enzymatic methods have been used to create covalently crosslinked hydrogels.[35]

1.2.1.1 Degradable hydrogels

There are many examples of enzymatic-degradable hydrogels in the literature. Many examples use natural molecules, such as polysaccharides and polypeptides, either on their own or in combination with biocompatible polymers, such as PEG. These hydrogels are designed to degrade only in the presence of specific enzymes, making them suitable for controlled release purposes (Figure 1.2).

In 1995 Shantha *et al.* [36] reported an example of a system designed to target specifically delivery of drugs in the colon: the hydrogel contained azoaromatic moieties as

crosslinking agent, which have the capacity to stabilize the gel, avoiding degradation by acidic stomach pH. These gels are easily degraded by azoreductases, enzymes produced in the microbial flora of the intestine, via reduction of azo-compounds in the presence of NADPH. In this way, after degradation of the azoaromatic moieties, the pH-responsive hydrogel is able to swell in the colon's basic conditions allowing the release of the drug (Table 1.3, Entry 1).

In another example aimed at colon-targeted drug delivery, Kim and Oh[37] used a dextran based polymer, cross-linked with acrylic acid, to obtain a dextranase/pH degradable hydrogel. Dextranases hydrolyse dextran to smaller oligosaccharides and are naturally occurring enzymes in the colon. 5-Aminosalicylic acid, an anti-inflammatory drug, was used as model payload. The authors simulated *in vitro* the colon conditions and monitored the drug release. They reported an increased release of 5-aminosalicylic acid due to the swelling and degradation of the hydrogel when exposed to the enzyme, which cleaves the α-1,6 dextran bonds (Table 1.3, Entries 1,2).

Lévesque and Soichet[38] reported on a dextran-based hydrogel, whose backbone was functionalised with p-maleimidophenyl isocyanate to avoid the presence of hydrolysable esters. The system was cross-linked with a modified peptide sequence which is a substrate for a matrix metallo protease, gelatinase A (MMP-2). This hydrogel was found to be stable in physiological conditions and to degrade, releasing the payload molecules, upon the action of MMP-2 (Table 1.3, Entries 2, 3).

Another example comes from Anseth and co-workers[39] that reported a PEG based hydrogel cross-linked by thiol-ene photopolymerisation of an enzyme substrate. The peptide sequence was selectively cleaved by human neutrophil elastase, a protease which is expressed in inflammation sites. The rate of hydrogel degradation can be tailored adjusting the peptide reaction constant, the concentration of HNE and of the peptide substrate. Indeed, the payload, albumin bovine serum and carbonic anhydrase, was released at different rates depending on the kinetics of the enzyme and the hydrogel formulation (Table 1.3, Entry 3).

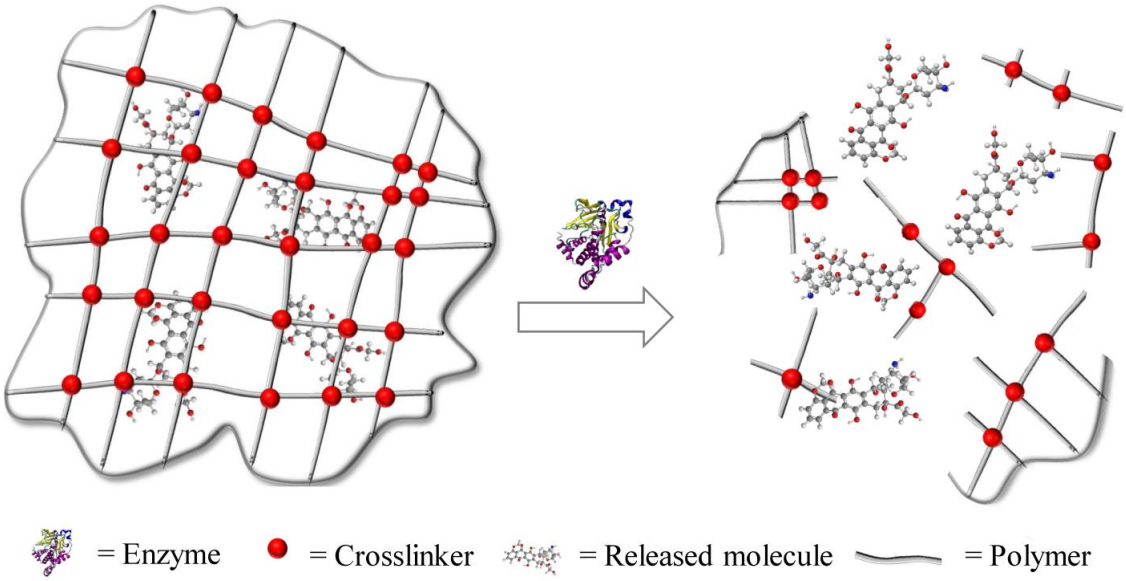

Figure 1.2 Schematic representation of a degradable hydrogel. The crosslinkers are designed to be an enzymatically degradable substrate. Upon cleavage of the substrate, the hydrogel degrades leading to the release of the payload.

	Enzyme	Crosslinker	Released molecule	Polymer
1	Oxidoreductase [28]	Azo linker [28]	Drug [28,29]	Acrylate derivative [28,29]
2	Transferase [29]	Dextran [29]	Fluorophore [30]	Dextran [30]
3	Hydrolase [30,31]	Peptide [30,31]	Protein [31]	PEG [31]

Table 1.3 The table describes the main characteristics of the degradable hydrogels presented in Paragraph 1.2.1.1.

1.2.1.2 Triggered swelling hydrogels

An alternative strategy to obtain an enzyme-responsive cross-linked hydrogel is to attach to it pendant enzyme-sensitive moieties. In this case the initial polymeric structure will stay intact, while the macroscopic transition will be expressed as a swelling/change of the material. Thornton *et al.*,[40] reported on a chemically crosslinked polyethylene glycol acrylamide (PEGA) hydrogel that demonstrated a different level of molecular accessibility in response to three different proteases, which had different substrate selectivity. The hydrogels were functionalized with peptide sequences, made of zwitterionic peptides flanked by oppositely charged amino acids that had a high affinity only for one kind of protease used in the studies. After the enzymatic cleavage of the sequence, a swelling of the hydrogel is observed, due to the specific interaction of the target enzyme with the peptide sequence and the removal of anionic aspartic acid groups. Fluorescently labelled dextran and avidin were used as payload molecules in order to monitor the diffusion and release profiles upon swelling.

In a following study,[41] the authors further developed this system by functionalising PEGA hydrogels with peptide sequences that, after enzymatic cleavage, would give a different overall charge to the beads. Using this method it was possible to selectively release oppositely charged proteins, albumin and avidin, due to the electrostatic repulsion between the payload and the hydrogel. This example shows that the molecular release mechanism may be matched to the properties of the payload.

A further development of this system has been achieved increasing the charge density of pendant amino acid sequences attached to the polymer adding zwitterionic branched peptide actuators.[42] This study showed the feasibility to achieve a controlled release of a template payload triggered upon the catalytic activity of proteases on micro-sized hydrogel particles under physiological conditions - the increased overall charge allowed the beads not to be affected by salt concentration in solution which hinders charges. This system enables the possibility of loading a model drug exploiting hydrogel swelling due to an induced pH change and releases it only upon the action of a specific enzyme.

However, it should be noted that a more biocompatible matrix would be required for translation to clinical therapeutics.

Another example that exploits enzyme substrates to achieve specificity for drug delivery is reported by Tauro *et al*.[43] In this study, a cross-linked poly(ethylene glycol)diacrylate was functionalised with pendant peptide sequences that are substrate for matrix MMPs. Platinum, a chemotherapy agent, was complexated with a lysine containing peptide. The release of platinum was showed to be influenced by the peptide sequence chosen as substrate of MMP, higher affinity meant higher release. Moreover, *in vitro* experiments on malignant glioma cell line showed significant decrease of cellular proliferation when the platinum containing hydrogels and MMPs were added. This example, different to the ones made by mentioned above, does not rely on the polymer swelling to trigger the drug release. Instead, the platinum ions are held in place by anion interactions with the positively charged Lys residues, which are cleaved by the enzyme, releasing the payload.

1.2.1.3 Supramolecular hydrogels

Supramolecular assemblies consist of molecules that are held together by non covalent interactions, such as electrostatic interactions, hydrogen bonding, π-stacking, van der Waals forces, hydrophobic interactions or combinations of thereof in aqueous or organic solvent systems.[44] In the past decade there has been increasing interest in the possibility of using enzymes to trigger supramolecular assembly/disassembly.

A common strategy to achieve gelation to form a supramolecular hydrogel is to modify a drug molecule with a precursor of a hydrogelator functionalised with an enzyme sensitive trigger.

An example of this approach was reported by Vemula *et al*.[45] Acetaminophen, an analgesic and antipyretic drug, was covalently linked to a fatty acid through a lipase

cleavable linker. Enzyme addition after gelation led to cleavage of ester linker and release of acetaminophen. The authors incorporated curcumin, a hydrophobic drug, in the hydrogel network, which was released under the same conditions of acetaminophen, creating a multi-drug release system (Table 1.4, Entry 1).

The strategy of incorporating a drug into the hydrophobic core of the hydrogel fibres was previously reported by the same research group.[46] In this case, a low molecular weight hydrogelator, amygdalin (a glycoside present in nature), was synthesised exploiting enzyme catalysis. Under physiological conditions they showed the release of cumin using lipases to trigger the gel dis-assembly (Table 1.4, Entry 2).

A two-stage release system, triggered by enzyme and pH has been reported from Van Bommel *et al*.[47] In this case a model drug, 6-aminoquinoline (AQ), has been incorporated into a hydrogelator, a cyclohexane trisamide scaffold functionalised with two ethylene glycol units, through an enzyme cleavable linker, phenylalanine (Phe), which was not accessible to the enzyme when the hydrogel was in the assembled state. In response to a pH or temperature change, the gel fibres were found to dissociate into individual molecules that could be cleaved by α-chymotrypsin, resulting in the release of the loaded drug (Table 1.4, Entry 3).

Gao *et al.*[48] designed a hydrogel precursor based on taxol, a well-established antineoplastic agent. Drug molecules were covalently linked to a peptide motif that is known to self-assemble, Naph-Phe-Phe-Lys (Naph = Naphtalene), and a group that is cleavable by an enzyme, phosphorylated tyrosine (*p*Tyr). Upon the action of phosphatases, the phosphate group is removed and the precursor transformed into the hydrogelator, which self-assembles, leading to the formation of a nanofibrous gel. Moreover, they assessed that the taxol-functionalised gel fibres preserved their therapeutic efficiency. De/phosphorylation may provide powerful stimuli to control self assembly, since the addition or removal of anionic phosphate groups mainly drives changes in electrostatic interactions (Table 1.4, Entry 4). We can define the last two examples as prodrug/ERM combinations.

An alternative strategy to direct incorporation of drugs within gelator design, which partially applies to the example just described above, is to use peptidase building blocks to obtain supramolecular hydrogels. Peptide-based hydrogels (PBH) have recently generated great interest as potential drug delivery vehicles. The main advantage of using peptide is that they are among nature's building blocks and, hence, offer low toxicology profiles, an essential characteristic for biological applications. Examples of PBH have been reported for applications in the drug delivery field, e.g. for anti-inflammatory molecules[49] or as implants.[50] To the best of our knowledge only one example of enzyme-triggered drug release from PBH has been reported to date. However, a number ERMs based on PBH have been reported to demonstrate new concepts of potential interest in drug delivery, but which have not been tested with the incorporation of drug molecules. Some of these are summarised below.

Pioneering work on PBH was published in 2004 by Xu and co-workers.[51] They firstly reported how enzymes can trigger the formation of gels starting from simple building blocks as N-(9-fluorenylmethyloxycarbonyl) (Fmoc) amino acid. This concept has been further developed by a number of research groups (Table 1.4, Entry 5). Sadownik *et al.*[52] reported micelles (which will be treated in Paragraph 1.3) to fiber transition, upon enzymatic dephosphorylation of Fmoc-Phe-*p*Tyr (Table 1.4, Entry 6). This approach could be designed to have a molecule loaded into the micelle's hydrophobic core, and upon catalysis in the presence of overexpressed enzymes, the system would undergo gelation around the target area, isolating the damaged cells and releasing the payload in a specific fashion. However, this concept remains to be tested for its suitability for controlled release.

The strategy of selectively isolating the target area, e.g. cancer tissue, surrounding it with a hydrogel was previously reported by Yang *et al.*[53] using another enzyme. They designed a nonapeptide amphiphile to be a substrate for MMP. After enzymatic reaction the peptide was cleaved in the expected position and the self-assembly motif, whose

main interactions were driven by four repeating Phe units, led to hydrogelation (Table 1.4, Entry 7).

Reversibility represents an opportunity achievable using enzymes. Kinases and phosphatases are ideal enzymes to create reversible systems due to their antagonistic behaviour and biological relevance (Table 1.1). To achieve phosphorylation with kinase, adenosine-5'-triphosphate (ATP) must be present in solution because it is the source of phosphate that the enzyme uses to phosphorylate amino acids. Theoretically, ATP can be used as the "fuel" that drives the reaction having both the enzymes present. Xu and co-workers[54] exploited a pentapeptidic hydrogelator (Naph-Phe-Phe-Gly-Glu-Tyr). They achieved a gel-sol transition when kinases and ATP were added to the hydrogel due to the phosphorylation of Tyr residues leading to a more hydrophilic molecule. *Vice versa*, adding phosphatases the Tyr residues become dephosphorylated and the gel is restored. Moreover, they succeeded testing this system *in vivo* in a mouse model, suggesting new application for the engineering of biomaterials which may find use in drug delivery (Table 1.4, Entry 8).

Very recently, a similar approach has been reported by Stupp and co-workers.[55] Using the same antagonistic enzymes, they developed a system which forms filamentous nanostructures upon dephosphorylation and dis-assembles upon phosphorylation. To achieve this result they synthesised a nonapeptide, containing one serine unit, covalently attached to a C_{12} chain. To assess the feasibility of drug release from such a system, they incorporated doxorubicin into the fibres and studied the cytotoxicity against tumour cells which secrete kinases. Not only did they observe a faster release from phosphorylated peptide – not self-assembled- but also a higher level of toxicity against cells only when kinases were present. This example, despite some problems of doxorubicin leaking from the self-assembled system, represents a big step forward toward the application of an enzyme triggered release system PBH (Table 1.4, Entry 9).

Achieving good control over the hydrogel structure is important because it can greatly influence the hydrogel properties and, consequently, the drug release process. It is a

challenging matter that can be achieved studying the enzyme role in the self-assembly process and understanding its dynamics. E.g., Hirst *et al.*[56] showed how dramatically influenced is the structure of the hydrogel by the concentration of the enzyme used. The authors studied the self assembly rates of several Fmoc-dipeptides capped with methyl ester functionalities, which are hydrolysed by subtilisin, triggering the gelation. They found that the molecular order was increasing, resulting in stiffer gels, with enzyme concentration suggesting a role of the enzyme in the self-assembly process (Table 1.4, Entry 10). This approach suggests a route to processing these gels to control their release profile.

All the described systems are good candidates for sustained or controlled drug delivery applications as well as an interesting method to shield molecules with poor water solubility inside hydrogels. The ERMs treated in Paragraph 1.2.1.3 are summarised in Table 1.4.

	Starting material	Enzyme-sensitive component	Enzyme	Response	Ref
1	Apn*-O-$[C]_n$	Apn-O~C	Lipase	Gel-to-sol, release of Apn and curcumin	37
2	Amygdalin-O-$[C]_n$	Amygdalin-O~C	Lipase	Gel-to-sol, release of curcumin	38
3	G*-Phe-AQ	G~Phe~AQ	α-chymotrypsin	Gel-to-sol, release of AQ	39
4	Taxol-$(Phe)_2$-Lys-*p*Tyr	*p*Tyr	Phosphatase	Sol-to-gel, diffusion of taxol	40
5	Fmoc-*p*Tyr	*p*Tyr	Phosphatase	Sol-to-gel	43
6	Fmoc-Phe-*p*Tyr	*p*Tyr	Phosphatase	Micelles to fibers	44
7	$(Phe)_4$-Cys-Gly-Leu-$(Asp)_2$	Gly~Leu	Matrix Metallo Protease-9	Sol-to-gel	45
8	Naph-$(Phe)_2$-Gly-Glu-Tyr	Tyr/*p*Tyr	Kinase/ Phosphatase	Gel-to-sol/ sol-to-gel	46
9	Lys-$(Arg)_2$ -Ala-Ser-Val-Ala-Gly-Lys-$[C_{12}](NH_2)$	Ser/*p*Ser	Kinase/ Phosphatase	Gel-to-sol/ sol-to-gel, release of doxorubicin	47
10	Fmoc-Tyr-Leu-OMe	O~Me	Subtilisin	Sol-to-gel	48

Table 1.4 The table describes the main characteristics of the supramolecular hydrogels presented in Paragraph 1.2.1.3. (*Apn=Acetaminophen, G=gelling scaffold).

1.3 Enzyme-responsive micelles

Micelles are structures formed by surfactants, e.g. phospholipids, where a hydrophilic head is in contact with the water while a hydrophobic tail hides inside giving the overall spherical shape. When studied for drug delivery purposes and synthesized artificially, micelles are often made by amphiphilic co-polymers or by polymer bio-conjugation of hydrophobic polymer with polar biomolecule and *vice versa*.

The enzyme responsive micelles that are presented in this chapter have sizes in the nm range, which is generally suitable for administration purposes. Moreover, the chemical properties of micelles are very appealing for applications in the drug delivery field due to the possibility to load a hydrophobic drug in the formed pocket. E.g. Blanco *et al.*[57] exploited this strategy to target lung cancer, lowering drugs' cytotoxicity, improving half-life time and tumour accumulation.
We divided enzyme-responsive micelles, in two categories, according to the physical response of the micelle upon catalytic action of the enzyme.

1.3.1 Disruptive enzyme-responsive micelles

In this category we consider all the enzyme responsive micelles that, after enzymatic reaction, do not have the original structures of the micelle-composing molecules. The enzyme selectively cleaves a bond which divides the molecular structure in two or more parts that are not able to self-assemble separately (Figure 1.3).

A conceptually similar approach to prodrugs, is to bond the drug molecules through a linker to a polymer chain. In this case, the design of the polymeric part is essential to make a system a good candidate for drug delivery applications, e.g. the polymer should not affect the effectiveness of the drug. Uhrich and co-workers[58] first designed an amphiphilic macromolecule with a hydrophobic component, dodecyl carbon chains, and

a hydrophilic moiety, a PEG chain, attached to a mucic acid backbone which is conjugated to the drug through a hydrazone linker. The release of the drug, doxorubicin, was mainly intracellular and pH driven. The macromolecule was designed to be biocompatible and biodegradable. Macromolecules were exposed to pancreatic lipase and found to be totally degraded within 6 days, while they were stable in the same conditions without enzyme for weeks (Table 1.5, Entry 1).

Another potential drug delivery system exploiting lipases to degrade micelles was reported by Shi and co-workers.[59] They prepared micelles formed by two diblock copolymers, poly(lactide)-block-poly(ethylenglycol) (PLA-b-PEG) and poly(lactide)-block-poly(N-isopropylacrylamide) (PLA-b-PNIPAM). When the temperature exceeds the lower critical solution temperature (LCST) of NIPAM, a core-shell-corona structure is formed by PLA, PNIPAM and PEG, respectively. The corona structure, formed by PEG, allows an adjustable diffusion of lipase, an enzyme able to degrade PLA, through PEG arms into the micelles and hence a selective release of the ibuprofen payload molecules (Table 1.5, Entry 2).

Castelletto *et al.*[60] reported on a polymer-peptide conjugate that self-assembled forming micelles, the corona being formed by PEG while the core by the heptapeptide, which contains two β alanines and is mostly composed by hydrophobic amino acids that form helical structures. Upon exposure to α-chymotrypsin, the peptide sequence is cleaved and the micelles fall apart. The amino acid sequence chosen contains a self-recognition motif that can specifically bind to amyloid protein and the authors suggest that this method could be used in the future to develop an enzyme-responsive diagnostic to secrete enzymes involved in formation of amyloid proteins (Table 1.5, Entry 3).

Heise and co-workers[61] exploited the selectivity of a protease to cleave a polypeptide di-block copolymer. In this case the peptides are used as corona while the core is formed by the hydrophobic poly(n-butyl acrylate) and polystyrene copolymer. The peptide was formed by copolymers of poly(L-Glu) embedded with variable amounts of L-Ala. They found that the degradation in response to protease exposure was proportional to the

quantity of Ala contained in the polymeric peptide and suggest that the system could be designed to have particular degradation times. Moreover, this ERM could be designed to be responsive to different kinds of enzyme including different amino acids in the polypeptide chain as enzyme/substrate specificity guarantees that the system is unlikely to be affected by exposure to other enzymes (Table 1.5, Entry 4).

Another approach to obtain disruptive micelles is to use polymers which are themselves substrates of enzymes. Wang *et al.*[62] synthesised an amphiphilic alternating polyester polymer containing oligo(ethylene glycol) (OEG) pendant chains that self assembles into micelles in aqueous solution. As mentioned earlier, the OEG chains not only contribute to the self-assembly process but also confer to the system essential properties such as lowering nonspecific interactions. After encapsulating two hydrophobic drugs, doxorubicin and rifampin, they noticed that the release was increased in the presence of proteinase K or reduced pH of 5.5. Both mechanisms enable cleavage of polymer backbone, resulting in micelle degradation. Without the exposure to enzymes only 10% of the drug could be released. Moreover, *in vitro* studies showed that the micelles were able to penetrate cancer cells and release doxorubicin, obtaining higher efficacy than the drug alone (Table 1.5, Entry 5).

The final example of disruptive micelles, exploits amphiphilic dendrons as self-assembly material. Azagarsamy *et al.*[63] inserted an enzyme cleavable ester moiety between the hydrophobic and hydrophilic part of the dendrimers. Upon esterase exposure, the micellar aggregates were dis-assembled (Table 1.5, Entry 6).

The ERMs treated in Paragraph 1.3.1 are summarised in Table 1.5.

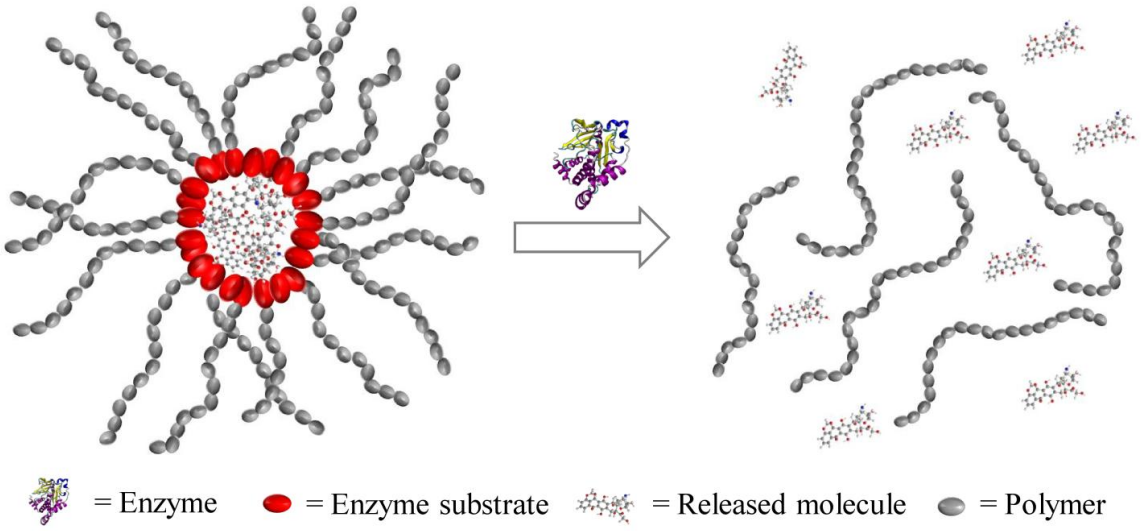

Figure 1.3 Schematic representation of a disruptive enzyme-responsive micelle. The enzyme substrate plays a critical role in the self-assembly process. Upon enzymatic catalysis, the polymeric structure is modified and the interactions leading to self-assembly are lost, as a result the structure disassembles and the payload is released.

	Enzyme	Enzyme substrate	Released molecule	Polymer	Ref
1	Pancreatic lipase	Hydrazone linker	Doxorubicin	PEG-[C_{12}](Mucic acid)$_4$	51
2	Lipase	PLA	Ibuprofen	PLA-b-PEG/PLA-b-PNIPAM	52
3	α-chymotrypsin	Phe~Phe	Amyloid peptide fragments	$(Ala)_2$-Lys-Leu-Val-$(Phe)_2$-PEG	53
4	Elastase, thermolysin	Ala~Ala	Amino acid fragments	*co*-poly(n butyl acrylate)-polystyrene-*b*-poly(Glu-*co*-Ala)	54
5	Proteinase K	Ester chains	Doxorubicin and rifampin	OEG-polyester	55
6	Porcine liver esterase	Ester linker	Pyrene	Dendrons	56

Table 1.5 The table describes the main characteristics of the disruptive enzyme-responsive micelles presented in Paragraph 1.3.1.

1.3.2 Switchable micelles

The common feature of switchable micelles is to allow self-assembly without disrupting the original polymer composition. All examples are based on the catalytic activity of phosphatases. This underlines the great interest that this class of enzymes, together with their antagonistic counterparts, kinases, is generating (as seen in Paragraph 1.2.1.3).

The first two examples were reported in close succession in 2009. Hawker and co-workers,[64] reported the self-assembly of a block-copolymer under physiological conditions. Incorporating vinyl monomers with an enzymatic activated substrate, which renders the monomer soluble, and copolymerising it with PEG macroinitiator, they

obtained a water soluble block copolymer. Upon action of phosphatases, the solubilising moieties, phosphate groups, are removed from the vinyl polymer backbone, turning it to hydrophobic. Consequently, the polymer becomes amphiphilic and undergoes self-assembly, forming colloidal nanostructures. The enzymatic reaction appears to be slow, the dephosphorylation is not complete after 7 days, probably due to the self-assembly of the polymer after only a partial conversion, which does not allow the enzymes to cleave all the phosphate moieties.

Kühnle and Börner,[65] synthesised a poly(ethylene oxide)-block-peptide copolymer (PEO-peptide conjugate). The bioconjugate had a peptide segment with a primary structure containing five repeating units of threonine and valine diads ($(Thr\text{-}Val)_5$), which have a strong tendency to adopt β-sheet aggregates in water. They suppressed this behaviour introducing three phosphorylated threonine residues into the $(Thr\text{-}Val)_5$ peptide aggregation domain. After the addition of phosphatase in the solution, they achieved the transition from random coils to β-sheets in overall fibrillar structures. Strictly, the formed structures are not micelles in this case.

A dual-responsive material has been recently developed to create a phosphatase/temperature responsive system.[66] In this study, poly(2-isopropyl-2-oxazoline) chains were functionalised with Fmoc-*p*Tyr that is known to self-assemble upon dephosphorylation.[43,67] This system, beside combining the numerous advantages of the polymer chain, such as stealth behaviour and low toxicity profiles, add to the system the temperature responsiveness. After enzymatic dephosphorylation the system forms micelles. When the temperature exceeds the LCST, the hydrophilic polymer corona structure becomes hydrophobic and collapses around the hydrophobic core formed by Fmoc-Tyr, reducing the particle size of the micelles. The enzyme responsiveness is reported to be fast compared to the ones reported above - enzyme conversion ends within one hour - due to the presence of only one phosphate group per polymer chain. Fmoc allowed to monitor the reaction by spectroscopy but it could be replaced by a more biocompatible molecule, ideally purely peptidic. Moreover, the thermal behaviour

is reversible, a feature that could be used to enhance tissue-targeting or help in loading the payload.

The last example exploits the same enzyme, but uses a different strategy: in this case phosphatases do not target polymer chains and their action lead to dis-assembly instead of self-assembly.[68] The authors synthesised a hydrophilic block copolymer methoxy-poly(ethylene glycol)-block-poly(L-lysine hydrochloride) (PEG-b-PLKC). The PLKC segment was chosen because it is positively charged and able to interact with negatively charged molecules. When ATP is added to the solution, the ionic interactions between ATP and PLKC physically bind the two components together, adding the hydrophobic adenosine functionalities and turning the polymer to be amphiphilic, leading to self-assembly into micelles. Upon enzymatic dephosphorylation, the ATP is degraded to adenosine and single charged phosphate groups, which are not able to bind anymore to PLKC and micelles fall apart.

The systems reported in this paragraph have not yet been tested as drug delivery systems, but provide unique properties such as good control over particle shape and the size and the manner of the structures formed. There are several issues to take into account, e.g. release time, but the great amount of work that has been done in the last few years in this direction make us believe that in the near future the drawbacks of these systems will be overcome and applications will be feasible.

1.4 Enzyme-responsive silica nanocontaniners

The last section of this chapter is dedicated to enzyme-responsive silica nanocontainers (SN). SN can be defined as mesoporous supports that can be used in the drug delivery field as scaffolds for storage of payload molecules which are released upon the catalytic action of enzymes (Fig. 1.4). Silica mesoporous supports provide many advantageous characteristics for drug delivery applications such as high loading due to large pore volume, biocompatibility and stability but also provide good protection of payload molecules because silica is not affected by external stimuli such as pH or temperature.[69] Silica supports have been used as support to release inorganic molecules[70] but, what makes these systems really interesting is the possibility to "cap" the pores with stimuli-responsive molecules to trigger the release of the payload molecules under certain conditions. The first example of silica support with capped pores was reported in 2003 by Mal *et al.*[71] that realised a light sensitive reversible gate system through the photodimerisation of coumarin. After this first study, a number of responsive systems were developed, example of reported triggers are pH,[72] temperature[73] or antibody-antigen interactions.[74]

The major drawback of this strategy is the lack of extensive *in vivo* studies about biocompatibility of silica nanoparticle and whether the toxicity is linked to specific characteristics of the material, e.g. particle size.[75] It is still to be demonstrated but studies suggest lung and liver toxicity.[76]

Since it is a new approach in the drug delivery field - the first SN has been reported in 2008 by Patel *et al.*[77]- most of the reports are proof of concept studies not yet used in drug delivery. In this first example, the authors first functionalised the mesoporous silica particles, having ~400 nm diameter and 2 nm pore diameter, to obtain a linker composed by ethylene glycol with a free azide group terminus. Following the loading of rhodamine B, a luminescent probe, by diffusion, the particles were incubated with α-cyclodextrin. After one day of incubation the pendant azide group was "clicked" on adamantyl

stoppers with pendant alkyne groups to obtain a [2]rotaxane. Two different adamantyl stoppers were synthesised, the first one had an ester linker, which is susceptible to esterase catalysis, while the second is an amide analogue, to serve as a control. After exposure to porcine liver esterase, it was found that rhodamine B was released only from the particles with the ester linked stopper while no release was detectable for the control. With the removal of the stopper, the α-cyclodextrin molecules were released, not being threaded any longer, leaving the pore open and allowing the diffusion of the luminescent probes (Table 1.6, Entry 1).

A second example exploiting cyclodextrins has been reported by Kim and co-workers[78] using smaller particles (~60 nm diameter) with the same pore size (2.5 nm diameter). A similar functionalisation strategy was used: first the surface was coated with alkyne groups and then the cyclodextrins were "clicked" on the surface after the loading with calcein, a fluorescent dye. When exposed to α-amylase, an enzyme that catalyses the degradation of starch into sugar, cleaving the α-1,4-glycosidic bond, the nanoparticles released calcein from the pores. No calcein release was noticed when the particles were not exposed to the enzyme or incubated with it on its denaturated form. Moreover, they synthesised a second population of dextran-based functionalised particles which had a different linker, containing an ester bond, without major changes to the functionalisation strategy. After exposure to lipases they found that the dye was released due to the cleavage of the ester bond (Table 1.6, Entries 1, 2).

A disaccharide, a lactose-derivate, was used by Bernardos *et al.*[79] to functionalise the particles having 2.4 nm average pore diameter. In this example, before coating the supports, the mesopores were loaded with $[Ru(bipy)_3]Cl_2$, a dye, to monitor the release upon enzymatic catalysis. They found that the release was taking place upon the catalytic action of β-D-galactosidase, able to cleave the 1→4 glycosidic bond between β-D-galactose and β-D-glucose monosaccharides which forms the structure of lactose. After the rupture of the bond, the cause of the steric hindrance, that was trapping the fluorescent dyes into the pores, is removed and the $[Ru(bipy)_3]Cl_2$ is able to freely

diffuse. The authors simulated pH conditions that this system should cross in an eventual application as drug delivery system. At pH 7.5, the value at which β-D-galactosidase is located in the intestine, negligible dye release was noticeable in absence of the enzyme. Similar behaviour was reported when the system was exposed to acid pH values, encountered in the stomach. Finally, the system was tested for selectivity with other enzymes, e.g. protease, but no significant loss of payload was reported (Table 1.6, Entries 1, 2).

The same authors further developed this system by functionalising the surface of the particles (100-200 nm diameter and 2.3 nm pore diameter) with different starch derivates, composed by various mixtures of polysaccharides.[80] After preliminary studies, they assessed that, when exposed to pancreatin, a mixture of different enzymes such as amylases and lipases extracted from the pancreas, there was a controlled release of the payload molecules. The release was progressive, sustained and proportional to the composition of saccharides used to functionalise the surface. Finally, they tested the starch-functionalised population which showed the best release profile through *in vivo* and *ex vivo* assays using doxorubicin as guest molecule instead of $[Ru(bipy)_3]Cl_2$. *In vitro* experiments showed the same release profile of the payload only when the enzyme was present. *Ex vivo* assays showed that the nanocontainers where internalised by the cell through endocytosis and then transported to the autolysosomes where enzymes able to degrade saccharides are present. After incubation of cancer cells with this SN loaded with doxorubicin the authors reported a decrease of cell viability and increased cell death (Table 1.6, Entries 1, 2).

An example of SN coated with a different material comes from Thornton and Heise.[81] The authors used a protease cleavable Fmoc-tetrapeptide sequence to functionalise the surface of the silica particles (5 μm diameter, 30 nm pore diameter) using FITC functionalised dextrans, rhodamin B and fluorescein as model payload to show the ability to trap molecules of various molecular weights. The particles were functionalised with two tetrapeptides with different affinities for two proteases, elastase and

thermolysin. Due to the hydrophobic and π-π interactions and the steric hindrance of Fmoc moieties, without enzyme addition the pores were closed and the payload retained. Upon exposure to the two proteases, depending on the substrate specificity for the selected protease and the concentration used, the tetrapeptides were cleaved and the dyes release in a controlled fashion (Table 1.6, Entries 1, 2, 3).

Coll *et al.*[82] reported another example where peptide sequences acted as enzyme-responsive gate guardians. In this study, they synthesised different peptides of various length that could be a substrate of proteolytic enzymes obtained from Streptomyces griseus and used them as substrate after trapping a dye inside the particles (~100 nm diameter, 0.9 nm pore diameter). They reported that the length of the peptide sequence had a strong influence to effectively cap the gate and trigger the release only upon the catalytic action of enzyme. The SN coated with the longest peptide (18 amino acids) showed zero release before exposure to enzyme, while the particles functionalised with shorter sequences (11 and 6 amino acids) show significant leakage (Table 1.6, Entries 1, 2, 3).

Another approach to obtain SN, reported by Schlossbauer *et al.*,[83] exploits the avidin/biotin interaction. In this study, the particle surface was modified with biotin and, after trapping a model payload, fluorescein, in the pores, avidin was added to the solution. Due to the strong interactions between biotin and avidin, the pores closed and no leakage of fluorescein was noticed. After exposure of trypsin, a protease that can digest avidin, amounts close to 100% of the payload were released in less than three hours after enzymatic addition. To further prove that the avidin/interaction was closing the pores, the authors monitored the release of dye increasing the temperature and found that, due to weaker affinity at higher temperatures, fluorescein was gradually released (Table 1.6, Entries 1, 3).

Finally, a different approach has been recently reported in two different papers by Hanagata and co-workers. So far, all the SN reported in this paragraph exploited enzyme catalysis to cleave one part of the molecule coating the surface, preventing steric

hindrace or self-assembly interactions, while their strategy uses the total degradation of coating molecules to trigger the release. Both the studies use particles which have up to 500 nm diameter and a pore size between 2.4 and 2.6 nm of diameter. In the first case,[84] after loading the supports with fluorescin as model payload, they functionalised them with positively charged linkers, applied by layer-by-layer deposition of a oligodeoxynucleotide and poly(L-Lys) negatively and positively charged, respectively. Upon exposure to α-chymotrypsin, they assessed *in vitro* the release of fluorescent dyes and genes due to degradation of the polymer (Table 1.6, Entries 1, 2, 3). In the second study,[85] they used the same strategy to coat the particles the oligodeoxynucleotide used in the previous report. Deoxyribonuclease was used to degrade the model gene and release fluorescein. This approach, besides exploiting non covalent interactions to coat the particles, allows the triggered release of a second molecule, *i.e.* oligonucleotides (Table 1.6, Entries 1, 2, 3, 4).

The ERMs treated in Paragraph 1.4 are summarised in Table 1.6.

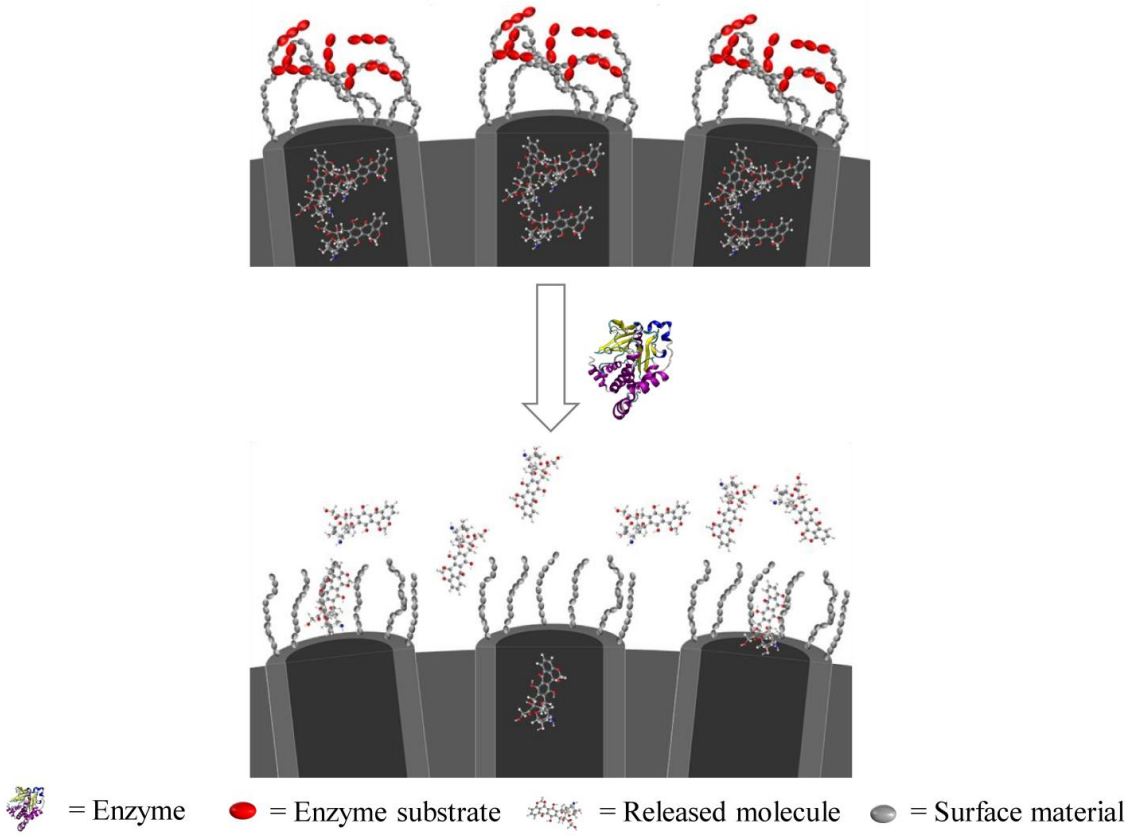

Figure 1.4 Schematic representation of an enzyme-responsive silica nanocontainer. Mesoporous particles are functionalised with enzyme substrates which obstruct the pores due to steric hindrance or weak interactions. Upon enzyme catalysis, the substrates are removed from the particles and the payload is released.

	Enzyme	Enzyme substrate	Released molecule	Surface material
1	Esterase [70,71,73]	Ester linker [70, 71, 73]	Fluorophore [70-78]	Saccharide [71-73]
2	Glycosyl hydrolase [71- 73]	Glycosidic bond [71-73]	Oligo-nucleotide [77, 78]	Peptide [74, 75]
3	Protease [74- 77]	Peptide [74- 77]		Oligo-nucleotide [77, 78]
4	Nuclease [78]	Oligonucleotide [78]		

Table 1.6 The table describes the main characteristics of the enzyme-responsive silica nanocontainers presented in Paragraph 1.4.

1.5 Conclusion

In summary, it has been shown how enzymes offer a number of advantages as potential tools to improve drug delivery. They are often involved in the development of diseases, making them extremely useful to address one of the biggest challenges of drug delivery: selectivity. The examples treated in this chapter illustrate how the versatility of enzymes offers multiple approaches to trigger drug release exploiting enzymes. Indeed, we have seen strategies that involve degradation, self-assembly, dis-assembly, cleavage and swelling, upon the catalytic action of enzymes finalised to the release of drugs. We reported studies where the release system was entirely composed by natural building blocks, where naturally occurring building blocks were conjugated to synthetic materials or the release system was solely composed of synthetic material. It is important to underline how the development of new biocompatible materials and polymers has a very important effect on the advances made from ERM in the biomedical field. In fact, many approaches rely on the availability of materials that show low cytotoxicity profiles or are FDA approved.

Most of the examples that are listed in this chapter are proof of concept, especially because we discussed the most advanced recent developments of ERM that have, among possible applications, drug delivery.

2. Phosphatase/temperature responsive poly(2-isopropyl-2-oxazoline)[†]

2.1 Introduction

Significant attention has recently been focused on the development of so-called ‘‘smart’’ materials[86] that can respond to external stimuli with a change in physical properties.[46,87] These materials can be tailored to respond to various stimuli, e.g. temperature,[88] ionic strength,[89] pH[90] or the catalytic activity of enzymes.[32,33,48,91] Systems that respond to combined stimuli, such as pH and temperature,[92] temperature and light,[93] and temperature and enzymatic activity[39] have also been described. Exploiting enzyme activity in this context has many advantages, including catalytic amplification of the self-assembly trigger, the ability to function under constant, physiological conditions and selectivity. Given the important role that enzymes play in biological pathways related to health and disease, this class of responsive materials may be expected to become increasingly important for future biomedical applications.[78]

Here, we focus on the use of phosphatase catalytic activity, combined with thermal responsiveness, to control polymer self-assembly. Phosphatases play a variety of vital roles in many organs in the human body where they are often expressed at cell surfaces, *i.e.* their catalytic sites are exposed and can interact with the cell’s external environment. Their expression levels commonly vary significantly during processes of relevance to health, disease and repair, as is the case for bone regeneration.[94] Moreover, their antagonistic disregulation with kinases is suspected to be involved in the development of cancer, diabetes and Alzheimer’s syndrome.[95]

[†] Published in part as: P.F. Caponi, X.P. Qiu, F. Vilela, F.M. Winnik, R.V. Ulijn, *Polymer Chemistry*, **2011**, 2, 306-308.

In 2004, Xu and co-workers[96] reported the first examples of phosphatase triggered molecular self-assembly, based on dephosphorylation of Fmoc-*p*Tyr to form the self-assembling Fmoc-Tyr, thereby controlling changes in electrostatic interactions. A number of responsive systems have since been developed based on de-phosphorylation of peptide derivatives.[33,39] More recently, similar switch systems have been introduced into polymeric materials, as demonstrated by Kühnle and Börner[57] and Amir *et al.*[56] These are elegant systems, but their response times were slow, at least in part because their kinetics are dictated by the enzymatic hydrolysis of multiple phosphate groups per polymer. Here, we describe a system which combines the self-assembly properties of Fmoc-Tyr,[83a] with the thermal responsive properties of poly(2-isopropyl-2-oxazoline) (PiPrOx), thus achieving a dual responsiveness (Fig. 2.1). In addition, we have developed a click chemistry route to polymer bioconjugation which will facilitate future development of similar hybrid polymeric/biomolecular systems with enzyme-responsiveness built-in.

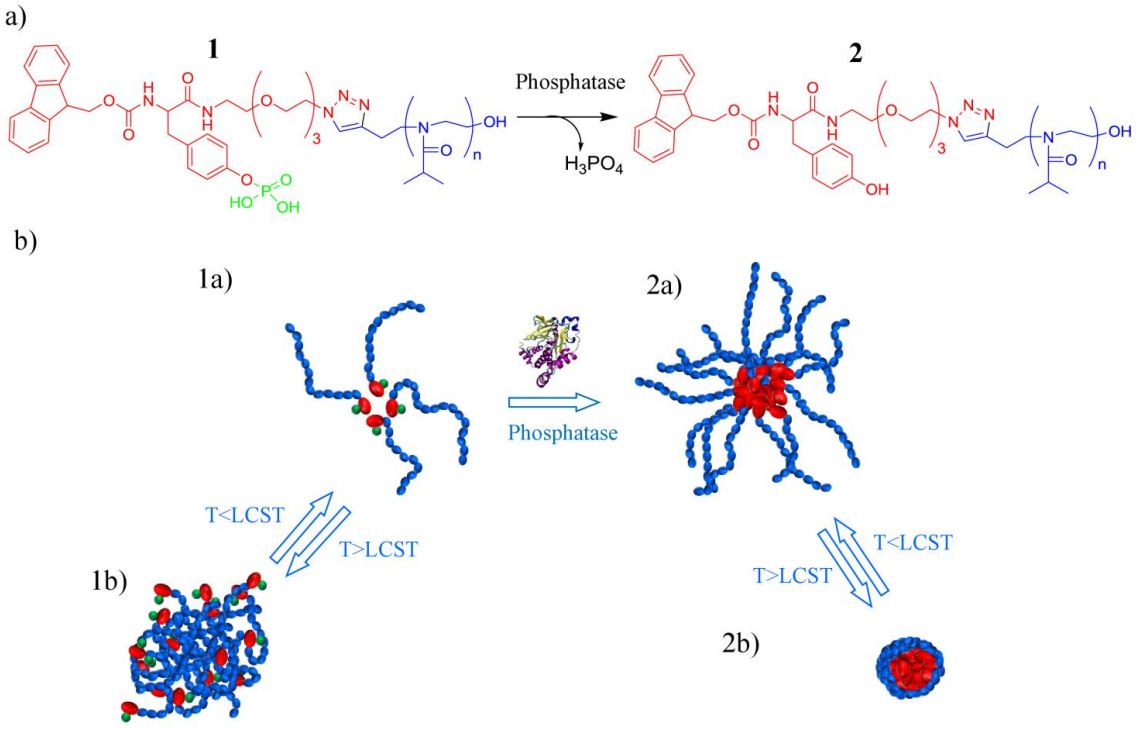

Figure 2.1 (a) Dephosphorylation of Fmoc-*p*Tyr-PiPrOx (**1**), catalysed by phosphatase, to obtain Fmoc-Tyr-PiPrOx (**2**). On average n=48. (b) Schematic representation of enzyme and temperature-induced self-assembly behaviour of the polymer bioconjugate. The phosphorylated polymer forms weak self-assembled structures due to the interaction between Fmoc-*p*Tyr moieties (1a). Above the LCST, random aggregates are formed (1b). After cleavage of the phosphate groups (**2**), Fmoc-Tyr moieties drive the self-assembly into micelles (2a). Above the LCST, the corona structure of the micelles collapses around the Fmoc-Tyr core (2b).

2.2 Result and discussion

A number of thermal responsive materials were reported in the last few years with poly(N-isopropylacrylamide) (PNIPAM) being the most widely studied.[97] A thermal responsive polymer shows a lower critical solution temperature which is the minimum temperature where all the phases are soluble.[98] Above the LCST the hydrogen bonds between the polymer chains and water are not entropically favoured, leading to the development of hydrophobic bonds between the polymer chains. Therefore, the phase transition is dictated by the hydrophobicity/hydrophilicity balance of the polymer. This process is often measured through the cloud point temperature which is the macroscopic effect, *i.e.* aggregation and precipitation, which follows the development of bonds among polymer chains and can be measured by spectrometry techniques, e.g. UV/VIS.

Compared to PNIPAM, PiPrOx has a number of advantages. First, poly(2-alkyl-2-oxazoline) has low toxicity[99]— indeed, two members of this family, *i.e.* poly(2-methyl-2-oxazoline) and poly(2-ethyl-2-oxazoline), have obtained FDA approval.[100] Second, they show a so-called ‘‘stealth’’ behaviour,[101] displaying reduced interactions with (immune system) proteins. Furthermore, the LCST of PiPrOx can be tailored by modifying the polymer end groups.[102] The synthesis of PiPrOx was performed by cationic ring opening polymerisation (CROP) of 2-isopropyl-2-oxazoline (Scheme 2.1a).[103] Propargyl tosylate was used as the initiator in order to introduce clickable alkyne groups to the α-end of the polymer chains (for details on polymerization and characterization see Paragraph 2.4.1). Fmoc-*p*Tyr was reacted with 11-azido-3,6,9-trioxaundecan-1-amine by a standard peptide synthesis procedure (Scheme 2.1b) (for details see Paragraph 2.4.2) to obtain a Fmoc-*p*Tyr-N_3 complex. Click chemistry was conducted in water using Cu(I) as catalyst generated in situ from the reduction of $CuSO_4$ by sodium ascorbate (Scheme 2.1c).[104] The level of end-functionalisation of the polymer was found to be 90%, as evaluated by UV/Vis exploiting the absorbance of Fmoc at 300 nm.

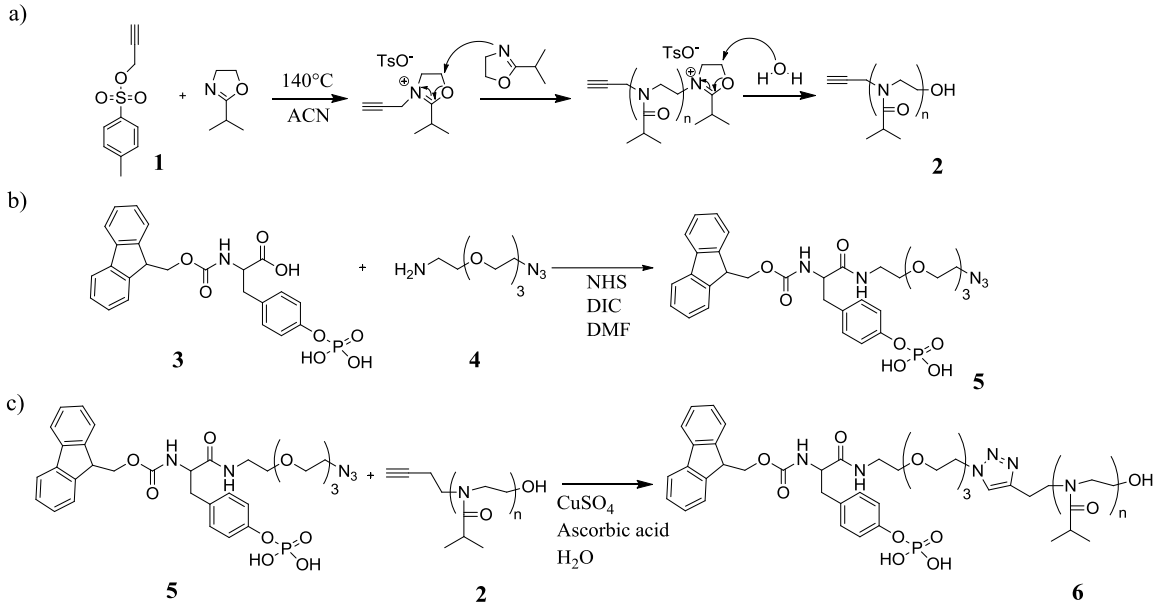

Scheme 2.1 (a) CROP used to obtain propargyl-PiPrOx-OH (2). Propargyl toluene-4-sulfonate (1) was used as initiator, while water was the terminating agent. (b) Coupling of Fmoc-*p*Tyr (3) with 11-azido-3,6,9-trioxaundecan-1-amine (4) using a standard coupling protocol to obtain Fmoc-*p*Tyr functionalized with a terminal azide group (5). (c) Click reaction used to obtain Fmoc-*p*Tyr-PiPrOx-OH (6).

Successful click coupling was indirectly evidenced by the changed phase transition temperature of aqueous propargyl-PiPrOx-OH before and after Fmoc-*p*Tyr incorporation (Fig. 2.2). The LCST of **3** in water was 46°C measured by UV transmittance, while **1** had a cloud point temperature value of 39.5°C. This decrease in phase transition is due to the presence of the hydrophobic Fmoc-*p*Tyr functionality. The change in LCST could also be used to monitor enzyme triggered supramolecular rearrangements proposed in Fig. 2.1. When an aqueous solution containing **1** was left overnight in the presence of 50 U of phosphatase, the cloud point temperature decreased by 2°C, due to the removal of hydrophilic phosphate groups, further enhancing the hydrophobicity (Fig. 2.2). The

unmodified polymer showed no significant hysteresis as previously reported.[105] Hysteresis was observed for the functionalised polymers **1** and **2**.

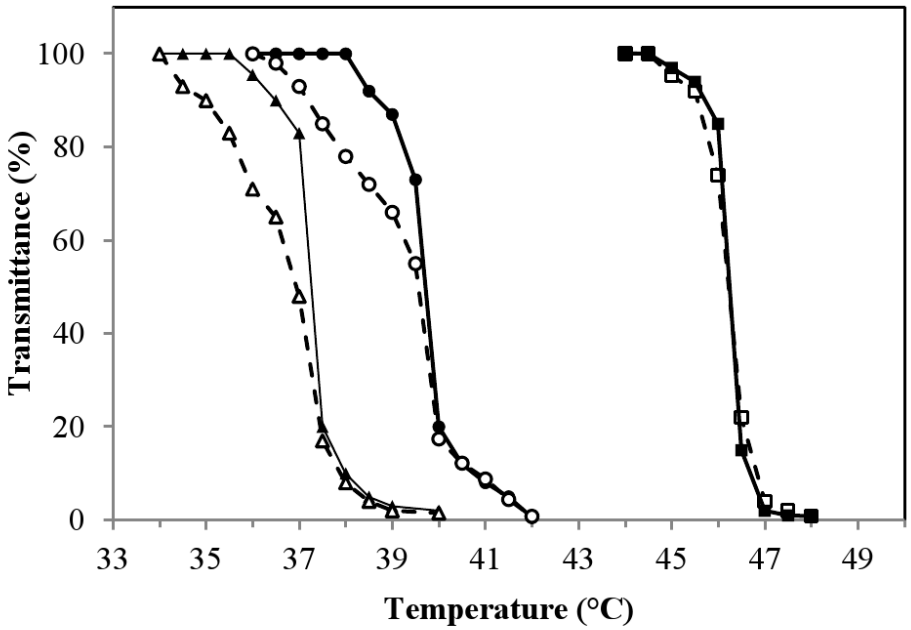

Figure 2.2 Reversibility of phase transitions of Fmoc-*p*Tyr-PiPrOx-OH (**1**) (●), Fmoc-Tyr-PiPrOx-OH (**2**) (▲) and propargyl-PiPrOx-OH (**3**) (■). Continuous line represents heating process while dotted line indicates cooling. Transmittance recorded at 600 nm.

To confirm the reversibility of the thermal response process, several cycles of heating and cooling (above and below the LCST) were completed for the polymer before (**1**) and after enzymatic (**2**) treatment. After several cycles, both the polymers (**1** and **2**) are capable to revert back to the initial soluble state (Fig. 2.3). Optical images were taken as further proof of the reversibility of phase transition (Fig. 2.4).

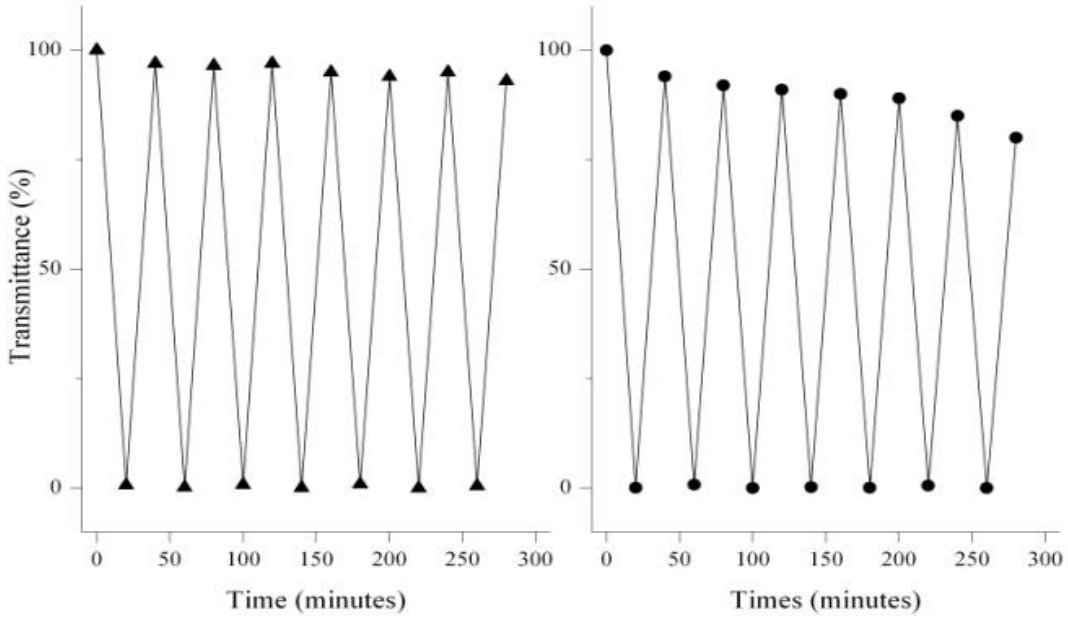

Figure 2.3 Study of the reversibility of thermal transition for ST OH-PiPrOx-*p*Tyr-Fmoc (**1**) (▲) and ST OH-PiPrOx-Tyr-Fmoc (**2**) (●). Higher values of transmittance correspond to 35°C while lower values to 45°C.

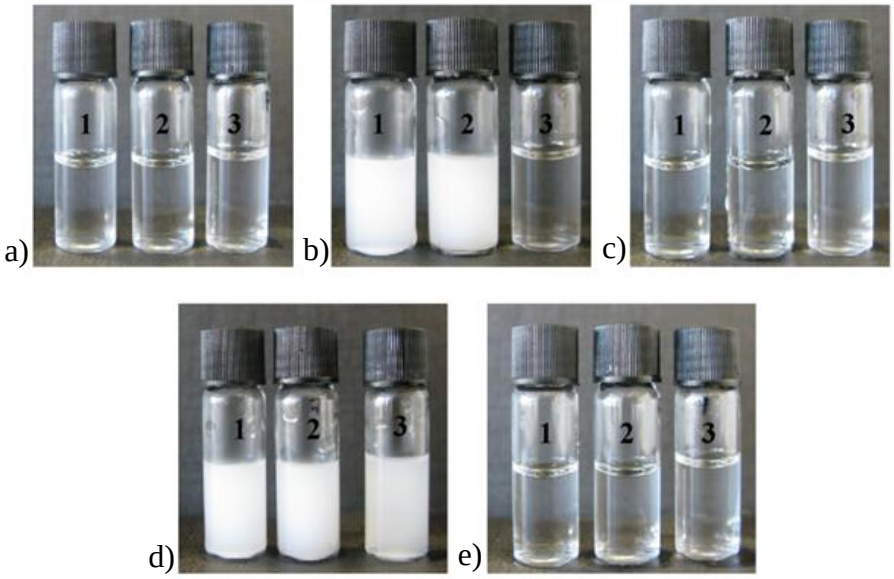

Figure 2.4 Optical images of **1**, **2** and **3** showing the reversibility of phase transition. a) Room temperature. b) After heating at 40°C. c) After cooling at room temperature d) After heating at 50°C. e) After cooling at room temperature.

The enzyme triggered self-assembly was also monitored by observing changes in fluorescence emission of fluorenes. 50U of enzyme were added to a 0.005 mg ml^{-1} solution of Fmoc-*p*Tyr-PiPrOx-OH. 10 minutes after enzyme addition, a decrease of fluorescence intensity at 305 nm was noticeable and after 3 hours the fluorescence spectrum did not show further changes. In addition to a peak at 305 nm, the emission spectra are characterised by relatively narrow peaks at approximately 320 nm and a broader peak at 370 nm. The latter is thought to represent fluorenyl excimers, indicative of Fmoc-Tyr aggregation (Fig. 2.5, inset). The ratio between the intensity of the 305 (monomer) and 370 (excimer) decreases with time, suggesting enzyme action induces Fmoc-Tyr aggregation (Fig. 2.5).

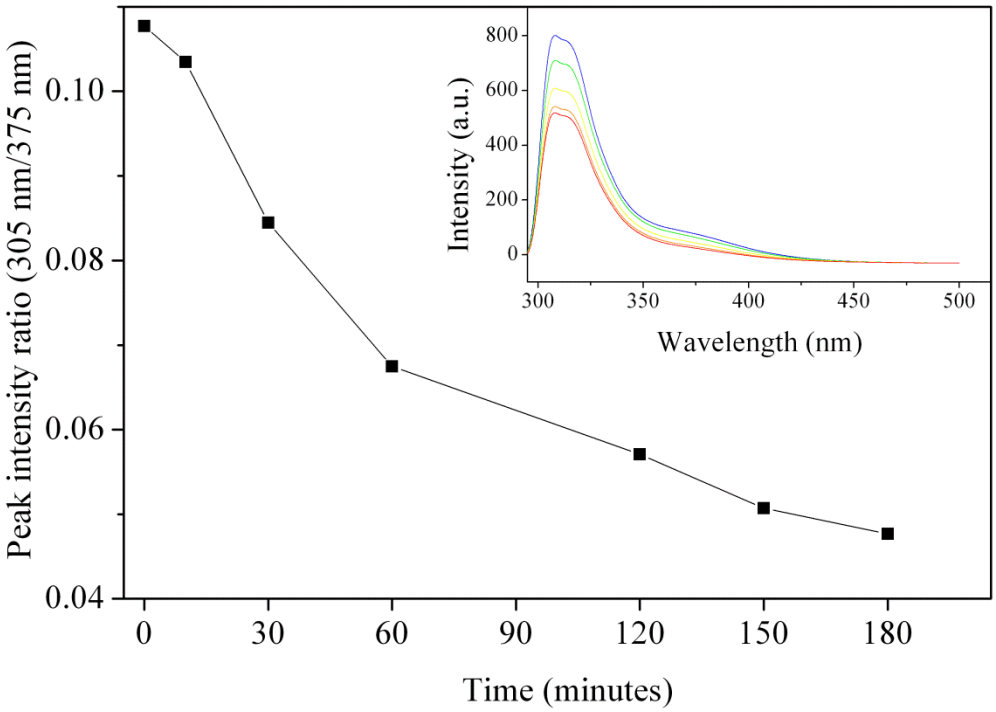

Figure 2.5 Enzymatic triggered self-assembly monitored by fluorescence spectroscopy. The inset graph shows the decrease in fluorescence intensity after addition of the enzyme over the course of 3 hour reaction (increasing time from top to bottom).

Finally, dynamic light scattering (DLS) was used to confirm that nano-objects with defined sizes formed upon enzyme action. The average hydrodynamic radius of **3** in aqueous solution at room temperature was ~2 nm (Fig. 2.6), while the R_h values of **1** and **2** were 44 and 92 nm, respectively. These observations indicate that before functionalization, the polymer (**3**) does not aggregate, while after functionalisation, micellar structures form (Fig. 2.1), with their sizes dictated by the presence of phosphate groups. Above the LCST, the polymer obtained after enzymatic treatment forms small mesoglobules (R_h = 21 nm) as a result of the dehydration collapse and aggregation of the poly(2-isopropyl-2-oxazoline) chains (Fig. 2.6 and 2.7).

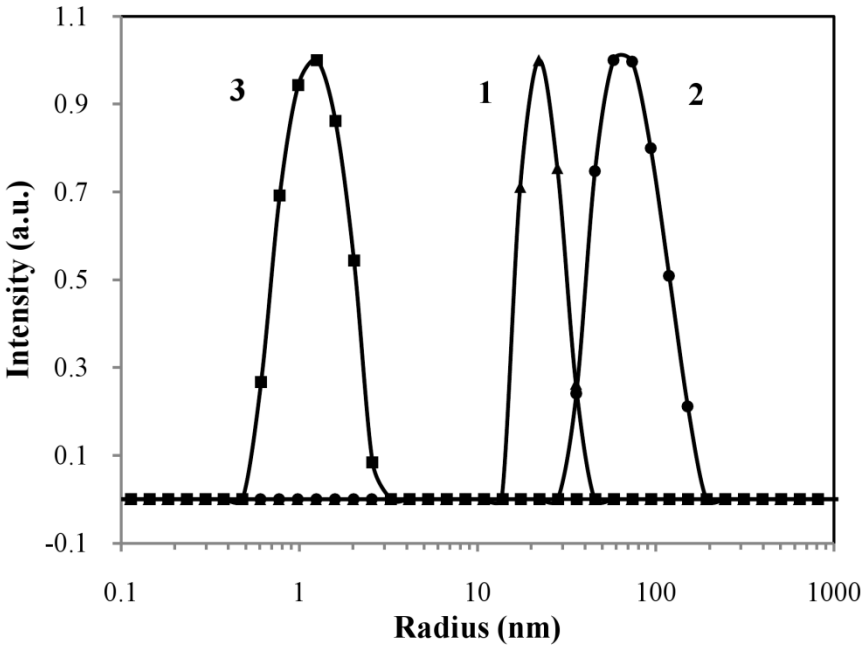

Figure 2.6 DLS data showing the average particle size dimension at room temperature being 44 nm for Fmoc-*p*Tyr-PiPrOx-OH (**1**) (▲), 92 nm for Fmoc-Tyr-PiPrOx-OH (**2**) (●) and 2 nm for propargyl-PiPrOx-OH (**3**) (■).

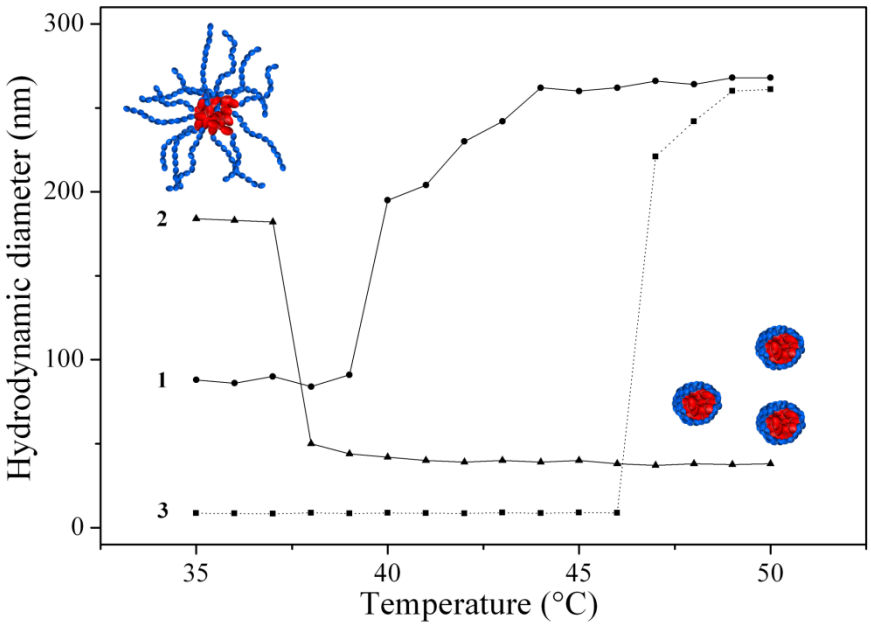

Figure 2.7 Hydrodynamic diameter of Fmoc-*p*Tyr-PiPrOx-OH (**1**) (●), Fmoc-Tyr-PiPrOx-OH (**2**) (▲) and propargyl-PiPrOx-OH (**3**) (■) as a function of the solution temperature (polymer concentration =2.5 mg ml^{-1}).

2.3 Conclusions

We hypothesise that **1** randomly collapses above LCST, while, upon enzymatic cleavage, aromatic interactions of Fmoc-Tyr[83a] give rise to shell–corona-like structures that above LCST form stable micelles. The system presented here is a first example of phosphatase/temperature dual responsive polymers. Starting from two well-known building blocks for stimuli-responsive materials we have been able to create a novel responsive material using a straightforward synthetic methodology which can be expanded to different responsive polymer/enzyme substrates. A further development for these materials could be to release bioactive payloads in response to cell surface phosphatases, in an effort to control and direct cellular behaviour.[106]

2.4 Materials and methods

Materials 2-Isopropyl-2-oxazoline (iPrOx, Tokyo Chemical Industry) was stirred overnight with calcium hydride (CaH_2), vacuum distilled and stored under nitrogen atmosphere. Alkaline phosphatase from calf intestine mucosa (New England BioLabs, 10.000 U ml^{-1}, one unit is defined as the amount of enzyme that hydrolyzes 1μmol of p-nitrophenylphosphate to p-nitrophenol in a total reaction volume of 1 ml in 1 ml at 37°C), propargyl p-toluenesulfonate (Fluka), 11-azido-3,6,9-trioxaundecan-1-amine (Aldrich), anhydrous N,N-dimethylformamide (DMF, Aldrich), dichloromethane (DCM, Aldrich), N-hydroxysuccinimide (NHS, Aldrich), N,N-diisopropylcarbodiimide (DIC, Aldrich), fluorenylmethoxyloxycarbonyl-phosphorylated tyrosine (Fmoc-*p*Tyr-OH, Aldrich), 3.5 kDa regenerated cellulose membrane (Triple Red Ltd), 500 Da cellulose acetate membrane (Aldrich), anhydrous acetonitrile (ACN, Aldrich) and tetrahydrofuran (THF, Aldrich) were used as received.

Instrumentation Fluorescence studies were performed on a Jasco FP-6500 spectrofluorometer. UV/Vis absorbance was measured on a Beckman Coulter DU 800 spectrophotometer equipped with a Beckman Coulter High Performance Temperature Controller. ^{1}H NMR spectra were recorded on a Bruker AV 300 at 292 K. DLS was performed on an AVL/LSE-5004 light scattering electronics and multiple tau digital correlator using an angle of 90°. ALV-Laser software was used to analyze the data and all sizes reported here were based on weight number. MALDI-TOF mass spectrometry was performed on a Kratos Analytical AXIIMA CFR using dithranol matrix. High performance liquid chromatography (HPLC) was carried out on a Dionex P680 HPLC system fitted with a UVD170U detector. An aliquot sample (100 μl) was injected into a Macherey-Nagel C18 column of the following dimensions: length 250 mm; internaldiameter 4.6 mm; particle size 5 μm; flow rate 1 ml min-1.

2.4.1 Polymer synthesis and characterisation

Polymerisation Polymerisation of iPrOx (Scheme 2.1a) was performed following a procedure reported in literature.[94] Microwave vials (0.5-2.0 mL) were left in a heating oven (125 °C) and cooled down to room temperature under nitrogen atmosphere. A solution containing 0.067 mmol of propargyl p-toluenesulfonate and 4 mmol of iPrOx was made directly in the microwave vial under nitrogen atmosphere and under stirring using ACN as the solvent. Total reaction volume was 1 ml. The vial was capped, and heated at 140 °C for 11 minutes. After the reaction, excess of H_20 was added to the vial, and the solution was extensively dialysed against water for 3 days. After dialysis the solution was freeze-dried.

^{1}H NMR The spectra were calibrated using the solvent signal ($CDCl_3$ 7.26 ppm, 300 MHz). Polymer concentration used was 2-5 mg ml^{-1} (Fig. 2.8).

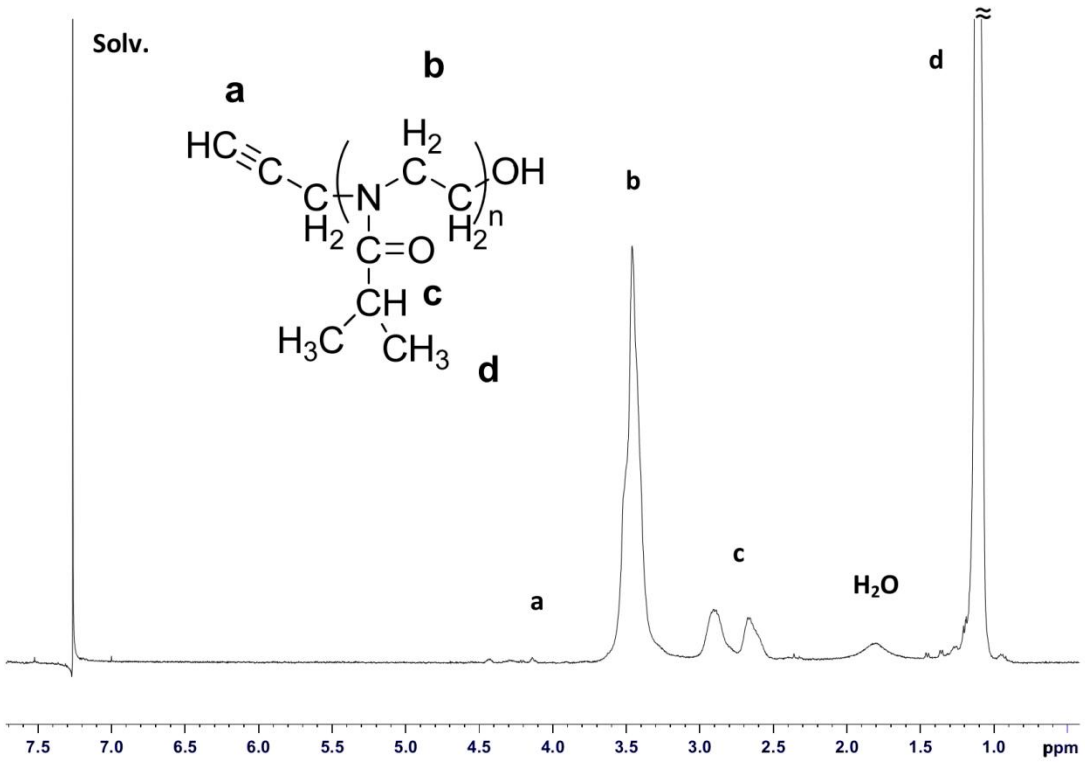

Figure 2.8 ^{1}H NMR spectra of ST propargyl-PiPrOx-OH in $CDCl_3$ (300 MHz).

Matrix-assisted laser desorption/ionisation-time of flight (MALDI-TOF) The samples were prepared by mixing THF solution of the polymer and matrix (20 mg ml^{-1}) in a ratio of 2:1 (v/v) (Fig. 2.9).

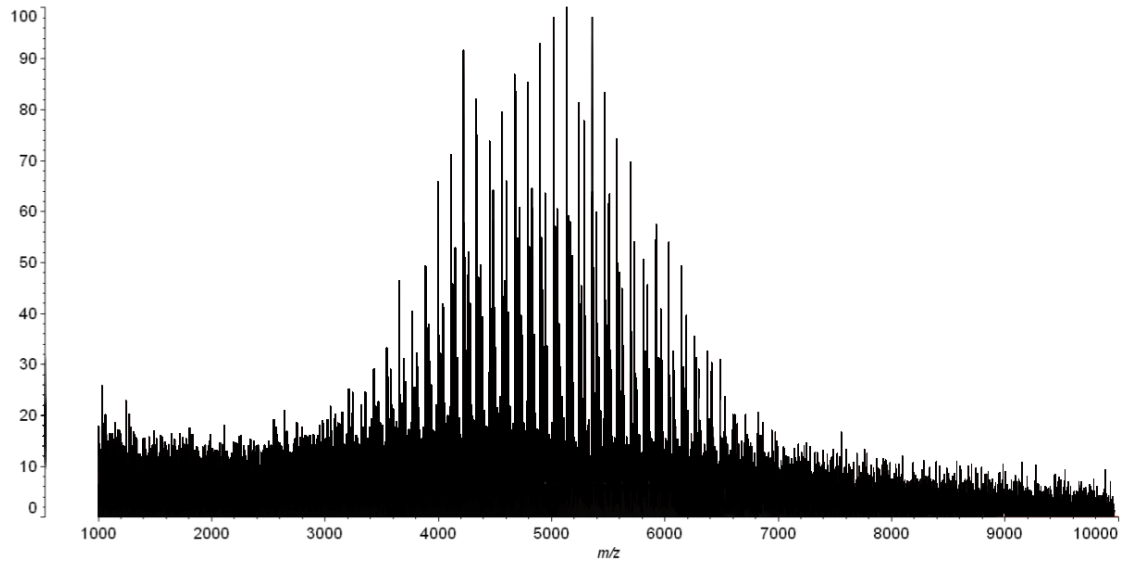

Figure 2.9 MALDI-TOF mass spectrometry spectra of ST propargyl-PiPrOx-OH.

2.4.2 Synthesis and characterisation of Fmoc-*p*Tyr bearing terminal N_3

Synthesis Synthesis of Fmoc-*p*Tyr bearing a terminal azide group was performed using a standard coupling procedure. The carboxylic terminus of Fmoc-*p*Tyr was activated during an overnight reaction in the rotator using 2 eq. of NHS and DIC in DMF/DCM (1:1). A solution containing 1 eq. of 11-azido-3,6,9-trioxaundecan-1-amine and 2 eq. of TEA in DMF/DCM (1:1) was added to the activated amino acid (Scheme 2.1b). The reaction lasted overnight under stirring. The dialysis, which was followed by freeze-drying, was performed with a membrane of regenerated cellulose (500 Da molecular weight cut off).

Characterisation The purity of the obtained compound after the purification process was assessed by HPLC (initial flow rate 40% H_2O, 60 % MeOH) dissolving 0.2 mg of Fmoc-*p*Tyr-OH in 1 ml of water, as a control experiment, and the same amount of Fmoc-*p*Tyr-N_3 complex (Fig. 2.10). Runtime = 20 minutes.

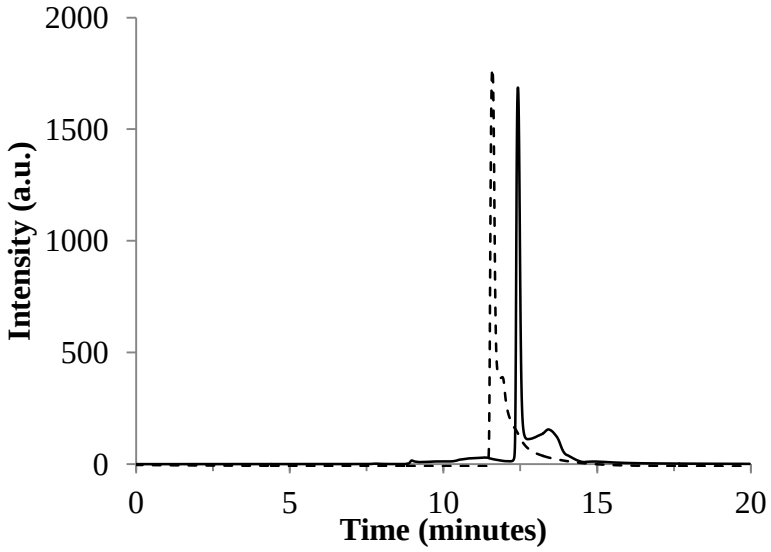

Figure 2.10 HPLC data showing the switch in the retention time between Fmoc-*p*Tyr-OH (dotted line, 11.5 minutes) and Fmoc-*p*Tyr-N_3 (continuous line, 12.5 minutes).

2.4.3 "Click coupling"

"Click" reaction (Scheme 2.1c) was performed in water, using $CuSO_4$ as catalyst and ascorbic acid as reducing agent to convert Cu (II) to Cu (I). The ratio used is the following: propargyl group/azide group/ $CuSO_4$ 1:2:0.3. 2 eq. of azide and 0.3 eq. of $CuSO_4$ and ascorbic acid were dissolved in a solution containing the polymer in water (final volume 7 ml). The reaction was left overnight on the rotator, before going through the purification process, using a membrane having a molecular weight cut off of 3.5 kDa.

Fmoc loading quantification The freeze-dried polymer was used to evaluate the Fmoc loading by UV absorbance of Fmoc at 300 nm, comparing it with the concentration/absorbance dependence of a calibration curve. Different calibration curves were calculated for each amino acid. A known amount of polymer (~0.5-1.0 mg) was dissolved in 1 ml of water. The obtained absorbance at 300 nm was used to evaluate the

concentration of Fmoc. The calibration curves were obtained taking the absorbance values of Fmoc-amino acid dissolved in H_2O, at different concentrations (Fig. 2.11).

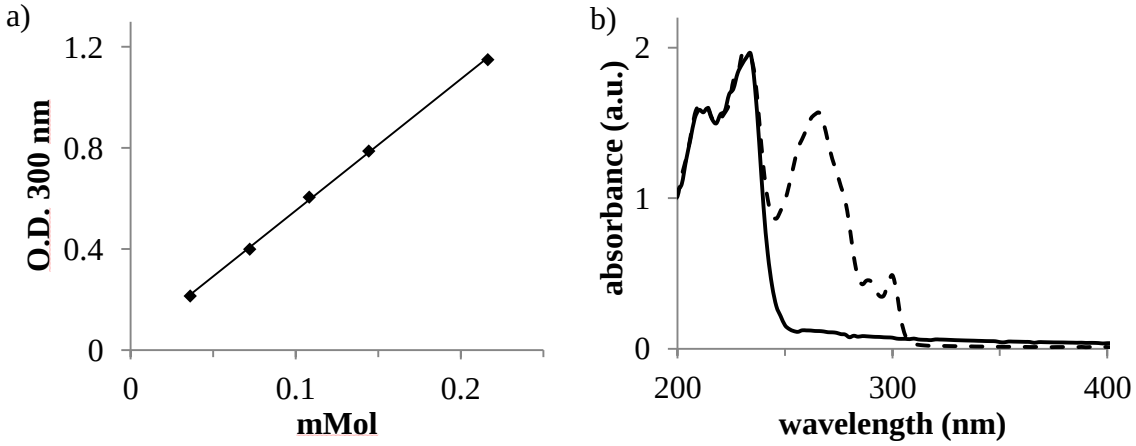

Figure 2.11 a) Plot of the calibration curve used for the quantification of the Fmoc-*p*Tyr loading on the polymers b) PiPrOx UV spectra before (continuous line) and after functionalisation (dotted line) with Fmoc-*p*Tyr.

2.4.4 Experimental

UV/Vis experiments-LCST A UV thermostatic cell was used to evaluate the cloud point temperature of the polymers. The absorbance of a known concentration of polymer dissolved in water (1 mg ml^{-1}) was read at 600 nm, in order to have no absorbance at room temperature. The sample was heated in the thermostatic cell with intervals of 0.2°C, within a temperature range of 25-60°C. The absorbance started to increase when the phase transition temperature of the polymer was reached and transmittance values plotted into a graph.

Fluorescence experiments An aqueous solution, containing a known amount of polymers (<0.01 mg), was used to take the initial measurement. The solution was left to incubate and measurements were taken every 12 hours. When the fluorescence spectrum

did not show further changes, 50 U of phosphatase (5 μL) were then added directly to the fluorimeter cuvette and changes in fluorescence spectrum recorded. Used excitation wavelength 290 nm, emission range 295-500 nm, band width (Ex) 3 nm, band width (Em) 3 nm.

DLS measurements Aqueous solutions of polymer (2.5 mg ml^{-1}) were used to determine the average particle sizes before and after the enzymatic reaction. Prior to the addition in the light scattering vial, the solution was filtered (PDV 0.2 μm filter) to eliminate impurities. After taking a first measurement, 50 U of phosphatase (5 μL) was added directly to the vial and the sample was left overnight at room temperature, before taking a second measurement standing for the average particle size after the enzymatic conversion. Each measurement was repeated 3 times to assess the reliability of the results.

3. Characterisation and self-assembly behaviour of two components Fmoc-a.a.-poly(2-isopropyl-2-oxazoline)[‡]

3.1 Introduction

Producing synthetic mimics of the adaptive compartmental systems of biological systems, through conformational changes under constant conditions, is a goal that has not been achieved.[107] This objective is often pursued through the use of polymers, whose properties and characteristics can be precisely tailored, but that need a change in environmental conditions, e.g. change in ionic strength or pH value, to undergo morphological changes.[108] The use of enzyme responsive materials has attracted significant interest thanks to their capacity to operate under constant environmental conditions. Moreover, the advantages of using enzyme for their catalytic action are well known, e.g. they work under physiological conditions and are biologically relevant and compatible, making these systems particularly appealing for biomedical applications.[43,109]

Among the structures that can be formed by enzyme-responsive materials, micelles are of particular interest due to the possibility to encapsulate drugs in the hydrophobic core to have it delivered in a specific tissue, e.g. where the target enzyme is over-expressed. The control over the size and chemical composition of structures formed is a key issue, especially if the aim is to develop systems that can have applications in the drug delivery field. A strategy that can be used to obtain enzyme-responsive materials that self-assemble into colloidal aggregates, as reported by Hawker and co-workers[56] and by Kühnle and Börner,[57] is to synthesize a diblock co-polymer which is completely hydrophilic but turns into amphiphilic upon enzymatic catalysis, leading to self-

[‡] Published in part as: a) P.F. Caponi, F.M. Winnik, R.V. Ulijn, *Soft Matter*, **2012**, 8, 5127-5130. b) P.F. Caponi, R.V. Ulijn, *Polymers*, **2012**, 4, 1399-1415.

assembly. Also Gianneschi *et al.*[110] exploited an amphiphile copolymer to enable enzymatically triggered aggregation. In their work, a polymer was functionalised with peptides substrates for phosphatases, kinases and matrix metalloproteinases, achieving different morphological changes, such as transition from micelles to networks or micelles to amorphous aggregates, depending on the enzyme used. An alternative strategy, which involves the use of a non-covalent "super"-amphiphile, has been reported by Zhang and co-workers.[111] In this case, a diblock co-polymer is used which bears positive charges (PEG- poly lysine) and, upon addition of negatively charged ATP, the system undergoes self-assembly due to ionic interactions between ATP and poly(lysine). Upon phosphatase catalysed hydrolysis, the negatively charged molecules are digested, leading to dis-assembly. This strategy shows dis-assembly upon enzyme catalysis, ideal for drug delivery purposes.

Enzyme substrates are mainly incorporated in the polymer chains as natural amino acids but also synthetic strategies can be exploited to add to polymers enzyme responsive moieties, as shown by Hawker and co-workers. Nevertheless, all the examples cited, highlight how important is the design of the system in order to create a self-assembly system and how the amino acid interactions can affect the self assembly process.

In Chapter 2, we reported a system of self-assembling micelles that respond to dephosphorylation. Poly(2-isopropyl-2-oxazoline) (PiPrOx), a thermal responsive polymer, were functionalised through a one-step synthetic strategy with fluorenylmethoxyloxycarbonyl-phosphorylated tyrosine, which is known to self assemble upon dephosphorylation.[83a] Upon phosphatase catalysed hydrolysis, the functionalised polymers were found to self assemble forming micelles. Moreover, the system kept the reversible thermal properties typical of PiPrOx, *i.e.* phase separation above the lower critical solution temperature (LCST).

We hypothesized that by mixing different populations of functionalized PiPrOx polymers, it may be possible to exploit the interactions that can occur between these amino acids (ionic and aromatic interactions). We could then create multi-component,

modular systems that could dis-assemble upon enzyme catalysis. This chapter has as main objectives to study the effect of amino acid chemical properties when used to functionalise PiPrOx, to create a multicomponent system by mixing different populations of Fmoc-amino acid-functionalised PiPrOx, demonstrating reconfiguration upon phosphatase catalysis.

To this end, we report on a systematic study of multicomponent enzyme-responsive systems exploiting a modular approach. The system was obtained combining the different properties of amino acids and PiPrOx. We functionalised several populations of PiPrOx with amino acids bearing different characteristics: Fmoc-phosphorylated tyrosine, a hydrophilic amino acid bearing a negative charge, Fmoc-Lysine, a hydrophilic amino acid bearing a positive charge, Fmoc-Tyrosine and Fmoc-Phenylanine, two hydrophobic amino acids.

3.2 Results and discussion

3.2.1 Single component Fmoc-amino acid functionalised PiPrOx systems

3.2.1.1 Polymer synthesis and functionalisation

CROP is a polymerization technique that provides good control over the molecular structure and a low polydispersity index (PDI). This polymerization technique was first reported in 1965 in a patent application[112] and it is receiving increasing interest thank to the Microwave-assisted CROP, a further improvement of this technique that was recently reported, which allows to shorten the polymerization time from hours to minutes.[113]

The polymerisation procedure is the same used in Chapter 2, reported by Schubert and co-workers.[114] In order to produce a larger amount of polymer with the same characteristics, the reaction was scaled up compared to the procedure reported previously. The ratio [M]/[I] was kept constant and the total reaction volume was 3 ml. Briefly, propargyl-tosylate (TsO^-) has been used as initiator provide an alkyne group as the α-terminus functionality while the ω-terminus functionality, a hydroxyl group, was introduced by the terminator, water (Chapter 2, Scheme 2.1). The ratio of monomer/initiatior used was 60:1, in dry ACN, 4 M and 0.067 M were the concentrations used, respectively. MALDI-TOF of the purified polymers showed an average molecular weight of 5 kDa (n=44) and a PDI of 1.1 (Fig. 3.1).

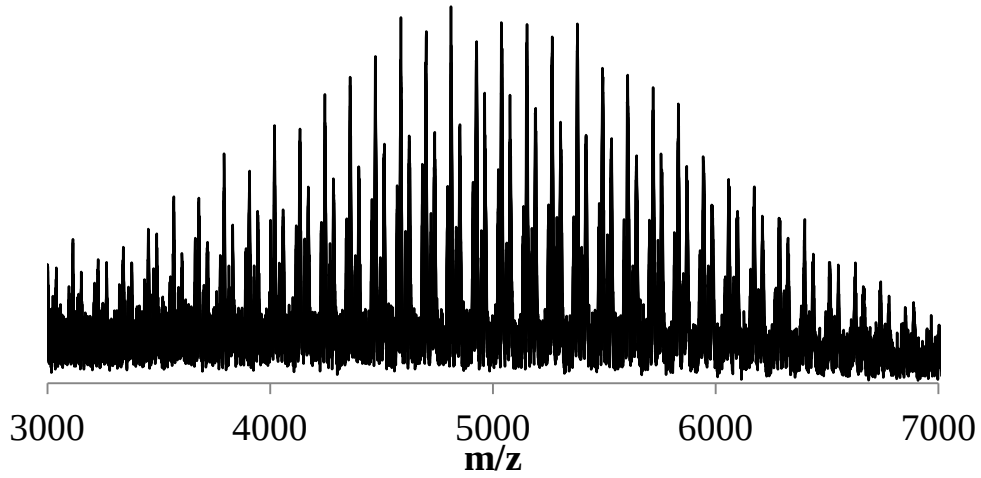

Figure 3.1 MALDI-TOF spectrum of poly(2-isopropyl-2-oxazoline). Average molecular weight=5 kDa.

In order to explore the self-assembly behaviour and the influence that Fmoc-amino acids have when attached to PiPrOx chains, we decided to chose a number of amino acids with different characteristics. The system we previously reported (Chapter 2) was functionalised with Fmoc-tyrosine and its phosphorylated form (Fmoc-Tyr/*p*Tyr).

To investigate the effects that amino acids have on the self-assembly properties of polymer, we chose a completely hydrophobic amino acid, Fmoc-phenylalanine (Fmoc-Phe) and another polar one bearing a positive charge, lysine (Fmoc-Lys). Polymers functionalized with Fmoc-*p*Tyr[§] (**1**) (Chapter 2, Scheme 2.1b) and Fmoc-Lys (**4**) (Scheme 2.1) were attached, through HBTU chemistry, to a linker bearing an azide group and then clicked on the α-terminus of the polymer (Route A). Tyr functionalised PiPrOx (**2**) were obtained enzymatically by dephosphorylation of **1** (Route B) (Chapter 2, Fig. 2.1). Details about functionalisation procedure and characterization are reported in Paragraph 3.4.2.

[§] Compared to Chapter 2 reagents were changed but the mechanism of the reaction remains the same. NHS was substituted with HBTU and DIC with DIPEA due to higher water solubility profiles.

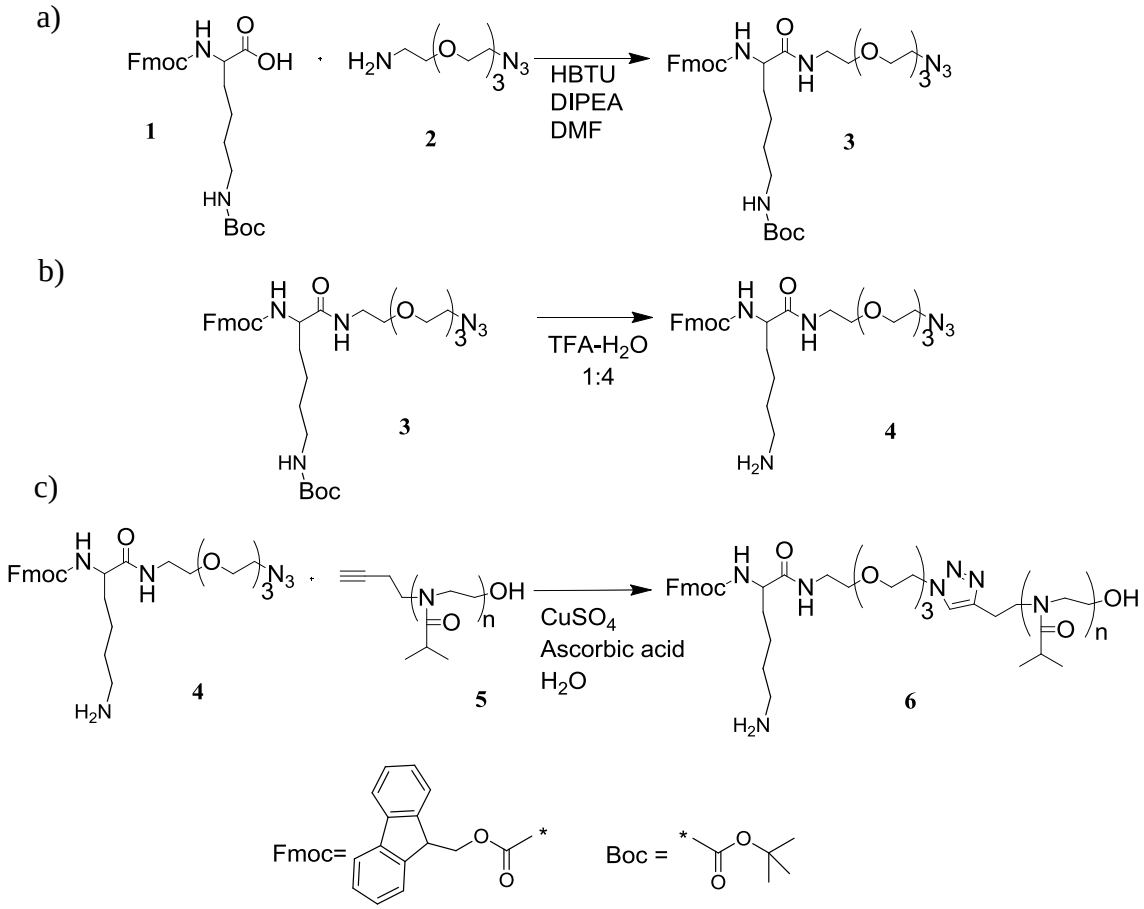

Scheme 3.1 Synthetic strategy used to obtain Fmoc-Lys functionalised PiPrOx. a) HBTU coupling used to functionalise the amino acid (1) with 11-azido-3,6,9-trioxaundecan-1-amine (2) to obtain Fmoc-Lys-N_3 (3). b) Lysine side chain deprotection reaction with TFA (4). c) Click reaction exploited to functionalise PiPrOx (5) with Fmoc-Lys-N_3 (4) to obtain semitelechelic Fmoc-Lys-PiPrOx-OH (6).

To obtain Fmoc-Phe functionalised PiPrOx (**3**) a different procedure was used. The click reaction to functionalise the polymer with the Fmoc-Phe-N_3 was not giving good yields (<30%), probably due to low solubility of the complex in water. The reverse procedure was found to be successful (Route C) (Scheme 3.2). Briefly, the azide-containing linker was first clicked onto the polymer, then Fmoc-Phe was attached to the pendant free amine group through HBTU chemistry. To assess that the first step was successful, the

LCST was checked prior and after the click reaction. There is a difference of 2°C in the phase transition temperature between the unfunctionalised polymer (51°C) and the polymer with the pendant amine group (53°C) (Fig. 3.2). The increased overall hydrophilicity of the polymer chains raises the phase transition temperature. This is due to the substitution of the alkyne group with the hydrophilic pendant amine group belonging to11-azido-3,6,9-trioxaundecan-1-amine, and it provides a first indication that the reaction was successful.

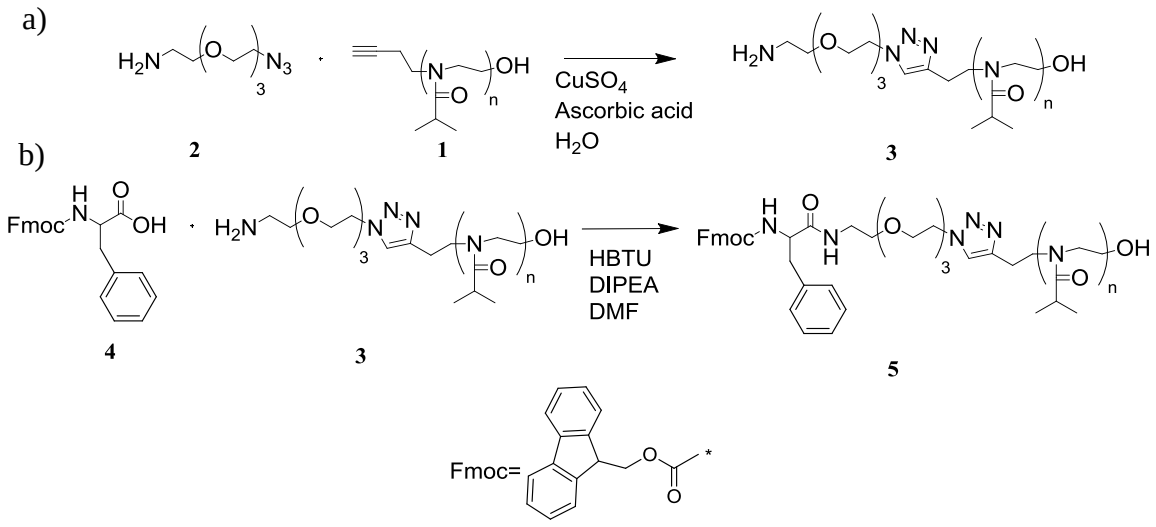

Scheme 3.2 Synthetic strategy used to obtain Fmoc-Phe functionalised PiPrOx (Route B). a) Click reaction was used to functionalise PiPrOx (1) with 11-azido-3,6,9-trioxaundecan-1-amine (2) to obtain PiPrOx bearing a primary amino group (3) . b) HBTU chemistry was exploited to couple PiPrOx bearing the primary amino group at the α-terminus (3) with Fmoc-Phe (4) to obtain semitelechelic Fmoc-Phe-PiPrOx-OH (5).

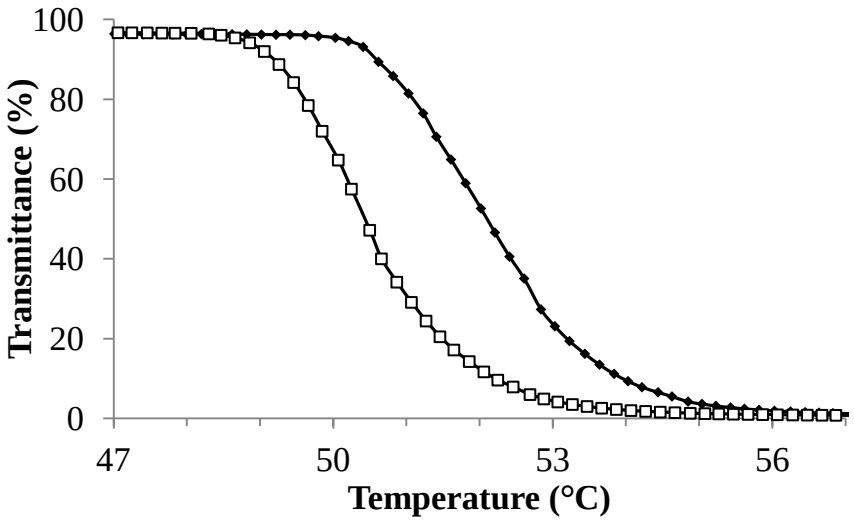

Figure 3.2 Cloud point determination of unfunctionalised polymer (□) and the polymer after click reaction with 11-azido-3,6,9-trioxaundecan-1-amine (■).

Attempts to functionalise PiPrOx with longer peptide sequences using the same synthetic strategy were made, starting off with Fmoc-dipepetides that showed interesting self-assembly properties such as Fmoc-Phe-*p*Tyr (**5**). Synthesis of Fmoc-Phe-*p*Tyr-N_3 complex was achieved through HBTU coupling (data not shown). Unfortunately, the loading yields achieved with Route A were low (~45%) despite several changes to the functionalisation strategy, e.g. substitution of solvent used for click reaction or altered reagent ratios. Route C gave even lower yields (~30%).

After attaching the Fmoc-amino acids on the polymer chain the loading was evaluated exploiting the absorbance of Fmoc at 300 nm. Loading values are excellent in each case (>90%) and summarized in Table 3.2.

3.2.1.2 Phase transition temperature studies

To assess if the polymer functionalisation affected the thermal properties of PiPrOx, we studied the thermal responsiveness of the polymers by measuring the transmittance by

UV at 600 nm. The polymer concentration (1 mg ml^{-1}) was kept constant through all the UV experiments. Figure 3.3 gives a schematic representation of the conformation of the single component systems below and above the LCST, while Figure 3.4 shows the phase transition profiles of the polymers, *i.e.* recorded transmittance against the temperature.

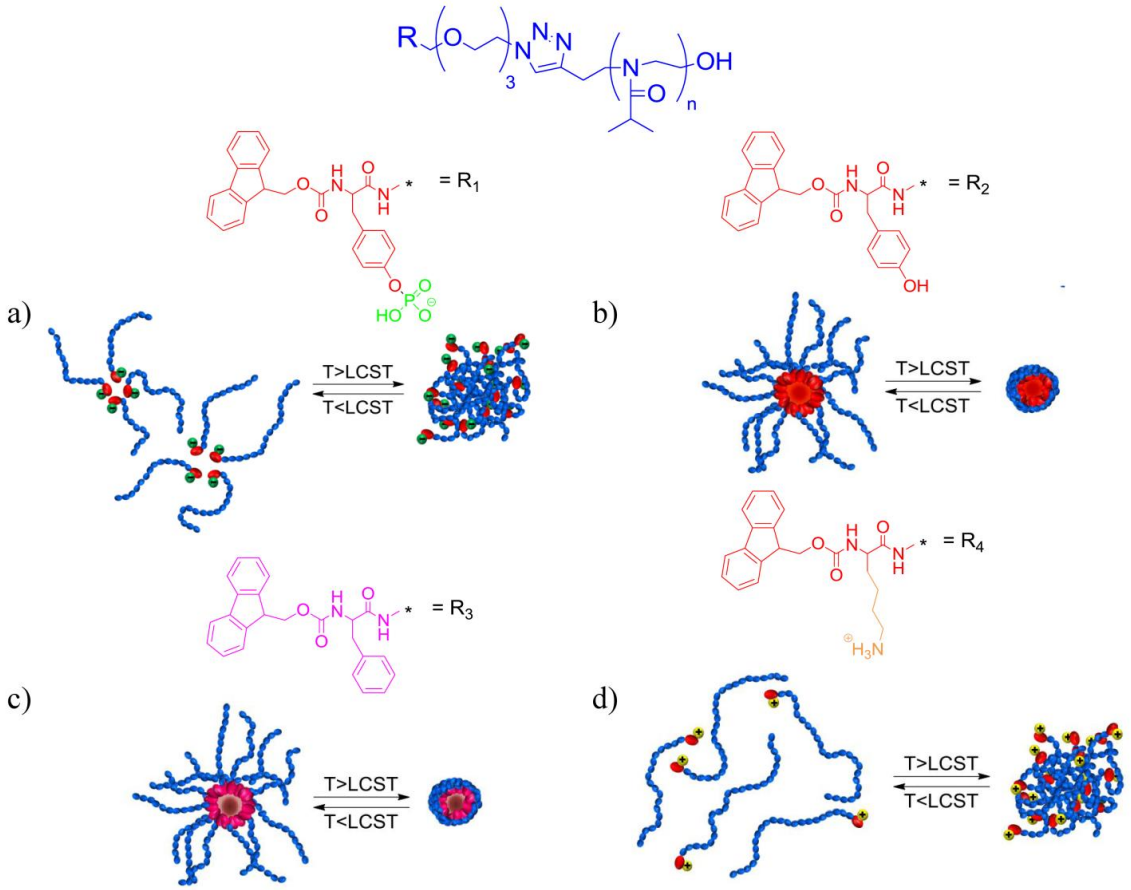

Figure 3.3 Schematic representation of self assembly behaviour of single component Fmoc-a.a. functionalised PiPrOx systems. a) **1** forms unstable aggregates at room temperature but precipitates above LCST as shown for the unfunctionalised polymer. b) **2** forms stable colloidal particles at room temperature which are kept when the temperature is increased. c) **3** forms stable colloidal aggregates as seen for **2** both below and above the phase transition temperature. d) **4** shows the same behaviour seen for the unfunctionalised polymer both at room temperature and above the LCST.

The phase transition temperature is contained within a range of 3°C (37.7-40.7°C) for **1**, **2** and **4**, while it drops to 31°C for **3**. Their values are summarized in Table 3.2. There is a good correlation between the phase transition temperature found for each functionalized polymer and the LogP value of amino acids (Table 3.1). The structural difference between **2** and **3** only consists in the hydroxyl group that is present on the tyrosine side chain and yet, this leads to a remarkable difference in the polymer behaviour. The presence of a charge on the amino acids Lys and *p*Tyr is expected to prevent close interactions between residues, hampering the development of effective π-π stacking interactions between Fmoc moieties. On the other hand, the presence of a hydrophobic residue, e.g. the phenyl functionality of Phe, not only is expected to favour the self-assembly process by increasing the overall hydrophobicity of the Fmoc-amino acid moiety but also improves the chances of interactions among amino acids/Fmoc functionalities.

Amino acid	**CLogP***
*p*Tyr	- 3.561
Tyr	- 2.223
Phe	- 1.556
Lys	- 3.561

Table 3.1 Estimated LogP of the amino acids used to functionalise PiPrOx. *Calculated LogP was assessed using ChemBioDraw chemical properties analysis tool.

The differences in phase transition temperatures clearly show the substantial effects on the self-assembly behaviour upon end-functionalisation of polymer chains (Fig. 3.4). The phase transition profile of **5** (which was only partially functionalised) showed a sinusoid curve, starting to decrease at temperatures around 35°C but reaching low

transmittance values only close to the phase transition temperature of the unfunctionalised polymer (~51°C) (Fig. 3.4., inset). This data demonstrates that only polymers functionalised in a homogeneous fashion present a sharp phase transition.

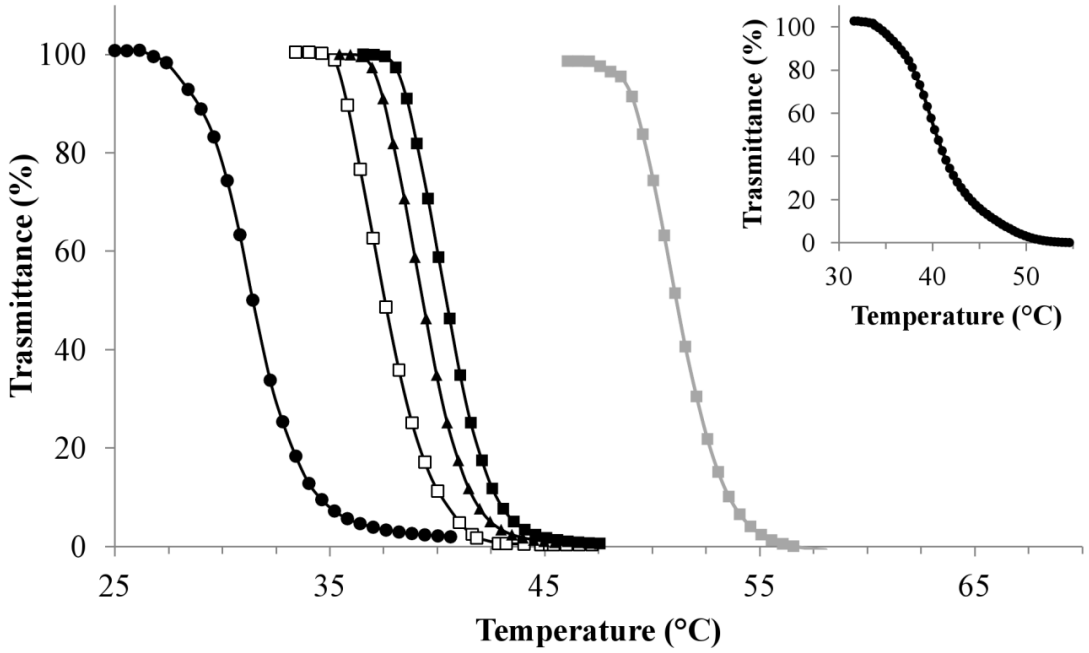

Figure 3.4 Cloud point behaviour of unfunctionalised polymer (■), **1** (■), **2** (□), **3** (●), **4** (▲) and **5** (●) (inset). (Polymer concentration used=1 mg ml^{-1}).

3.2.1.3 Dynamic light scattering studies

DLS was exploited to assess whether the functionalized polymer formed aggregates in solution (Fig 3.5). Solutions containing 2.5 mg ml^{-1} of polymer were dissolved in water and used to take the measurements. As previously reported, **1** forms aggregates with an average particle size of 35 nm below the LCST while it precipitates when the temperature increases. **2** forms colloidal structures at room temperature (~ 90 nm) that persist when the phase transition temperature is reached and the polymer chains collapse

around the hydrophobic core formed by Fmoc-Tyr moieties. **3** shows the same self assembly behaviour showed by **2**, both above and below the LCST forming colloidal structures having an average particle size of 85 nm and 20 nm, respectively. **4** behaves like the unfunctionalised polymer not showing self-assembly at room temperature and precipitating above the phase transition temperature.

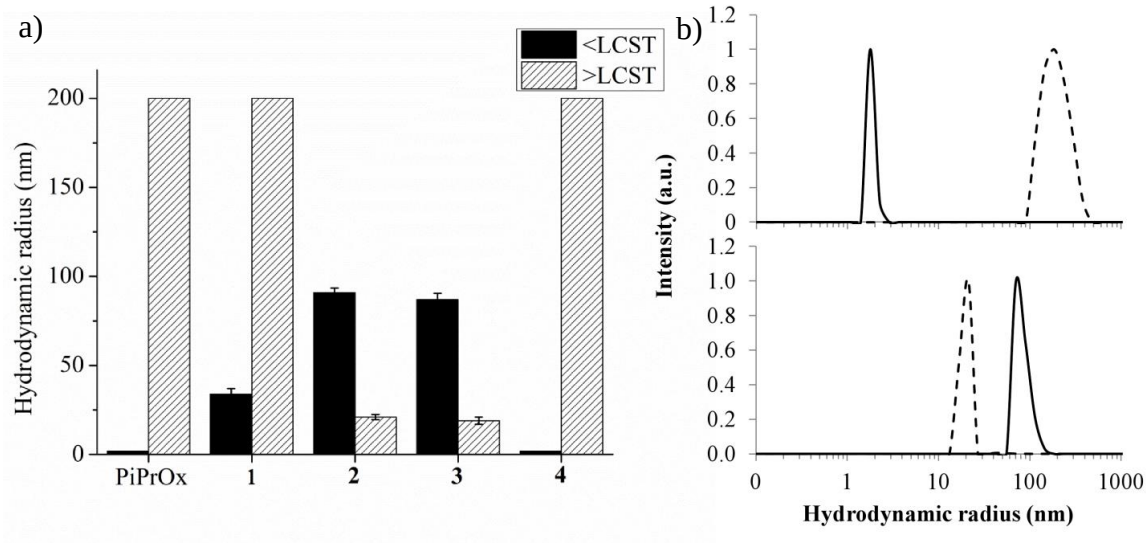

Figure 3.5 a) Histogram showing the average hydrodynamic radius below (black columns) and above the LCST (grey columns). b) Examples of DLS showing the hydrodynamic radius below (continuous line) and above the LCST (dotted line) of **4** (top) and **3** (bottom).

3.2.1.4 Critical micelle concentration studies

To confirm the presence of aggregates suggested by DLS, we investigated the critical micelle concentration (CMC) exploiting the fluorescence properties of pyrene. It has been reported that the ratio between the first vibrational band (373 nm) and the third vibrational band (384 nm) (I/III) of pyrene is related to the hydrophobicity of the

environment where the pyrene molecules are contained. The decrease of I/III ratio is dictated by an increase in the hydrophobicity of the environment.[115]

A 0.25 mM stock solution of pyrene in methanol was prepared and further diluted 20 times. Concentrations of polymers ranging from 0.02 mM to 0.5 mM were dissolved in a constant volume of water (1 ml). 50 µl of the diluted pyrene solution was added to each sample and fluorescence was read using an excitation wavelength of 334 nm. Figure 3.6 shows the CMC of single component systems studied. The unfunctionalised polymer, in addition to **1** and **4** do not show a decrease in the I/III ratio, which give comparable values through the range of concentration studied. I/III ratio for **2** and **3** decreases with concentration forming a slope that was used to calculate the CMC, which is 0.2 mM and 0.205 mM for **2** and **3**, respectively. The similarity of the two values suggests that the nature of the colloidal structures formed is comparable. The initial and final I/III ratio agrees with values found in literature that indicate the presence of colloidal structures.[56] The shoulder at ~ 420 nm, which stays constant all through the experiments, is reported in literature as a semi-excimer,[116] *i.e.* when two phenyl rings are only partially developing interactions.

Table 3.2 shows the characteristics of single component systems studied.

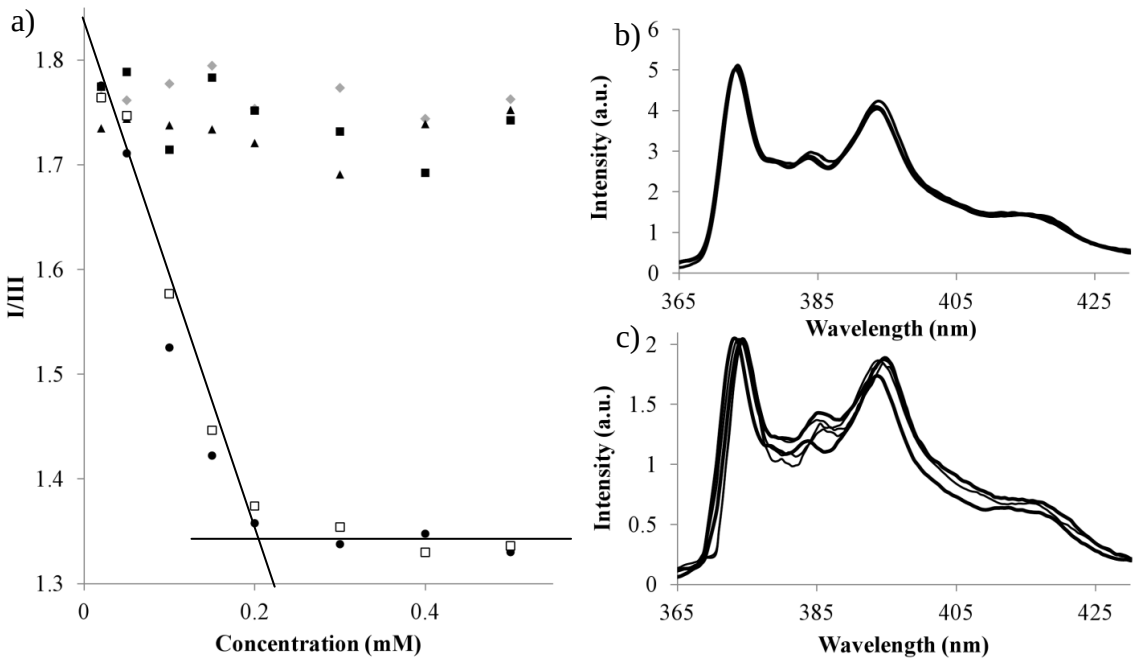

Figure 3.6 a) CMC of unfunctionalised polymer (■),**1** (■), **2** (□), **3** (●) and **4** (▲). Total volume of each sample 1.050 ml. b) Example of pyrene spectra where no changes are observed upon increase of polymer concentration (**4**). c) Example of pyrene spectra where I/III ratio decreases due to self-assembly (**3**).

Polymer	Functionalisation route	Functionalisation yield (%)	LCST (°C)	Radius (nm)		CMC (mM)
				< LCST	> LCST	
PiPrOx	/	/	51.5	1-2	>200	/
1	A	96	40.7	35-40	>200	/
2	B	/	37.7	80-90	15-20	0.20
3	A	94	31.4	75-85	15-20	0.21
4	C	93	39.2	1-2	>200	/

Table 3.2 Summary of characteristics of the single component systems studied.

3.2.2 Two-component Fmoc-amino acid functionalised PiPrOx systems

To provide further insight into the ability to produce multifunctional particle by mixing different functionalized polymers presented in Paragraph 3.2, we decided to mix the enzyme responsive polymers (**1**/**2**) with the other populations to see how the self-assembly properties, triggered upon the catalytic action of phosphatase, were affected. To this end, we mixed two populations of polymers: **1+3** and **1+4**, that, followed by the addition of 5 µl (50U) of enzyme, give **2+3** and **2+4** (Fig. 3.7). In this paragraph we aim to investigate different mechanisms to induce self-assembly of functionalised polymers. To this end, we tested both assemblies driven by electrostatics and aromatic or π- π stacking interactions.

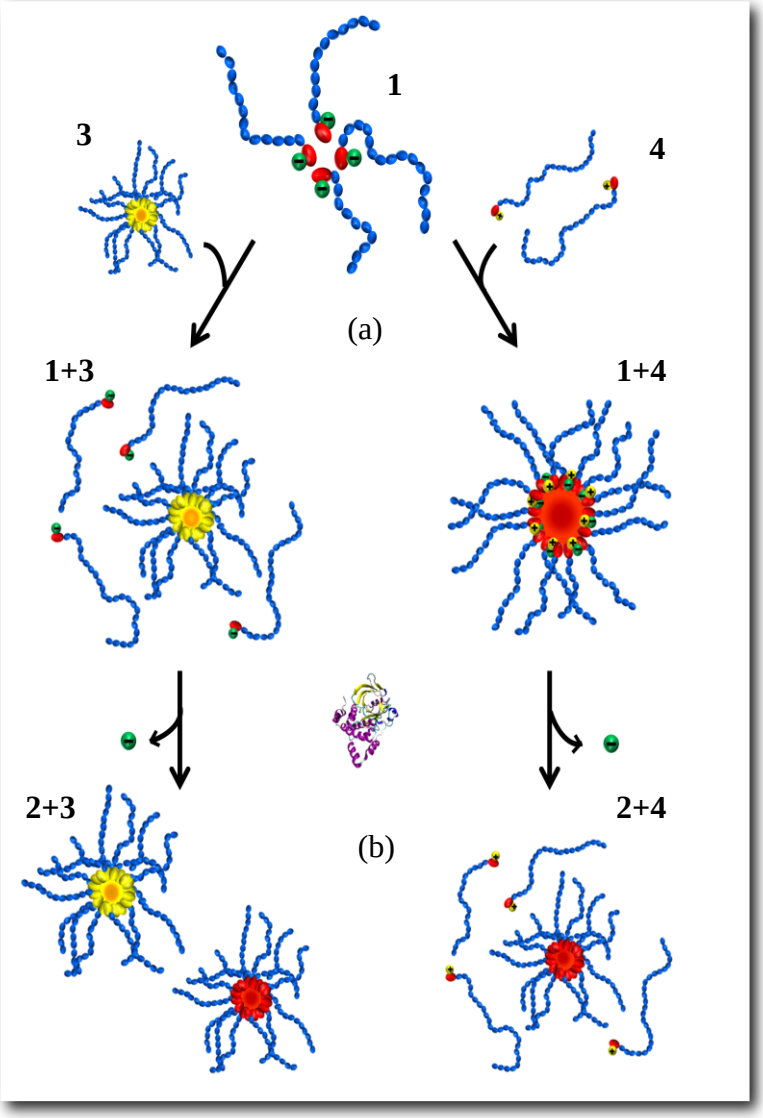

Figure 3.7 Schematic representation of self-assembly behaviour of dual component systems. a) When Fmoc-*p*Tyr-PiPrOx-OH (**1**) and Fmoc-Phe-PiPrOx-OH (**3**) are mixed, only **3** undergoes self assembly, while, when **1** and Fmoc-Lys-PiPrOx-OH (**4**) are mixed, both polymers self-assemble due to the contribution given by the opposite charges present on the amino acids. b) Upon enzymatic dephosphorylation of the tyrosine, Fmoc-Tyr-PiPrOx-OH (**2**) and **3** form distinct colloidal aggregates despite their chemical similarity, while **4** is expelled from the nanostructures which are now formed only by **2**.

3.2.2.1 Phase transition temperature studies

We proceeded to study the phase transition profiles of the dual component systems to investigate how the phase transition temperature was affected. All the LCST values observed were found to be the average of the two phase transition temperatures of the single component systems used in isolation. The total concentration was kept constant for all the LCST measurements, *i.e.* to achieve a 1 mg ml^{-1} concentration 0.5 mg of each polymer were dissolved in the solution. The cloud point temperature was found to be 36.4°C and 40.5°C for the dual systems before dephosphorylation (**1+3** and **1+4**, respectively), decreasing by roughly 2°C after enzymatic reaction (Fig. 3.8, Table 3.3). The decrease of the phase transition temperature shows that dephosphorylation is still taking place.

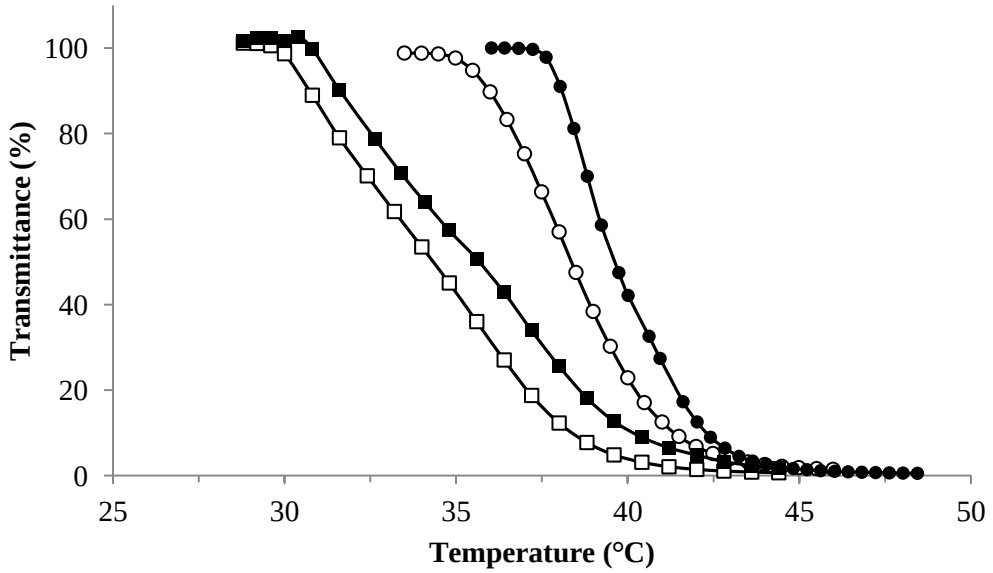

Figure 3.8 Cloud point behaviour of **1+3** (■), **2+3** (□), **1+4** (●) and **2+4** (○). (Polymer concentration used=1 mg ml^{-1}).

3.2.2.2 Dynamic light scattering studies

We used DLS to assess whether the mixed polymers were forming colloidal structures (Fig. 3.9). All systems investigated showed the presence of colloidal structures in the range of 90-135 nm at room temperature. This behaviour was expected for all the systems containing at least one population that undergoes self-assembly, *i.e.* **1+3**, **2+3**, **2+4**, as shown in Paragraph 3.2. The self assembly behaviour of **1+4**, which gives large aggregates, is probably driven by the opposite charges present on the *p*Tyr and Lys side chains.

Above the phase transition temperature the average particle size of all the systems decreases. In the case of **2+3** and **1+4** the PiPrOx chains forming the corona-like structure of the aggregates precipitates around the cores formed by Fmoc-amino acid interactions. **1+3** and **2+4** have only one component forming aggregates while the population not taking part to structure formation is monodisperse in solution. Upon heating **1** and **4** precipitate around the core formed by **3** and **2**, respectively, explaining the increased particle size above phase transition temperature.

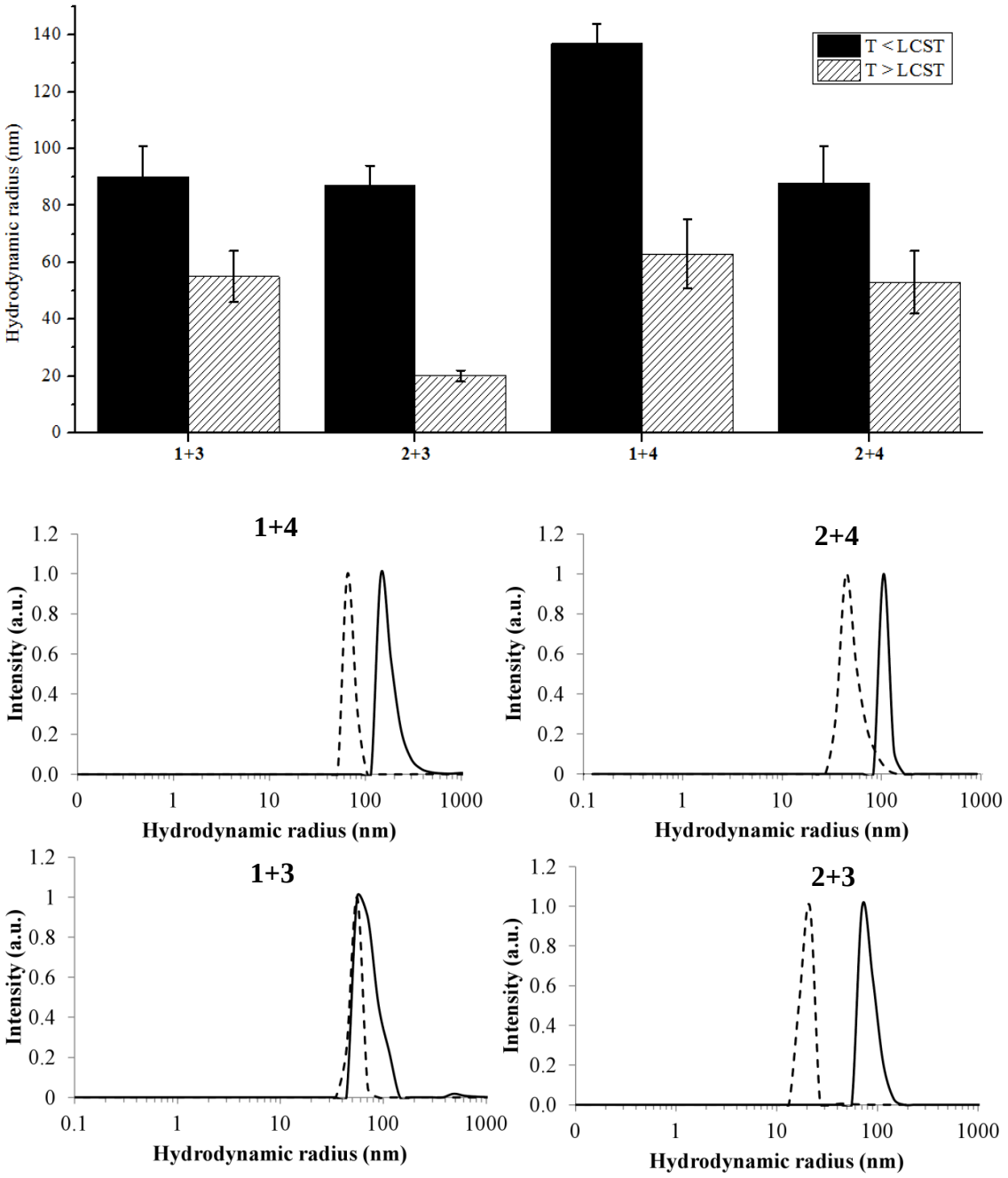

Figure 3.9 (Top) Histogram showing the average hydrodynamic radius below and above the cloud pint temperature. (Bottom) Examples of DLS data showing the hydrodynamic radius below (continuous line) and above the phase transition temperature (dotted line) of two component systems.

3.2.2.3 Critical micelle concentration studies

The CMC was determined using the same parameters used for the single component system and it gives useful indications about the structures of colloidal aggregates formed (Fig. 3.10, Table 3.3). **2+3** has the lowest CMC value (0.2 mM) which is comparable to the value obtained for **2** and **3** separately. **1+4** has a slightly higher CMC of 0.22 mM, which can be explained by the different nature of the interactions that lead to self assembly and by the presence of the charges that make the environment inside the aggregates slightly less hydrophobic. The two remaining systems, **1+3** and **2+4** have a CMC profile which is almost identical, suggesting that only one of the two polymer populations is taking part to the aggregate structures since the CMC value (0.34 and 0.35 mM, respectively) is much higher than that found for **3** and **1** alone.

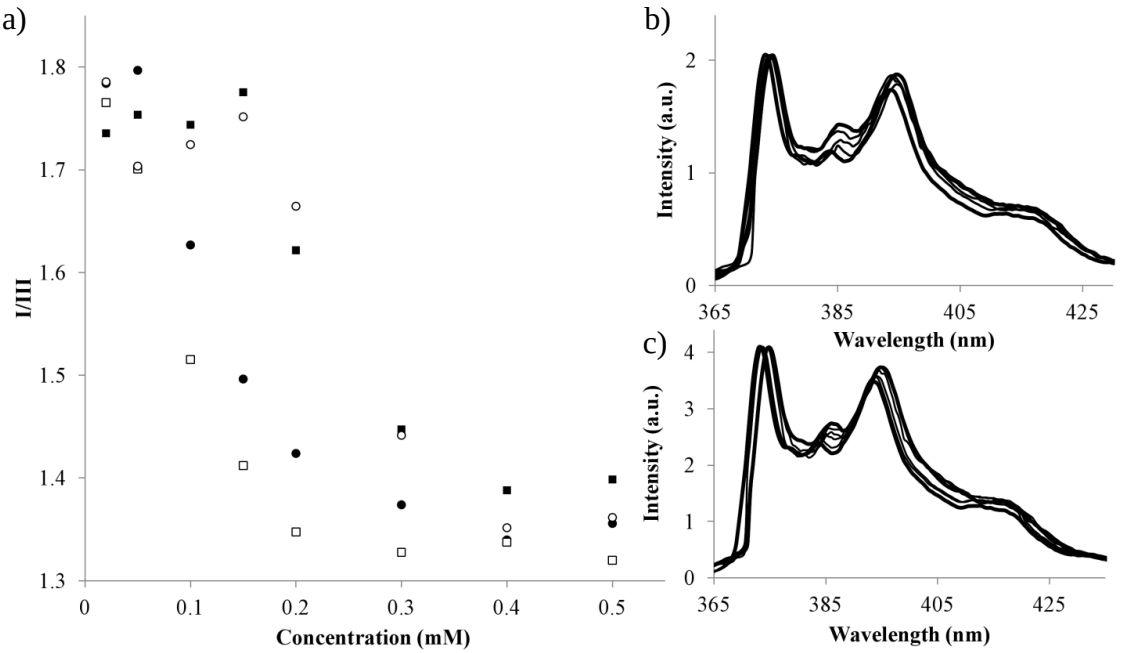

Figure 3.10 CMC of **1+3** (■), **2+3** (□), **1+4** (●) and **2+4** (○).Total volume of each sample 1.050 ml. b) Example of pyrene spectra where I/III ratio decreases at lower polymer concentrations (**2+3**). c) Example of pyrene spectra where I/III ratio decreases at higher polymer concentrations (**1+3**). The CMC value was calculated as shown in Figure 3.6.

Polymer	LCST (°C)	Radius (nm)		CMC (mM)
		< LCST	> LCST	
1+3	36.4	91	56	0.34
2+3	36.6	89	20	0.20
1+4	40.3	136	63	0.22
2+4	38.8	92	53	0.35

Table 3.3 Summary of characteristics of the dual component systems studied.

3.2.2.4 Kinetic and microscopy studies

We managed to achieve a system, which would be favourable for drug delivery application only in the case of **1+4→2+4**, as there is an actual change and composition in the nanostructure morphology that would allow to encapsulate a payload molecule releasing it upon the shrinkage of the colloidal aggregate. Since such a system looked promising we decided to investigate the kinetics and the nanostructure morphology achieved.

To monitor the kinetic of the self-assembly process, we followed the reaction through fluorescence exploiting the fluorescence intensity of Fmoc at 305 nm (Fig. 3.11). Upon mixing of Fmoc-*p*Tyr-PiPrOx + Fmoc-Lys-PiPrOx the fluorescence slowly decreases, reaching a stable fluorescence profile after 24 hours. *Vice versa*, upon addition of the enzyme we noticed a slow increase in the Fmoc peak intensity, which reached a stable value after 24 hours. We think that the fluorescence intensity of Fmoc is directly related to its self-assembly state. When it decreases it suggests a higher structural order. We believe that the fluorescence increase after enzymatic addition is related to the expulsion of Fmoc-Lys-PiPrOx from the aggregates. The kinetics show a slower self-assembly behaviour, compared to that previously found for Fmoc-*p*Tyr-PiPrOx where the self assembly process was completed within 3 hours (Chapter 2). This behaviour can be explained by a higher degree of complexity of the colloidal aggregates formed.

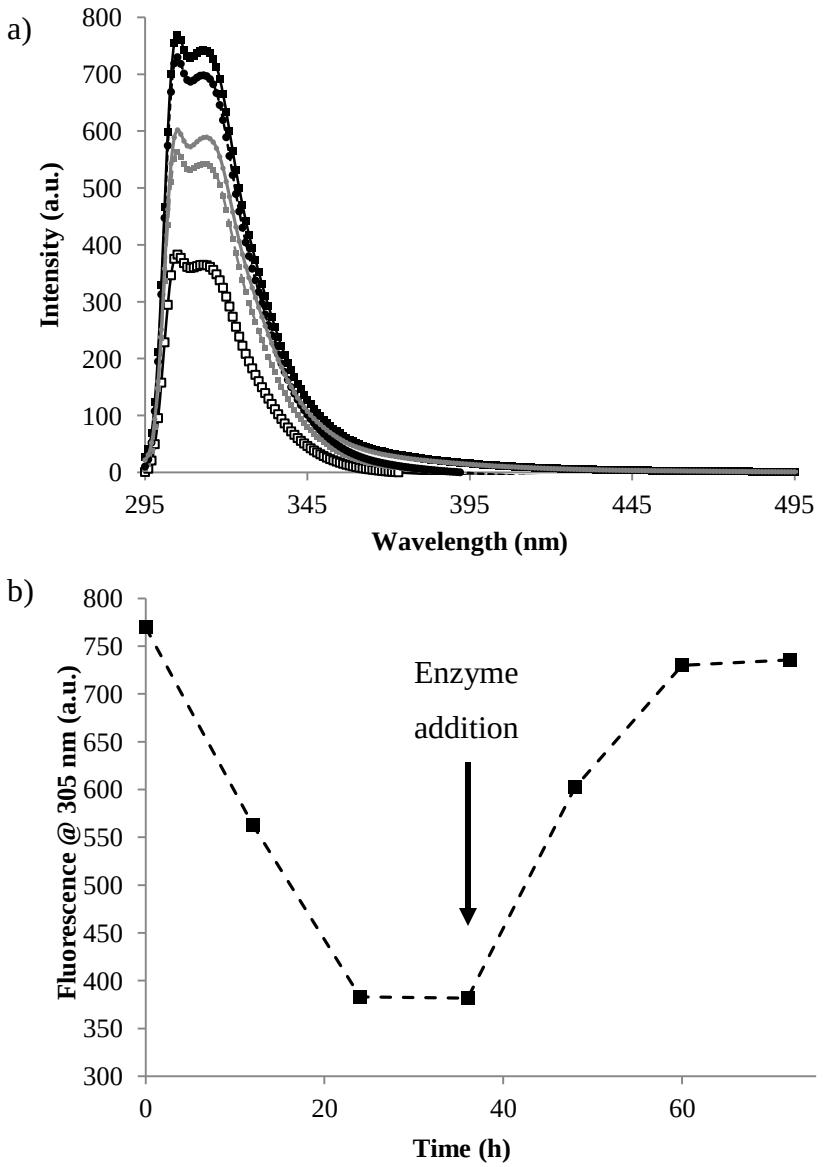

Figure 3.11 1+4→2+4 self-assembly kinetics followed by fluorescence exploiting the Fmoc peak at 305 nm. a) Dissolution of the polymers (■), 12 hours incubation (■), 24 hours incubation, enzyme addition (□), 12 hours after enzyme addition (●), 24 hours after enzyme addition (●); b) Fmoc intensity @ 305 nm plotted against time (Enzyme addition at 36 hours).

Atomic force microscopy (AFM) was run to assess the size and the dimensions of the colloidal aggregates found. Unfortunately, the sample preparation, which consists of

drying a solution of polymers on a small surface, seems to have a critical effect on the size of our system (Fig. 3.12). Spherical aggregates with a diameter in the µm order are noticeable both for **1+4** and **2+4**, even if smaller aggregates are present only after enzymatic reaction. Nevertheless, the shape of the nanostructures showed by AFM agrees with the formation of spherical aggregates.

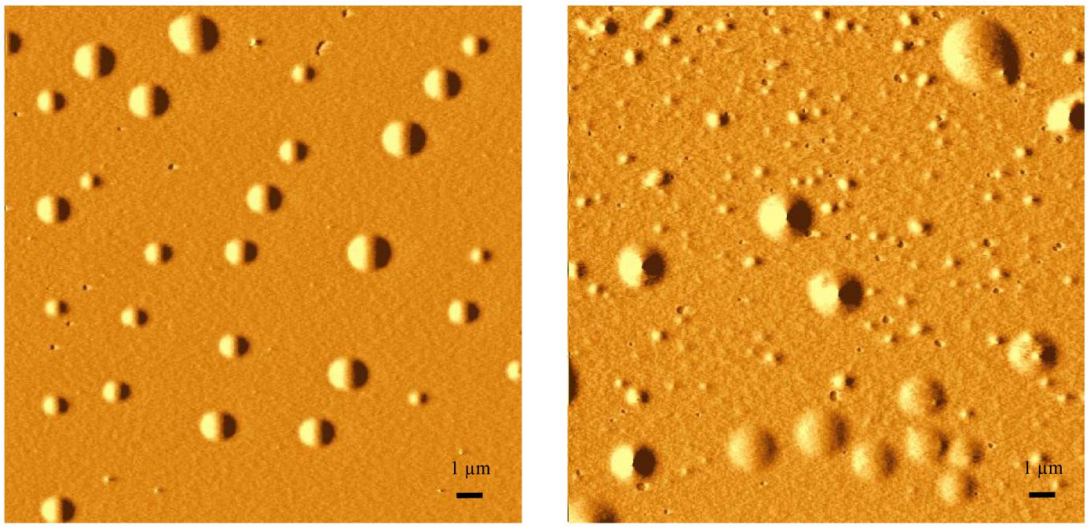

Figure 3.12 AFM images showing aggregates formed by **1+4** (a) **2+4** (b).

3.3 Conclusions

We report a modular approach to achieve compartmental systems that can be selectively triggered upon catalytic action of phosphatase, achieving reconfiguration of the nanostructures formed. Functionalising PiPrOx with different Fmoc-amino acid, we can dictate the morphology and temperature responsiveness of self-assembly tailoring the dimension of structure formed. We studied four different amino acids having different characteristics that drastically influence the self-assembly behaviour of the system. As shown, amino acids provide a powerful toolbox and the characteristics provided by other amino acids still remain to be explored.

The novelty introduced in this chapter by combining two different populations of polymers gives a further insight to how the self assembly process is influenced and characterized by the properties of each amino acid. Moreover, the straight forward synthetic strategy used, combined with the advantages provided by the Fmoc molecule, makes this system useful to build a platform that can be used for systematic studies on modular compartmental systems. Fmoc has been used for its self-assembly and fluorescence properties but we envisage that it could be replaced by a more biocompatible aromatic functionality still able to develop interesting self-assembly interactions through π-π stacking, e.g. fully peptidic self-assembly moieties. The development of such a system could lead to application in the drug delivery field due to the low cytotoxicity profiles showed by POx family[117] and the "switchability" introduced by enzyme catalysis.

3.4 Materials and methods

Materials 2-Isopropyl-2-oxazoline (iPrOx, Tokyo Chemical Industry) was stirred overnight with calcium hydride (CaH_2), vacuum distilled and stored under nitrogen atmosphere. Alkaline phosphatase from calf intestine mucosa (New England BioLabs, 10.000 U ml^{-1}, one unit is defined as the amount of enzyme that hydrolyzes 1μmol of pnitrophenylphosphate to p-nitrophenol in a total reaction volume of 1 ml in 1 ml at 37°C), propargyl p-toluenesulfonate (Fluka), 11-azido-3,6,9-trioxaundecan-1-amine (Aldrich), anhydrous N,N-dimethylformamide (DMF, Aldrich), O-(Benzotriazol-1-yl)-N,N,N′,N′-tetramethyluronium hexafluorophosphate (HBTU, Aldrich), N,N-Diisopropylethylamine (DIPEA, Aldrich), 3.5 kDa regenerated cellulose membrane (Triple Red Ltd), 500 Da cellulose acetate membrane (Aldrich), anhydrous acetonitrile (ACN, Aldrich), tetrahydrofuran (THF, Aldrich), fluorenylmethoxyloxycarbonyl-phosphorylated tyrosine (Fmoc-*p*Tyr-OH, Aldrich) fluorenylmethoxyloxycarbonyl-lysine (tert-butyloxycarbonyl) (Fmoc-Lys(Boc)-OH, Aldrich), trifluoroacetic acid (TFA, Aldrich) fluorenylmethoxyloxycarbonyl-phenylalanine (Fmoc-Phe, Aldrich) were used as received.

Instrumentation Fluorescence studies were performed on a Jasco FP-6500 spectrofluorometer. UV/Vis absorbance was measured on a Beckman Coulter DU 800 spectrophotometer equipped with a Beckman Coulter High Performance Temperature Controller. DLS was performed on an AVL/LSE-5004 light scattering electronics and multiple tau digital correlator using an angle of 90°. ALV-Laser software was used to analyze the data and all sizes reported here were based on weight number. MALDI-TOF mass spectrometry was performed on a Kratos Analytical AXIIMA CFR using dithranol matrix. High performance liquid chromatography (HPLC) was carried out on a Dionex P680 HPLC system fitted with a UVD170U detector. An aliquot sample (50 μl) was injected into a Macherey-Nagel C18 column of the following dimensions: length 250 mm; internal diameter 4.6 mm; particle size 5 μm; flow rate 1 ml min^{-1}. Atomic Force Microscopy (AFM) was performed on a Veeco Innova Scanning Probe Microscopy. The

tip was a Phosphorous doped Si tapping mode tip and the instrument was operated in tapping mode. Images were processed using a 2D plane fit using the software included in the instrument.

3.4.1 Polymer synthesis and characterization

Polymerisation Polymerisation of iPrOx was performed following a procedure reported in literature.[94] Microwave vials (2.0-5.0 ml) were left in a heating oven (125 °C) and cooled down to room temperature under nitrogen atmosphere. A solution containing 0.067 mmol of propargyl p-toluenesulfonate and 4 mmol of iPrOx was made directly in the microwave vial under nitrogen atmosphere and under stirring using AcN as the solvent. Total reaction volume was 3 ml. The vial was capped, and heated at 140 °C for 11 minutes. After the reaction, excess of H_20 was added to the vial, and the solution was extensively dialyzed against water for 3 days. After dialysis the solution was freeze-dried.

3.4.2 Synthesis and characterisation of Fmoc-amino acids bearing terminal N_3

Synthesis Synthesis of Fmoc-*p*Tyr bearing a terminal azide group was performed using a standard coupling procedure. The carboxylic terminus of Fmoc-*p*Tyr was activated using 2 eq. of HBTU and DIPEA in DMF/DCM (1:1). A solution containing 1 eq. of 11-azido-3,6, 9-trioxaundecan-1-amine in DMF/DCM (1:1) was added to the activated the amino acid**.** The reaction lasted overnight under rotation. The dialysis, which was followed from freeze-drying, was performed with a membrane of regenerated cellulose (500 Da molecular weight cut off).

Characterisation The purity of the obtained compound after the purification process was assessed by HPLC (initial flow rate 40% H_2O, 60 % ACN) dissolving 0.2 mg of

Fmoc-*p*Tyr-OH in 1 ml of ACN/H_2O (1:1 ratio), as a control experiment, and the same amount of Fmoc-*p*Tyr-N_3 complex (Fig. 3.13).

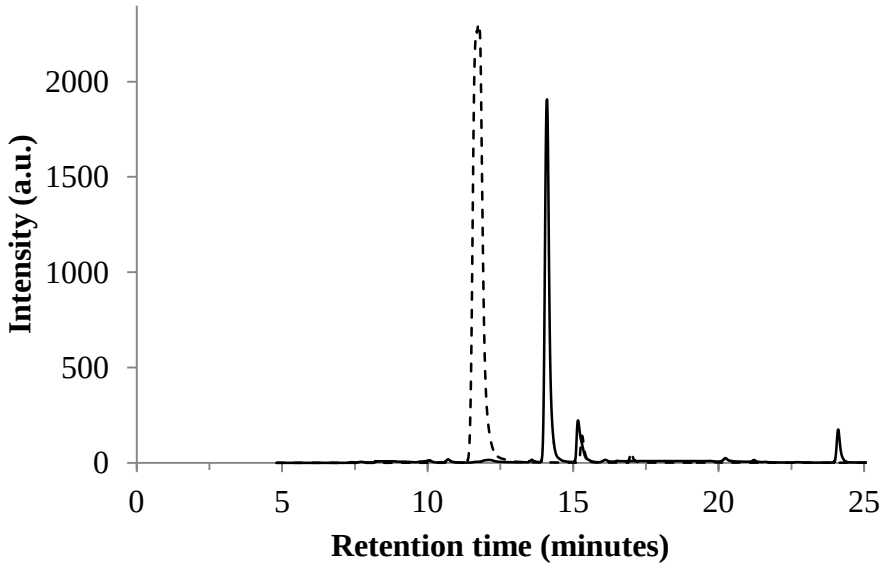

Figure 3.13 HPLC graph showing Fmoc-*p*Tyr (dotted line) and Fmoc-*p*Tyr-N_3 (continuous line) retention time. Purity = 93%.

Synthesis Synthesis of Fmoc-Lys(Boc)-OH bearing a terminal azide group was performed using a standard coupling procedure. The carboxylic terminus of Fmoc-Lys(Boc)-OH was activated using 2 eq. of HBTU and DIPEA in DMF. A solution containing 1 eq. of 11-azido-3,6,9-trioxaundecan-1-amine in DMF was added to the activated amino acid**.** The reaction lasted overnight under rotation. The dialysis, which was followed from freeze-drying, was performed with a membrane of regenerated cellulose (500 Da molecular weight cut off).

Removal of Boc protecting group was performed using a solution of TFA/H_2O (1:4 ratio). The reaction lasted overnight and the solvents were removed using a vacuum pump. A cycle of dialysis and freeze drying followed.

Characterisation The purity of the obtained compound after the purification process was assessed by HPLC (initial flow rate 40% H_2O, 60 % AcN) dissolving 0.2 mg of Fmoc-Lys(Boc)-OH in 1 ml of ACN/H_2O (1:1 ratio) , as a control experiment, and the same amount of Fmoc-Lys(Boc)-N_3 complex (Fig. 3.14).

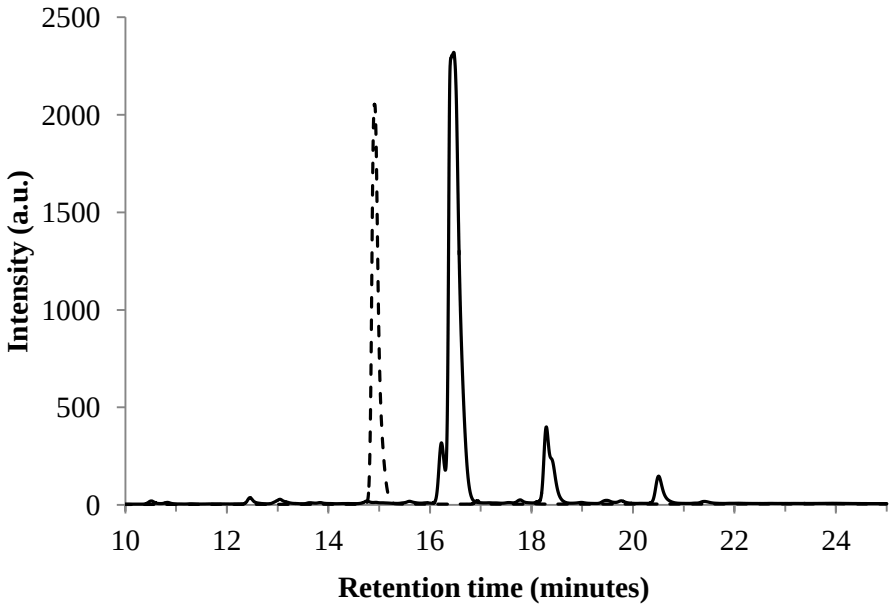

Figure 3.14 HPLC graph showing Fmoc-Lys(Boc)-OH (dotted line) and Fmoc-Lys(Boc)-N_3 (continuous line) retention time. Purity = 87%.

After deprotection the Fmoc-Lys-N_3 was analyzed through MS to check the reaction was successful (Fig. 3.15).

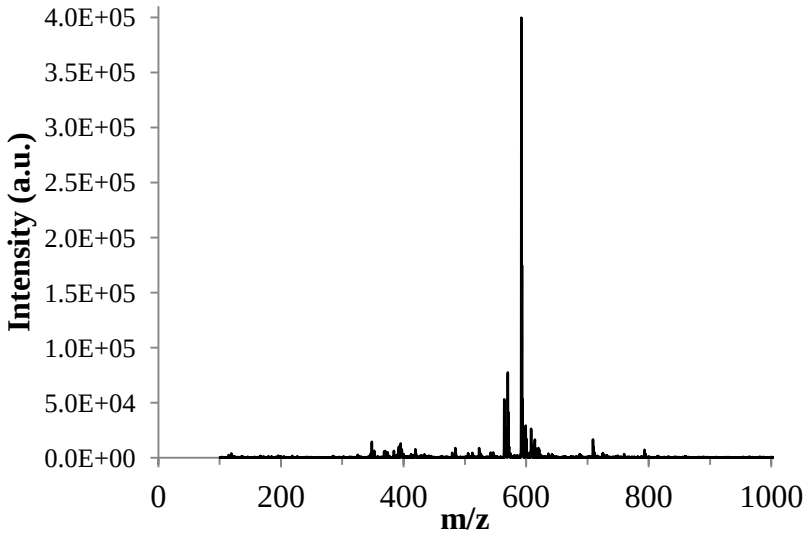

Figure 3.15 MS showing molecular weight profile of purified Fmoc-Lys-N_3. The main peak has a value of 592 corresponding to the sodium adduct of Fmoc-Lys-N_3 ([M]=569).

3.4.3 "Click" coupling

Please refer to Paragraph 2.4.3

3.4.4 Experimental

Please refer to Paragraph 2.4.4.

4. Peptide-based hydrogels for pheromone controlled release

4.1 Introduction

Insect pheromones are intraspecific semiochemicals that can be used in direct and indirect control against moths. Pheromones offer a number of advantages compared to the use of traditional chemical pesticides, *i.e.* they are specie-specific, environmentally friendly, not toxic to other insect species/animals, they do not induce resistance. Despite many challenging issues that still need to be resolved, *i.e.* higher costs compared to chemical pesticides, unsuitability to certain weather conditions, specific systems required that are matched to each kind of plant, it is a field that generates increasing interest.[118]

Semiochemicals are natural products produced by organisms that provide information either intraspecifically (pheromones) or interspecifically (allelochemicals) to the benefit or detriment of the individual. They provide information that is ecologically important to organisms and can control their behaviour.[119] As such, they offer an environmentally benign method to combat insect pests of arable crops or human health by altering behaviour to human advantage. Semiochemicals may also act as signals which switch on the chemical defences of plants in response to a pest or pathogen so by timely introduction can prepare or prime plants against attack. Semiochemicals are small lipophilic molecules and are mediated either through the air as volatile chemicals or through the soil rhizosphere both as volatile and non-volatile signals. Their detection and transfer to olfactory neurones in insect olfactory sensilla involves transport across an aqueous medium, the mechanism of which is unknown though involves olfactory binding proteins.[120] To improve the application of semiochemicals in the field it is

important to find formulations for dispensing volatile chemicals and study their movement in aqueous environments, whether it is soil water or insect antennae.

We propose to exploit the advantages of biomolecular gels based on aromatic peptide amphiphiles[48,121] to enhance the controlled release of pheromones by creating a gel that can release host molecules over time. The advantages of this system would increase the stability and durability of pheromone release formulation. The gel, which may be designed from components that interact non-covalently with active molecules that are volatile, hydrophobic and often sensitive to oxidation. By varying their molecular structure their ability to entrap water may be tailored to match weather conditions (heat and drought) that can often compromise the efficacy of the treatment.

Our group recently reported a phosphorylated peptide derivative (Fmoc-Phe-*p*Tyr), that forms micelles and upon dephosphorylation form stable, self-sustained hydrogels.[44] We hypothesised that adding pheromones to the phosphorylated dipeptide solution, they would be trapped in the hydrophobic core of the micelles, preventing evaporation. Upon phosphatase catalysis, the micelles turn into fibres expelling the pheromones due to the self assembly interactions developed among the Fmoc-dipeptide molecules and trapping the pheromones in the hydrogel's aqueous part. This mechanism would allow to have a constant release of pheromones along with water evaporation (Fig. 4.1). Moreover, this system could potentially be tailored by varying the composition of the hydrogel or by making multi-layer hydrogels where the pheromone is not equally present.

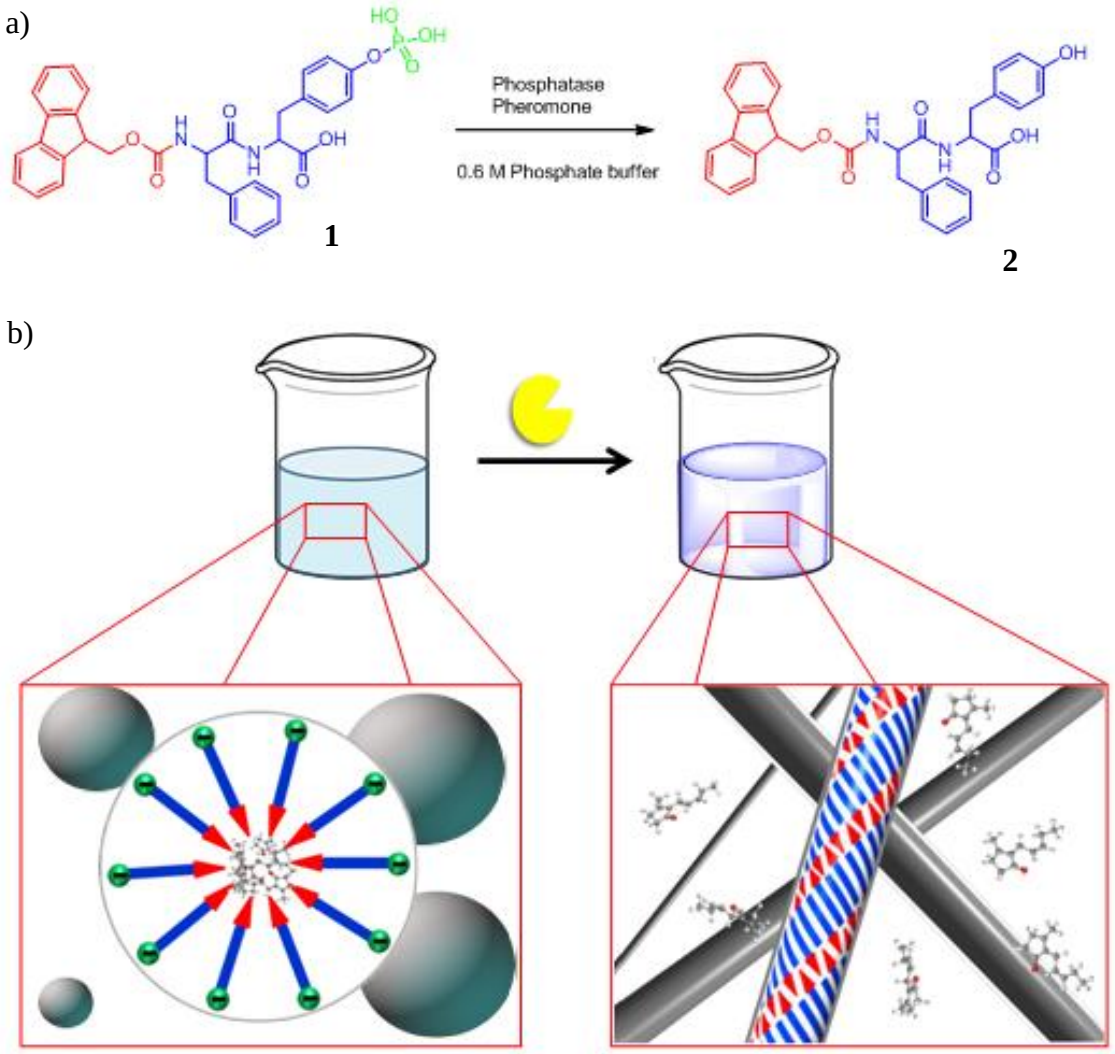

Figure 4.1 a) Fmoc-Phe-*p*Tyr dephosphorylation mechanism. Upon phosphatase catalytic activity Fmoc-Phe-*p*Tyr (1) is dephosphorylated becoming Fmoc-Phe-Tyr (2). b) Proposed mechanism for the controlled release of pheromones. When micelles are present, pheromone molecules hide into the hydrophobic cores (left), while, upon fibre formation, the pheromones are expelled and trapped in the hydrogel aqueous part (right).

In order to assess how pheromone presence would influence gel formation, we decided to start the study with two different pheromones: cis-jasmone, a volatile hydrophobic molecule, and isovitexin, a non-volatile hydrophilic molecule.

Cis-jasmone (Fig. 4.2a) has been has been firstly reported at Rothamsted Research.[122] It is a semiochemical that has a role in plant defence and occurs naturally in flower volatiles but can also be produced by damaged plants.[123] The production of this particular pheromone by damaged tissue could be a signal to alert neighbouring plants of being attacked by phytophagous insects in order to enhance their defensive response to pests.[124] This process is called priming: primed plants exhibit a higher and faster level of protection mechanisms.[125] Moreover, other effects are attributed to cis-jasmone, e.g. to attract beneficial insects[126] and to induce antibiotic effects.[127]
The major issue with treating plants with cis-jasmone is that the effect is not prolonged, *i.e.* the pheromone is applied and, due to its highly volatile nature several applications are needed, making it hard to achieve a long lasting effect. Creating a formulation that would allow a controlled release on a longer time scale would probably enhance cis-jasmone effect on plants.[6]

Isovitexin (Fig. 4.2b) belongs to a family of molecules called flavonoids, that are biosynthesised by plants. Flavonoids are thought to have a number of functions within the plant biological pathways,[128] the main one may be as a UV shield.[129] Moreover, flavonoids have been investigated as medical resources, e.g. antioxidant and antitumoral.[130] In particular isovitexin is known to promote root and seed growing.[131] It has been chosen due to the presence of phenyl groups that could help incorporation into the gel fibres as well for its hydrophilic features that could help dissolution in aqueous environment.

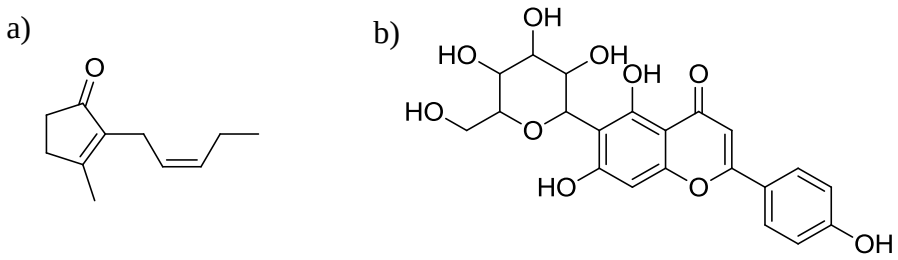

Figure 4.2 Chemical structure of cis-jasmone (a) and isovitexin (b).

4.2 Results and discussion

4.2.1 Preliminary studies

Different concentrations of Fmoc-Phenylalanine-phosphorylated Tyrosine (Fmoc-Phe-*p*Tyr) (3, 10 and 20 mM) were dissolved in 1 ml of phosphate buffer 0.6 M. Different concentration of cis-jasmone (0.54-3.3 mg) were suspended in the samples. 1 equivalent of cis-jasmone was added to sample 3FY, 10FY, 20 FY, while 1 μl was added to 20FY-1.

Only one sample of isovitexin containing hydrogel was made due to the low availability of the pheromone. 0.1 mg of isovitexin was added to a sample containing 10 mM of Fmoc-dipeptide.

Two controls (3 and 20 mM) were made without the addition of cis-jasmone to monitor the gelation time and to confirm its reliability at low and high peptide concentrations.

Finally, 5 μl of phosphatase (50 U) were added to all the samples, including the controls. All the sample vials were capped, sealed and left at room temperature. After 4 days the lids were removed and the samples were weighed. Sample names were given according to composition and are indicated in Table 4.1.

Sample name	Peptide concentration (mM)	Pheromone added	Enzyme added (µl)	Pheromone added (µm)	Gelation time (days)*
3 CONTROL	3	/	5	/	<1
20 CONTROL	20	/	5	/	<1
3 FY	3	CIS-Jasmone	5	2.86	13
10 FY	10	CIS-Jasmone	5	9.53	13
20 FY	20	CIS-Jasmone	5	19.03	13
20 FY-1	20	CIS-Jasmone	5	5.72	8
10 FY-ISO	10	Isovitexin	5	0.23	<1

***** The gelation time value is referred to the sample state after the lid is removed and it is left in contact with air.

Table 4.1 Composition of sample prepared for the preliminary study.

After the addition of the enzyme only the controls and 10FY-ISO formed self-sustained gels within a day. While the controls were clear, 10FY-ISO formed a yellow gel due to the presence of isovitexin. 3FY and 10FY turned to a turbid solution after one day of incubation while 20FY turned turbid after three days (Fig. 4.3).

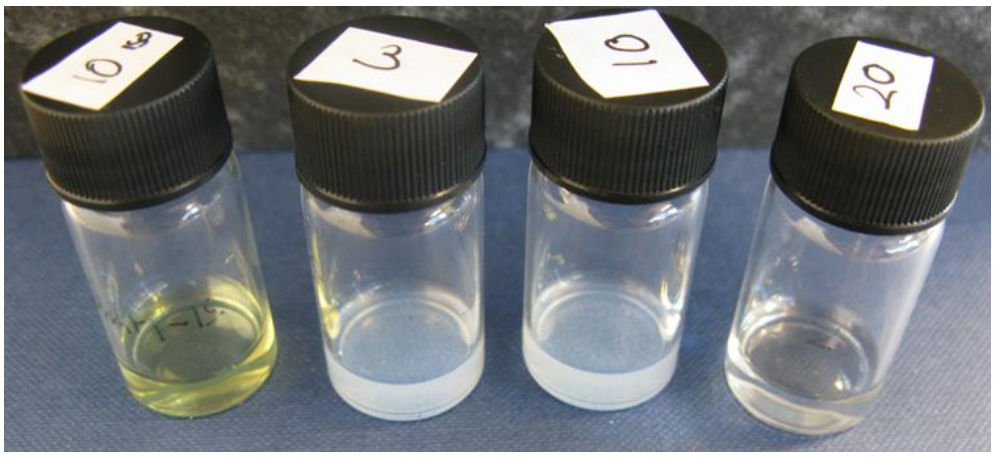

Figure 4.3 FY-ISO, 3FY, 10FY, 20FY (from left to right) after one day of incubation at room temperature.

After four days of incubation, all the samples except the controls and 10FY-ISO, appeared as a viscous, turbid solution (Fig. 4.4).

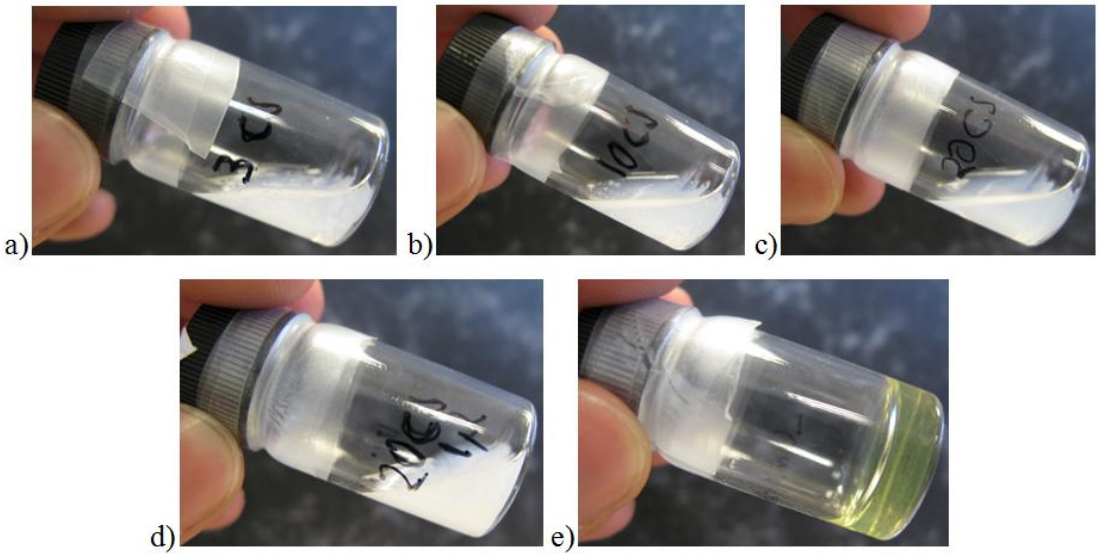

Figure 4.4 Samples after 4 days of incubation at room temperature. a) 3FY, b) 10FY, c) 20FY, d) 20FY-1, e) 10FY-ISO.

After the fourth day of incubation, the lids were removed and the samples left in contact with air. Eight days following the removal of the lids, the situation was unchanged for all the samples except for 20FY-1, which formed a self-sustained gel (Fig. 4.5a), and 10FY, which shows the presence of white aggregates (Fig. 4.5b).

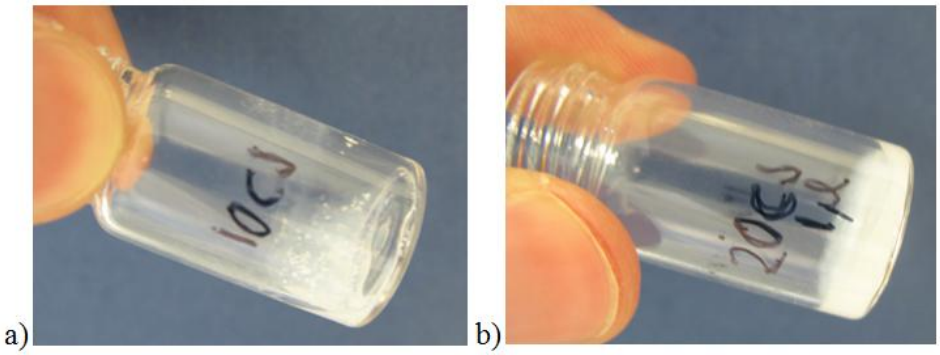

Figure 4.5 Samples after 8 days in contact with air. a) 3FY, b) 20FY-1.

After 13 days from the removal of the lids, all the samples formed gels (Figure 4.6). At this point, the water loss for each sample was around 90% (Fig. 4.7). Water loss is comparable for all the samples, whether they form gels or not, so we can assume that the gel formation does not alter the evaporation of water from the sample.

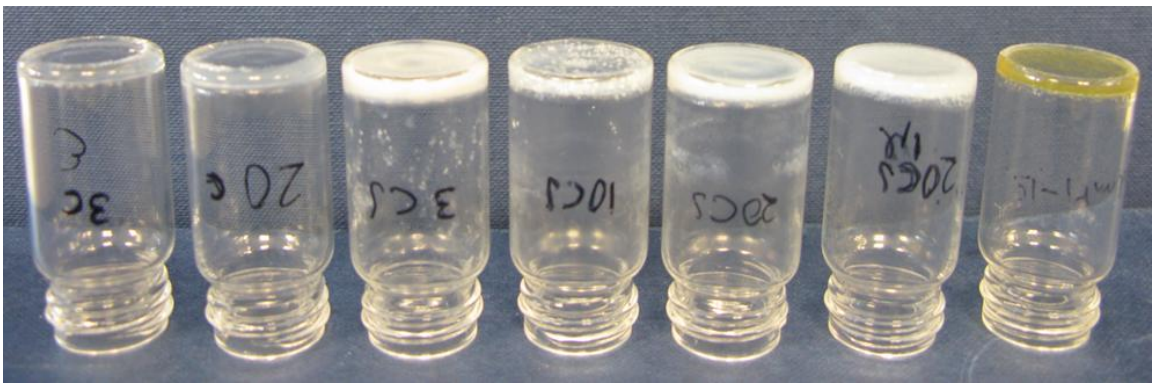

Figure 4.6 3CONTROL, 20CONTROL, 3FY, 10FY, 20FY, 20FY-1, 10FY-ISO (from left to right) after 13 days without lids.

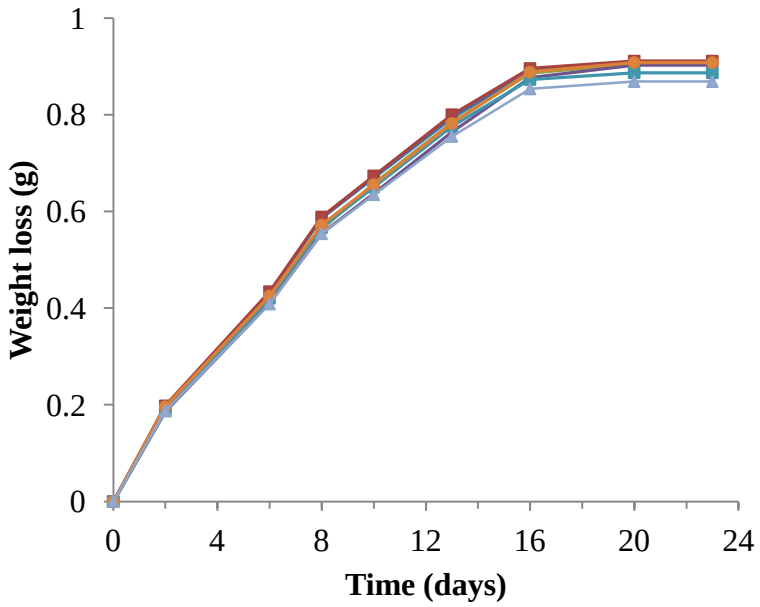

Figure 4.7 Weight loss due to water evaporation from samples. No samples have been notated due to the similar behaviour of weight loss profiles.

After three weeks there is no further loss of weight due to water evaporation. The dry samples look morphologically different even at a macroscopical level (Figure 4.8).

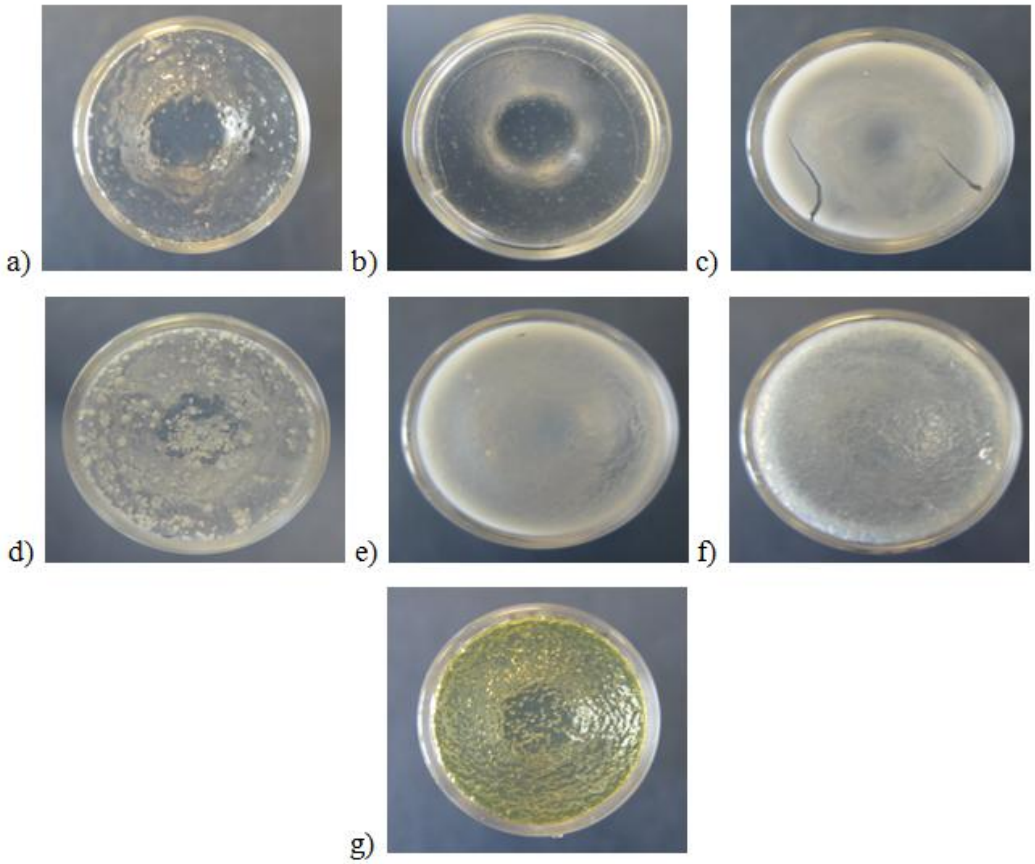

Figure 4.8 Picture of the bottom of the vials taken after 21 days. a) 3CONTROL, b) 20CONTROL, c) 3FY, d) 10FY, e) 20FY, f) 20FY-1, g) 10FY-ISO.

This preliminary study was merely done to observe how the hydrogel formation is affected by the presence of pheromones and to evaluate if the water evaporation rate is influenced by the peptide concentration. We decided not to pursue further the incorporation of isovitexin in the hydrogel due to its non-volatile behaviour and its

function, *i.e.* it would hardly develop towards an application. Moreover, due to its hydrophilic nature it is likely to be dissolved in the water layer of the gel for the whole process.

On the other hand, cis-jasmone, seemed either to interfere with gel formation or to be incorporated into the fibres matrix. In order to assess the role of cis-jasmone in hydrogel formation and its evaporation rate, we decided to run a time course experiment monitoring it through high performance liquid chromatography (HPLC).

4.2.2 Time course studies

To investigate whether the pheromone remains within the gel fibres, a new batch of samples with different concentration both of peptide and cis-jasmone were made. Two controls were made without the addition of the enzyme to monitor if the loss of pheromone was influenced by the micelles formed by Fmoc-Phe-*p*Tyr. Two peptide concentrations were used (20 and 30 mM) with a content of pheromone ranging from 0.47 to 2.35 mg ml^{-1}. Moreover, this batch was prepared on a 2 ml volume of buffer to further investigate the gelation and the water evaporation process (Table 4.2).

Figure 4.9 shows three examples of traces obtained through HPLC analysis that were used to assess the remaining pheromone in the hydrogel and the peptide conversion. The HPLC runs were calibrated in such a way to have a good separation between each peak and kept constant throughout the study. The remaining pheromone was calculated by the ratio of Area mA.U. (peptide)/Area mA.U. (cis-jasmone) and relating the obtained value with the initial one which was set as 100%. Similar calculation was made for the conversion, with the initial ratio of mA.U. Fmoc-Phe-Tyr/ Fmoc-Phe-*p*Tyr.

10-30 µl aliquots of sample were taken from different parts of the gel using a micropipette to assess volumetric reliability of the sample taken. The aliquot was then injected directly in an HPLC vial containing 1 ml of a solution of 1:1 ACN/H_2O + 0.1% TFA. To assess the reliability and avoid mistakes due to the non-homogenous

distribution of cis-jasmone in solution, each measurement was repeated two or three time, *i.e.* two or three aliquots were taken for each measurement and run individually. Nevertheless, some data points appear unreliable. Indeed, samples that form gels at earlier stages of the study (20/0.5, 30/0.5) present steady and reliable profiles, both for pheromone content and peptide conversion calculation.

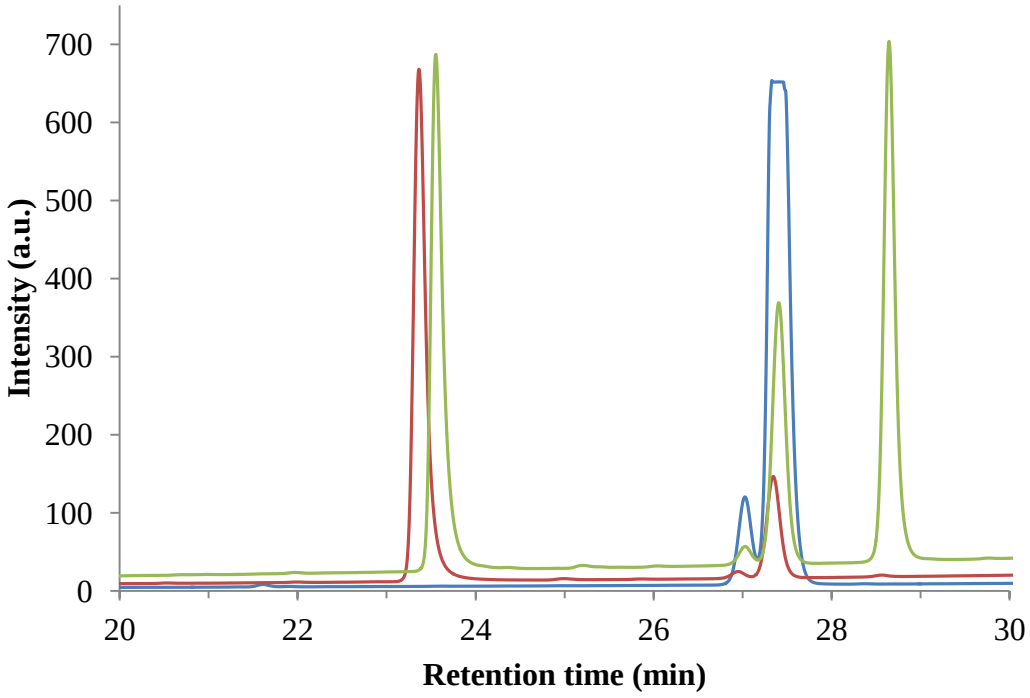

Figure 4.9 HPLC traces showing the retention time of cis-jasmone (blue line), Fmoc-Phe-*p*Tyr + cis-jasmone (red line) and dephosphorylated Fmoc-Phe-Tyr + cis-jasmone + phosphatise (green line, conversion ~50%). Peak legend: 23.5 min = Fmoc-Phe-*p*Tyr, 27.5 min = cis-jasmone, 28.75 min = Fmoc-Phe-Tyr. The shoulder visible at 27 min is probably trans-jasmone. Data were normalized due to different concentration used for the experiment.

Sample name	Peptide concentration (mM)	Enzyme added (µl)	Pheromone added (µm)	Gelation time (days)*
20 CONTROL	20	/	5.72	14
20/0.5	20	5	2.86	10
20/1.0	20	5	5.72	13
20/1.5	20	5	8.58	13
30 CONTROL	30	/	5.72	14
30/0.5	30	5	2.86	<1
30/1.0	30	5	5.72	13
30/1.5	30	5	8.58	13
30/2.5	30	5	14.3	13

* The gelation time value is referred to the sample state after the lid is removed and it is left in contact with air.

Table 4.2 Composition of the samples prepared for the time course study.

The 20 mM samples releasing profiles appear to be gradual only for 20/0.5, where the remaining pheromone signal after 24 days is 20% compared to the signal obtained when the pheromone was added to the sample. The other 20 mM samples, including the control, after 24 days have a pheromone content which is considerably higher (40-60%) (Fig. 4.10a). The conversion is between 60 and 70%, with small variations depending on the pheromone concentration (Fig. 4.10b).

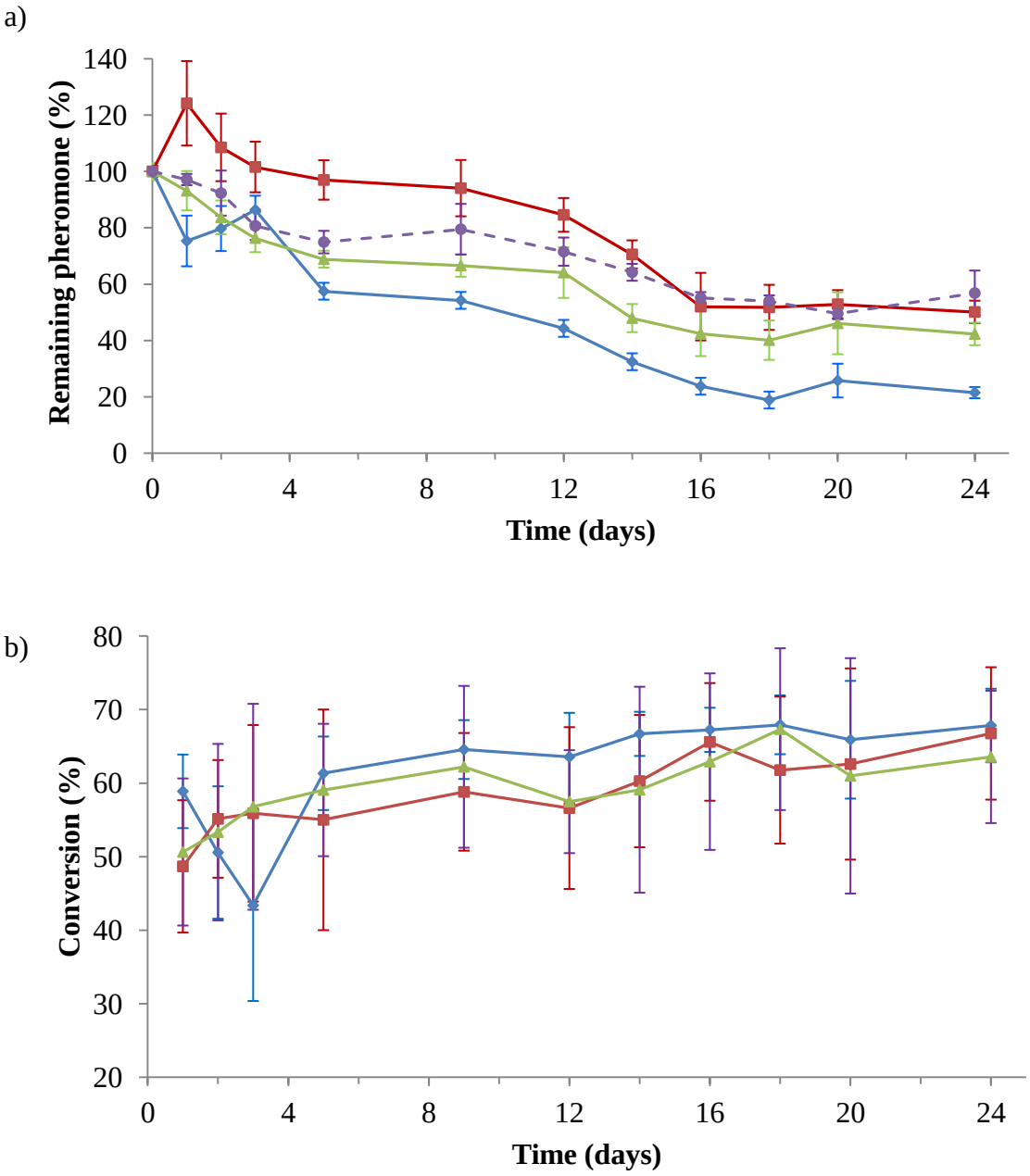

Figure 4.10 20 mM samples remaining pheromone concentration (a) and peptide conversion (b) plotted against time. 20/0.5 = ♦; 20/1.0 = ■; 20/1.5 = ▲; 20 CONTROL = ●, dotted line.

The 30 mM samples release profiles seem affected by the gelation time and the cis-jasmone concentration present in each sample. Only 30/0.5 has a neat release profile that reaches the same values of remaining pheromone found for 20/0.5 (~20%) (Fig. 4.11a). 30/2.5, the sample with the highest concentration of cis-jasmone, achieve the lowest conversion (~50%) (Fig. 4.11b), whereas, normally, samples prepared with the same peptide and enzyme concentrations reach conversion values above 90%. Similar values both for release and conversion are observed for 30/1.0 and 30/1.5.

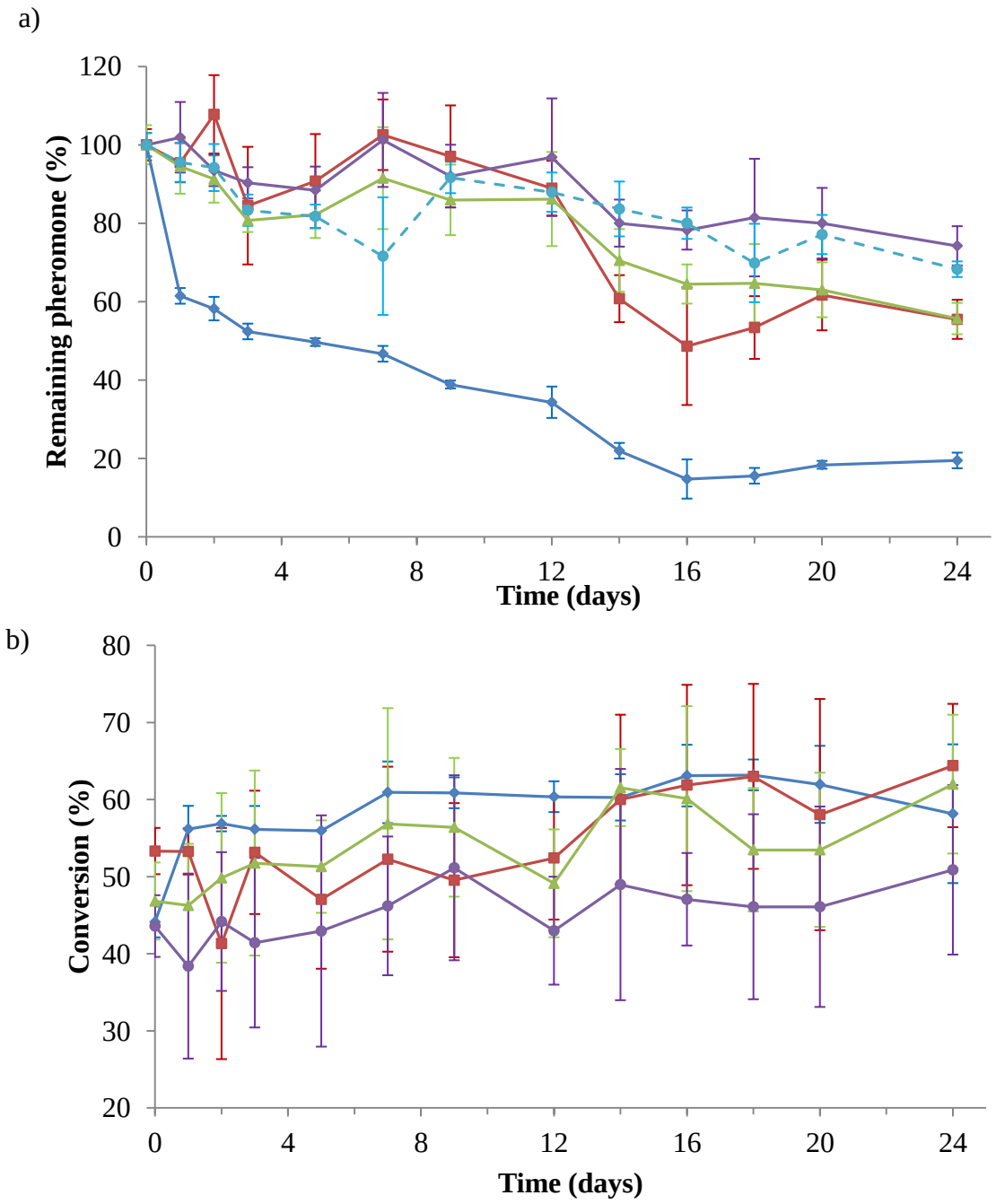

Figure 4.11 30 mM samples remaining pheromone concentration (a) and peptide conversion (b) plotted against time. 30/0.5 = ♦; 30/1.0 = ■; 30/1.5 = ▲; 30/2.5 = ♦; 30 CONTROL = ●, dotted line.

Observing the releasing profiles of both the controls, that have a remaining pheromone percentage very close to the samples with added enzyme, we can assume that the cis-jasmone is conserved inside the hydrophobic pockets of micelles and not released even after the complete evaporation of water. It appears that the release of the cis-jasmone is related to the gelation time of the sample, especially for 30/0.5, which gels after 36 hours of incubation and has a smooth release curve until it reaches a plateau after 16-18 days (Fig. 4.11a). A similar behaviour is noticeable for 20/0.5 even if the gelation takes place after 10 day by the removal of the lid (Fig. 4.10a). Overall, a lower conversion is directly related to higher pheromone content.

Water loss is comparable to what was found for previous samples (Fig. 4.12). A slight increase of water loss is noticeable for the control sample which contains only water, probably because the gel fibres trap some water preventing it from evaporating.

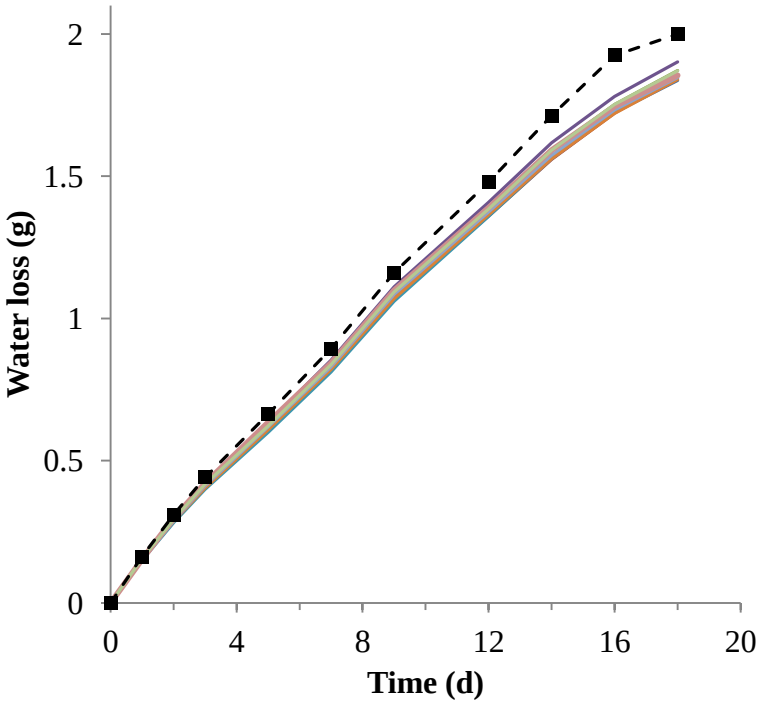

Figure 4.12 Weight loss due to water evaporation from samples. Only the water control (■, dotted line) has been marked due to the similar behaviour of the other samples.

4.2.3 Time course studies with higher enzyme concentration

To compensate for the incomplete conversion, we decided to increase the enzyme concentration added to each sample to check whether the pheromone acted as an inhibitor against phosphatase (Table 4.3). To this end, 20 µl of enzyme were added to each sample. Moreover, to make the system more appealing toward applications, we decide to add to the sample a higher amount of cis-jasmone, up to 4.7 mg ml^{-1}. Within 24 hours by enzyme addition all the samples gelled achieving excellent conversions in all the cases (> 95%). Compared to the hydrogels formed without the addition of cis-jasmone the samples appear milky, probably due to the presence of the suspended pheromone in the aqueous phase. An example of gelation achieved within 24 hours is showed in Figure 4.13.

The amount of enzyme added to the sample has been increased four times against an increase of pheromone addition of two to ten times. It cannot be excluded that the cis-jasmone inhibits the enzyme as the samples are equally affected by the pheromone concentration whether the pheromone is present in low (30/1.0HC) or high (30/5.0HC) concentrations. We can hypothesise that the pheromone generates a time-dependent inhibition on the phosphatase catalytic activity. Therefore, having a higher amount of enzyme present at the beginning of the reaction, it leads to faster dephosphorylation. On the other hand, when only 50 U of enzyme are added to the peptide solution the dephosphorylation proceeds in a slower fashion, *i.e.* the time required to obtain high conversion is increased, and the pheromone molecules have more time to interact with the phosphatase catalytic pocket. Crystallography or molecular modelling would be required to elucidate the eventual interactions that are developed between cis-jasmone and the catalytic site of phosphatase.

Sample name	Peptide concentration (mM)	Enzyme added (µl)	Pheromone added (µm)	Gelation time (hours)*
20/5.0HC	20	20	28.6	2
30/1.0HC	30	20	5.72	2
30/5.0HC	30	20	28.6	2

***** The gelation time value is referred to the sample state after the lid is removed and it is left in contact with air.

Table 4.3 Summary of characteristics of sample prepared.

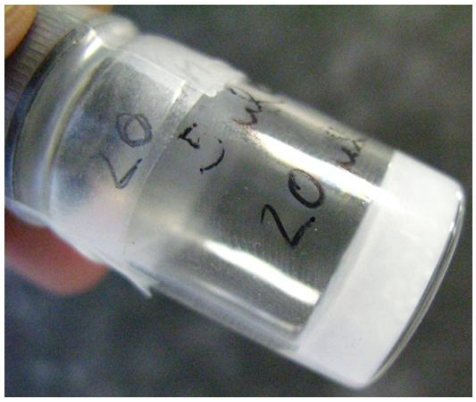

Figure 4.13 Optical image of 20/5.0HC after 24 hours from enzyme addition.

The hypothesis that the gel state has a relevant influence over the release of pheromone is confirmed in this new batch of samples (Fig. 4.14). All the samples formed self sustained gels by the time that the time course study started. The time course study for 20/5.0HC stopped earlier than the 30 mM samples due to the lower amount of peptide contained in the sample.

Nevertheless all the samples have a smooth and reproducible release profile. In particular, 30/5.0HC and 20/5.0HC are closely matched, indicating that the peptide concentration does not influence the release of cis-jasmone. This agrees with the observation that the water evaporation rate is independent on gelator concentration and it suggests that the pheromone molecules that diffuse into the air are contained in the aqueous phase of the hydrogel. We can assume that a portion of the pheromone is always contained into the fibres and it depends on the total concentration added to the sample, e.g. 30/1.0HC has a remaining pheromone concentration of about 50% (~0.45 mg), while for 30/5.0HC it is 35% (~1.6 mg) when the only difference between the two samples is the cis-jasmone added.

Finally, comparing the remaining pheromone after 24 days of 30/1.0HC (47%), 30 CONTROL (78%) and 30/1.0 (57%) (both described in Paragraph 4.2.2), is sensibly lower for the first, showing that both the conversion and the gelation affect the release of cis-jasmone.

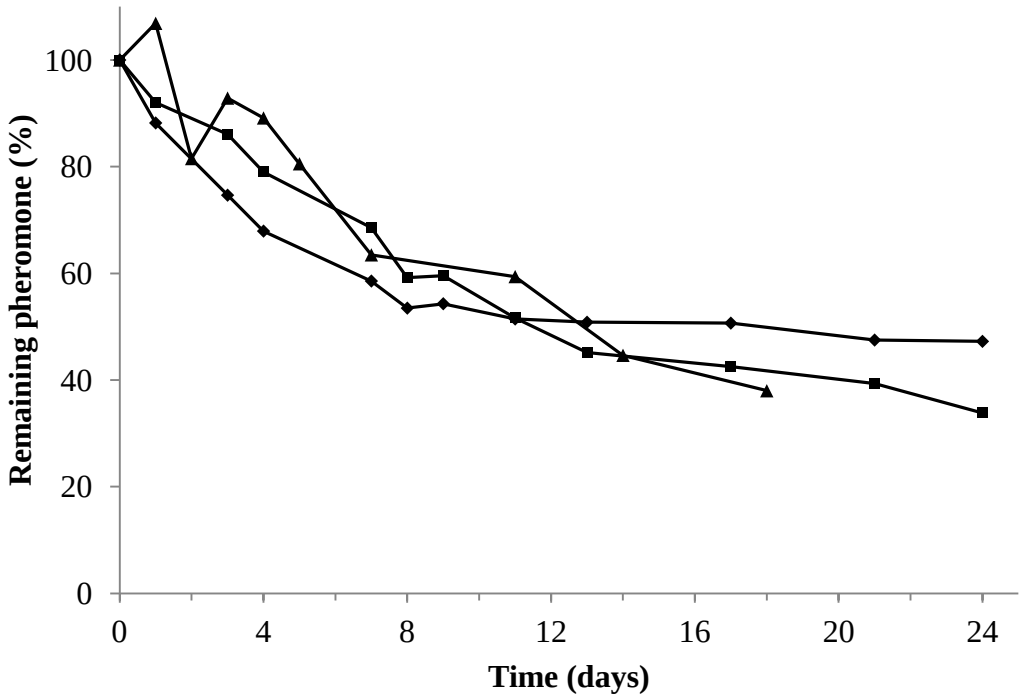

Figure 4.14 HPLC data plotted against time. ▲= 20/5.0HC; ♦ = 30/1.0HC; ■ = 30/5.0HC.

4.2.4 Air entrainment studies

To assess reliability of HPLC time course study and confirm the obtained results, we performed air entrainment studies (Fig. 4.15). This technique consists in trapping a sample in a closed environment. An air flow is forced through the chamber where the sample is contained and has to pass through an outlet containing a silica filter. The filter traps all the organic substances and is replaced at established time points. After the filter is removed, it is washed with ether and the resulting solution run on gas chromatography (GC) (Fig. 4.16). Using this technique we are able to determine with precision the amount of pheromone released with time. The air flow was set to 400 cubic centimetres per minute, with the chamber having a total volume of ~2000 cc^3. The filter was

changed every two/three days. Finally, to avoid contaminations, a moisture trap was placed before the inlet of the chamber containing the sample. At given time points the filter (Fig. 4.15c) was washed with ether and analysed to calculate the amount of pheromone released.

Two samples were prepared and analysed on different systems: a 30 mM Fmoc-Phe-*p*Tyr with 4.7 mg of cis-jasmone and 20 µl of phosphatase and a control with 4.7 mg of cis-jamone.

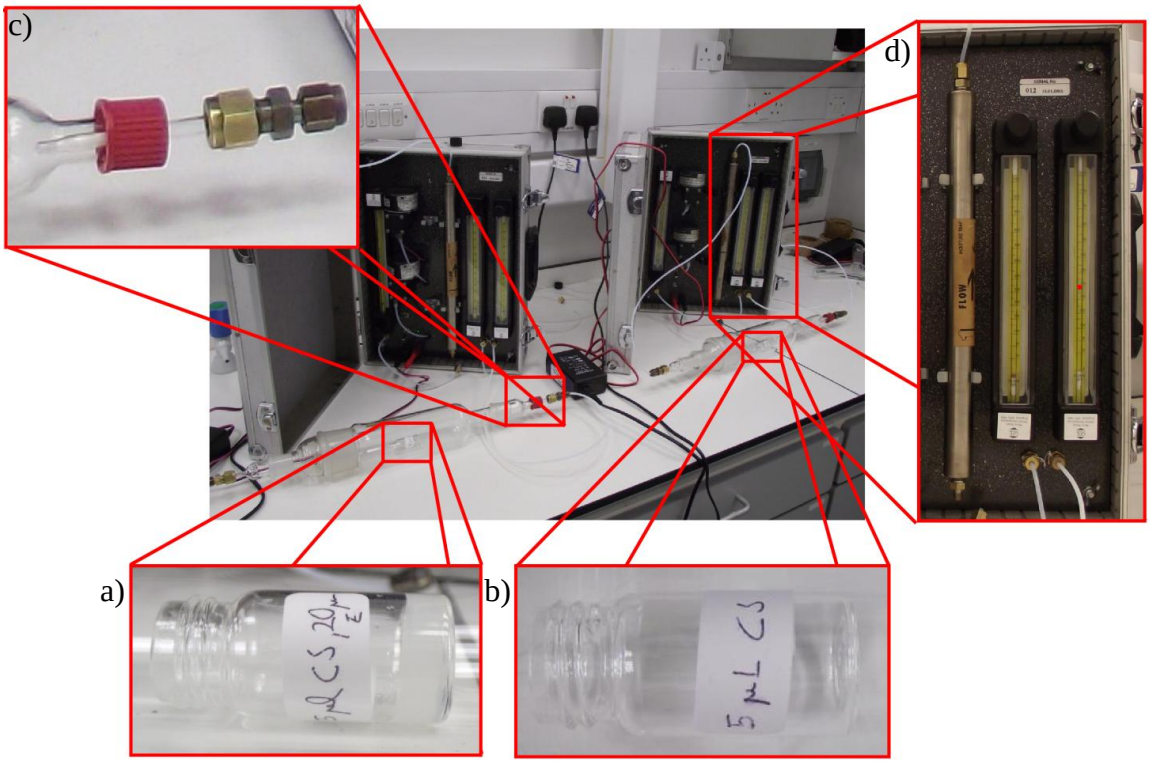

Figure 4.15 Air entrainment system used to monitor the release of cis-jasmone at Rothamsted Research. a) 30 mM Fmoc-Phe-Tyr hydrogel. b) Cis-jasmone control. c) Air outlet with filter. d) Air flow manometers and moisture trap.

Figure 4.16 GC system used to analyze the trapped cis-jasmone at Rothamsted Research.

According to the GC data, the gel releases the pheromone in a more constant fashion compared to the control (Fig. 4.17). The maximum release is reached after 4 days for the control while 2 more days are required for Fmo-Phe-Tyr in order to achieve the maximum release peak. Moreover, the release from the gel seems to be constant up to 15 days while the control has a constant and significant decrease of cis-jasmone release all through the duration of the experiment. The residual presence of pheromone in the gel is probably due to the collapse of the sample as it dries out, *i.e.* a small amount of cis-jasmone is trapped inside the gel fibres, as suggested from the HPLC data.

In theory, the area under the curve used to calculate the amount of cis-jasmone released shown in Figure 4.17 should be the same in both cases, *i.e.* the same amount of pheromone was added to the samples. The difference could be due to much higher pheromone volatility and consequent loss of cis-jasmone during sample preparation/handling.

The results obtained with the air entrainment experiment can only be partially compared to the results obtained with the HPLC time course study, as they have been performed using two different controls, only pheromone and a solution containing phosphorylated peptide and pheromone, respectively. To confirm the results obtained a further experiment performed with the same control would be required.

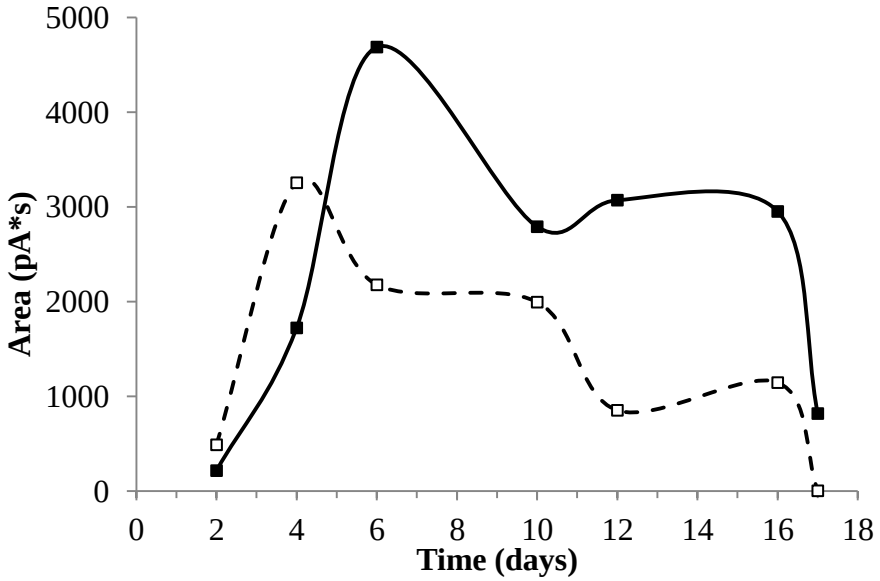

Figure 4.17 Cis-jasmone release from Fmoc-Phe-Tyr gel (■) and from control (□) monitored by GC.

4.3 Conclusion

This study aimed to prove the versatility of peptide based hydrogels for controlled release applications. Starting from an enzyme triggered hydrogel, we report of an innovative system that has the potential to become a vehicle for controlled release of volatile substances, such as pheromones. The release profile of the gel compared to the peptidic solution shows a significant increased release profile due to the conformational change after dephosphorylation, *i.e.* transition from micelle to fibres. The preliminary results obtained by the time course study show the cis-jasmone is released in a more controlled fashion compared to the pheromone in solution are promising. Nevertheless more studies are needed to confirm whether extended release rates can be achieved. The main issue is related to the collapse of the gel when the water evaporates but it could be overcome by monitoring larger systems or controlling the evaporation rate.

In conclusion, this exploratory chapter provides with good starting basis to realise a peptide based system for controlled release using effective monitoring protocols through HPLC and air entrainment studies. Moreover, this approach has tremendous potential for improvement as the self-assembly peptide system are numerous and can provide a wide range of characteristics and properties that can be exploited to tune the release profiles of volatile substances.

4.4 Materials and methods

Materials Alkaline phosphatase from calf intestine mucosa (New England BioLabs, 10.000 U ml^{-1}, one unit is defined as the amount of enzyme that hydrolyzes 1 μmol of p-nitrophenylphosphate to p-nitrophenol in a total reaction volume of 1 ml in 1 ml at 37°C), Fmoc-Phe-*p*Tyr **(**CS Bio Co.) and all the solvents (Aldrich) were used as received. Cis-jasmone and isovitexin were kindly provided by Dr. A.M. Hooper and used as received.

4.4.1 Gel formation

According to the desired final peptide concentration in the gel, precise amounts of Fmoc-Phe-*p*Tyr were weighed directly inside glass vials (7 ml volume). Then, 1/2 ml of 0.6 M phosphate buffer (pH 8) were added and the vial was shaken until a clear solution was obtained. Finally, 5/20 μl of alkaline phoshpatase were taken directly from the supplier's container and added to the solution. The vial was then capped, sealed and left to incubate at room temperature. The gelation was confirmed by inversion of the vial assessing that the hydrogel was self-sustained.

4.4.2 HPLC-monitored time course

A Dionex P680 HPLC system equipped with a Macherey-Nagel C18 column of 250 mm length, 4.6 mm internal diameter and 5mm particle size was used to analyze the mixtures of peptide derivatives. The gradient used was a linear exchange between 40% acetonitrile in water at 4 min to 80% acetonitrile at 40 min using a flow rate of 1 ml/min and detection wavelength of 225 nm. Sample preparation involved mixing 10-30 μl of sample with acetonitrile/water (1 ml, 50:50 v/v mixture) containing 0.1% trifluoroacetic acid.

4.4.3 Gas cromatography

GC was performed using a Hewlett-Packard HP6890 gas chromatograph fitted with an HP-1 capillary column (50 mm x 0.25 mm id x 25 μm film thickness) with a cool on-

column injector and flame ionisation detection operated from 30°C to 150°C at 5°C/min and at 10°C/min to 250°C and held for a further 30 min.

5. Conclusion

This thesis describes how simple enzyme substrates can be used to create new systems for controlled release that have the potential to find applications both in the biomedical and agricultural field.

The literature review underlines the huge effort that is being put by research groups all over the world to develop enzyme responsive materials. The aim is to develop a system that could find applications in the biomedical field, e.g. as drug delivery system. Three main systems have been found as principal research topics: hydrogels, micelles (or nanostructures) and nanocontainers. Each category has been shown to have unique advantages but to present many issues that need to be solved before this exciting research field can translate into applications. Among the issues that are still to be solved there are often inefficient loading capacity, lack of *in vitro/vivo* study and sensitivity to enzyme concentrations present in our bodies.

Among the described systems, enzyme responsive self assembly materials have good potential, e.g. their size is tuneable and can to be excreted without need of degradation. Their hydrophobic core could be exploited to host and trap hydrophobic molecules and, as for all the enzyme responsive systems, releasing them where needed. In this thesis we decided to address two issues that arise specifically with the development of enzyme responsive self assembly systems: the need to use a biocompatible material and to understand the dynamics of self-assembly.

To this end, we decided to study the self assembly dynamics of a polymer, whose family is been reported to be biocompatible, poly(2-isopropyl-2-oxazoline). This thermal responsive family of polymers is considered as “new” as it started to be studied in the last decade. In particular, few studies were published on isopropyl functionalized monomers even if they offer an interesting hydrophobic/hydrophilic balance.

Firstly, we developed a new, high yielding functionalization route exploiting "click chemistry" that enabled us to attach to polymer chains different Fmoc-amino acid moieties using a single step procedure. This strategy - with minor modifications - has been used like a platform to create a library of several amino acid functionalized polymers.

In a first proof of concept study, we functionalised the polymers with Fmoc-*p*Tyr moieties and monitored their self assembly behaviour and thermal properties with a number of techniques before and after enzymatic dephosphorylation. As a result, we reported the first example of phosphatase/temperature responsive polymer, which undergoes self-assembly after enzymatic catalysis, keeping intact its thermal responsive behaviour. Moreover, this part of the study gave first indications on how small alterations, *i.e.* the presence of an anionic groups, have such a significant impact on the self-assembly properties of the polymers.

Exploiting the results obtained in the first part of the study, in the second experimental chapter we increased the level of complexity adding other amino acids, pTyr/Tyr, Lys and Phe, all having different properties, in order to gain further insight on how electrostatic/ionic and hydrophobic/π-π interactions among different amino acids could direct and influence the self assembly process. Using a systematic approach, we proceeded to study both the single and mixed polymer populations. Our findings indicate that the interactions developed within Fmoc-amino acids can be exploited to tailor the aggregates formed by a mixture of ionic and hydrophobic interactions. Moreover, by mixing different polymer populations, we created a system able to respond to enzyme catalysis with dramatic conformational changes making this system more suitable for application in the drug delivery field.

The final explorative chapter provides an example on how enzyme-responsive materials have the potential to find useful applications also in the agricultural pest control field. Through careful design and choice of amino acids, we conducted a preliminary study on the controlled release of cis-jasmone by a peptidic derivative self-assembled hydrogel.

Fmoc-Phe-*p*Tyr/Tyr, self assembles into micelles trapping the pheromones before catalysis and forms stable hydrogel after dephosphorylation. These particular characteristics were exploited both to decrease the instability of the pure pheromone, *i.e.* when trapped in the hydrophobic cores of micelles, and to create a controlled release systems with improved release profiles compared to the water formulation, *i.e.* when gelation occurs. Moreover, we developed an effective protocol to monitor in real time the diffusion of cis-jasmone in the environment by HPLC that, together with the established procedures used at Rothamsted Research Centre, could constitute a reliable method for further studies on pheromone-containing hydrogels for controlled release. Many drawbacks will have to be improved in order to consider this first trial for commercial applications. Nevertheless, the system offers several advantages and has a wide potential of improvement.

6. Future work

Enzyme-responsive materials are a new and exciting research field with great potential towards a number of applications, as shown in this thesis. We are confident that enzyme responsive materials will play a key role in the next few decades for the development of new systems in the biological and biomedical fields.

As with most of studies, there are many questions left out to be answered. Although we introduced new polymer conjugates that increased our understanding on self-assembly dynamics, a lot of work still needs to be done in order to fully understand these complicated processes. ThankS to the new conjugation strategies introduced in this thesis, this objective could be easier to undertake. As a first step, it would be interesting to investigate how other amino acids with peculiar properties, e.g. histidine or proline, behave when attached to polymer chains and how their self assembly behaviour/interactions, thermal responsive profiles as single or mixed populations are affected. This study would allow further understanding on how to influence and direct amino acid interactions to tailor self-assembly materials with precise characteristics.

To make such a system suitable for biological applications, a main target would be to substitute the fluorenyl moiety attached to the amino acid to make the whole system more biocompatible. The fluorenyl group played a key role in helping understanding the self assembly dynamics thank to its fluorescence properties but also increasing the development of hydrophobic/π-π interactions that facilitate self-assembly. Nevertheless, it should be replaced by biocompatible self assembly segment, e.g. a fully peptidic sequence. To this end, molecular modelling would be a perfect tool to predict good peptides which could easily develop interactions. Being able to design self assembly bioconjugated polymers would allow to expand the study, taking into account different substrates/enzymes.

The main advantage of this system is that it has the potential to be tailored to target any kind of enzyme, *i.e.* designing the self assembly moiety to be also the enzyme substrate, and theoretically any kind disease caused by enzymatic disregulation or where, as a result of the pathological state, a particular kind of enzyme is overexpressed. In order to develop a system for controlled drug release in the human body, a number of toxicity tests would be needed. *In vivo* and *in vitro* tests would be required to evaluate the cytotoxicity of the modified polymers. Although our study showed that the colloidal aggregates are still accessible to enzymes, sensitivity of these systems to the concentration of enzymes expressed in physiological and pathological conditions within the human body should be carefully considered, e.g. sensitivity to cell secreted enzymes. Last but not least, loading capacity of the aggregates needs to be studied as well as release, degradation and excretion profiles.

The peptidic based hydrogels for the controlled release of pheromone gave interesting results and, although preliminary, very promising. To assess the real potential of the system, analysis method, sample preparation and composition should be tuned to confirm and eventually improve/tailor the release of the pheromone. Again, molecular modelling would give useful indications on the interactions developed between the peptides and pheromone molecules and would suggest how to improve the system.

As mentioned before amino acids provide a powerful toolbox to tailor such as release system to operate in the desired way. Careful design of the amino acid sequence would give us the opportunity to tune the development of pheromone/peptide interactions and to calibrate the release profile. Moreover, to further develop the release system, more peptide-based hydrogels should be investigated in order to study the influence of the characteristics of the peptidic fibres on the pheromone release.

During our study, we always compared the release profiles of our hydrogel systems against aqueous emulsions of pheromones: it would be interesting to compare them with commercially available products for the controlled release of pheromone to evaluate the effectiveness of our system. Further tests on pheromone stability under long storage

conditions within peptidic solutions and field trials, to assess how the plants vital cycle reacts to the concentration of pheromone release by the hydrogels, could constitute the proof that the controlled release of pheromones by peptide-based hydrogel works and will probably be undertaken at Rothamsted Research Centre.

7. References

[1] P. Ehlrich, *Lancet*, **1907**, *2*, 351.

[2] a) K.R. Schultz, W. P. Bowman, A. Aledo, W.B. Slayton, H. Sather, M. Devidas, C. Wang, S.M. Davies, P.S. Gaynon, M. Trigg, R. Rutledge, L. Burden, D. Jorstad, A. Carroll, N.A. Heerema, N. Winick, M.J. Borowitz, S.P. Hunger, W.L. Carroll, B. Camitta, *J. Clin. Oncol.*, **2009**, *27*, 5175. b) H. Kantarjian, N.P. Shah, A. Hochhaus, J. Cortes, S. Shah, M. Ayala, B. Moiraghi, Z. Shen, J. Mayer, R. Pasquini, H. Nakamae, F. Huguet, C. Boqué, C. Chuah, E. Bleickardt, B. Bradley-Garelik, C. Zhu, T. Szatrowski, D. Shapiro, M. Baccarani, *N. Eng. J. Med.*, **2010**, *362*, 2260.

[3] R.C. Gallo, L. Montagnier, *Nature*, **1987**, *326*, 435.

[4] D.D. Richman, D.M. Margolis, M. Delaney, W.C. Greene, D. Hazuda, R.J. Pomerantz, *Science*, **2009**, *323*, 1304.

[5] D.D. Richman, *Nature*, **2001**, *410*, 995.

[6] H.A. Chapman, P. Bertozzi, J.J. Reilly, *CHEST*, **1988**, 93, 1256.

[7] D.S. Smith, P.A. Humphrey, W.J. Catalona, *Cancer*, **1997**, 80, 1853.

[8] S. Singhal, M.C. Taylor, R.T. Baker, *BMC Biochem.*, **2008**, 9:S3.

[9] P.J. Rosenthal, *J. Exp. Biol.*, **2003**, 206, 3735.

[10] J.M. Matés, C. Pérez-Gómez, I. Núñez De Castro, *Clinical Biochem.*, **1999**, 32, 595.

[11] B.J. Clodfelder-Miller, A.A. Zmijewska, G.V.W. Johnson, R.S. Jope, *Diabetes*, **2006**, 55, 3320.

[12] M. Freeman, L. Kuiken, J.B. Ragland, S.M. Sabesin, *Lipids*, **1976**, 12, 433.

[13] F. Liu, Z. Liang, C.X. Gong, *Panminerva Medica*, **2006**, 48, 97.

[14] J. Rautio, H. Kumpulainen, T. Heimbach, R. Oliyai, D. Oh, T. Järvinen, J. Savolainen, *Nat. Rev. Drug Discov.*, **2008**, *7*, 255.

[15] P.A. Vasey, S.B. Kaye, R. Morrison, C. Twelves, P. Wilson, R. Duncan, A.H. Thomson, L.S. Murray, T.E. Hilditch, T. Murray, S. Burtles, D. Fraier, E. Friegerio, J. Cassidy, *Clin. Cancer Res.*, **1999**, *5*, 83.

[16] Y. Singh, M. Palombo, P.J. Sinko, *Curr. Med. Chem.*, **2008**, *15*, 1802.

[17] K. Knop, R. Hoogenboom, D. Fischer, U.S. Schubert, *Angew. Chem. Int. Ed.*, **2010**, *49*, 6288.

[18] M.P. Napier, S.K. Sharma, C.J. Springer, K.D. Bagshawe, A.J. Green, J. Martin, S.M. Stribbling, N. Cushen, D. O'Malley, R.H.J. Begent, *Clin. Canc. Res.*, **2000**, *6*, 765.

[19] V.T. DeVita, T.S. Lawrence, S.A. Rosenberg, eds. *Cancer: Principles and Practice of Oncology*, 8th ed. Philadelphia, WoltERM Kluwer/Lippincott Williams & Wilkins; **2008**.

[20] a) Z. Ram, K.W. Culver, S. Walbridge, R.M. Blaese, E.H. Oldfield, *Cancer Res.*, **1993**,*53*, 83. b) S. Schepelmann, C.J. Springer, *Curr. Gene Ther.*, **2006**, *6*, 647.

[21] a) R. Satchi, T.A. Connors, R. Duncan, *Br. J. Cancer*, **2001**, *85*, 1070. b) Y. Singh, M. Palombo, P.J. Sinko, *Curr. Med. Chem.*, **2008**, *15*, 1802.

[22] S.M. Moghimi, A.C. Hunter, C.J. Murray, *FASEB J.*, **1995**, *19*, 311.

[23] J.A. Champion, Y.K. Katare, S. Mitragotri, *J. Control. Rel. Rev.*, **2007**, *121*, 3.

[24] H. Maeda, J. Wu, T. Sawa, Y. Matsumura, K. Kori, *J. Control. Rel. Rev.*, **2000**, *65*, 271.

[25] K. Greish, *J. Drug Target.*, **2007**, *15*, 271.

[26] M. Goldberg, R. Langer, X. Jia, *J. Biomater. Sci. Polymer Ed.*, **2007**, *18*, 241.

[27] a) T. Graham, *J. Chem. Soc.*, **1862**, *15*, 216. b) T. Graham, *P. Roy. Soc. Lond.*, **1864**, *13*, 335.

[28] M. Hamidi, A. Azadi, P. Rafiei, *Adv. Drug. Deliv. Rev.*, **2008**, *60*, 1638.

[29] R.V. Ulijn, N. Bibi, V. Jayawarna, P.D. Thornton, S.J. Todd, R.J. Mart, A.M. Smith, J.E. Gough, *Materialstoday*, **2007**, *10*, 40.

[30] F. Carpi, E. Smela, eds. *Biomedical applications of electroactive polymer actuators*, John Wiley & Sons Ltd., **2009**.

[31] T. Traitel, Y. Cohen, J. Kost, *Biomaterials*, **2001**, *21*, 1679.

[32] J. Kost, T.A. Horbett, B.D. Ratner, M. Singh, *J. Biomed. Mater. Res.*, **1985**, *19*, 1117.

[33] W. Zhao, H. Zhang, Q. He, Y. Li, J. Gu, L. Li, H. Li, J. Shi, *Chem. Commun.*, **2011**, *47*, 9459.

[34] W.E. Hennink, C.F. van Nostrum, *Adv. Drug. Deliv. Rev.*, **2002**, *54*, 13.

[35] J.J. Sperinde, L.G. Griffith, M*acromolecules*, **2000**, *33*, 5476.

[36] K.L. Shantha, P. Ravichandran, K.P. Rao, *Biomaterials*, **1995**, *16*, 1313.

[37] I.-S. Kim, I.-J. Oh, *Arch. Pharm. Res.*, **2005**, *28*, 983.

[38] S.G. Lévesque, M.S. Soichet, *Bioconjugate Chem.*, **2007**, *18*, 874.

[39] A.A. Aimetti, A.J. Machen, K.S. Anseth, *Biomaterials*, **2009,** *30*, 6048.

[40] P.D. Thornton, R. Mart, R.V. Ulijn, *Adv. Mater.*, **2007**, *19*, 1252.

[41] P.D. Thornton, R.J. Mart, S.J. Webb, R.V. Ulijn, *Soft Matter*, **2008**, *4*, 821.

[42] T.O. McDonald, H. Qu, B.R. Saunders, R.V. Ulijn, *Soft Matter*, **2009**, *5*, 1728.

[43] J.R. Tauro, B.-S. Lee, S.S. Lateef, R.A. Gemeinhart, *Peptides*, **2008**, *29*, 1965.

[44] G.M. Whitesides, B. Grzybowsky, *Science*, **2002**, *295*, 2418.

[45] P.K. Vemula, G.A. Cruikshank, J.M. Karp, G. John, *Biomaterials*, **2009**, *30*, 383.

[46] P.K. Vemula, J. Li, G. John, *J. Am. Chem. Soc.*, **2006**, *128*, 8932.

[47] K.J.C. Van Bommel, M.C.A. Stuart, B.L. Feringa, J. Van Esch, *Org. Biomol. Chem.*, **2005**, *3*, 2917.

[48] Y.G. Gao, Y. Kuang, Z.F. Guo, Z. Guo, I.J. Krauss, B. Xu, *J. Am. Chem. Soc.*, **2009**, *131*, 13576.

[49] A. Altunbas, S.J. Lee, S.A. Rajasekaran, J.P. Schneider, D.J. Pochan, *Biomaterials*, **2011**, *32*, 5906.

[50] L. Liang, X.-D. Xu, C.-S. Chen, J.-H. Fang, F.-G. Jiang, X.-Z. Zhang, R.-X. Zhuo, J. *Biomed. Mater. Res. B Appl. Biomater.*, **2010**, *93B*, 324.

[51] Z. Yang, H. Gu, D. Fu, P. Gao, J.K. Lam, B. Xu, *Adv. Mater.*, **2004**, *16*, 1440.

[52] J.W. Sadownik, J. Leckie, R.V. Ulijn, *Chem. Commun.*, **2011**, *47*, 728.

[53] Z. Yang, M. Ma, B. Xu, *Soft Matter*, **2009**, *5*, 2546.

[54] Z. Yang, G. Liang, L. Wang, B. Xu, *J. Am. Chem. Soc.*, **2006**, *128*, 3038.

[55] M.J. Webber, C.J. Newcomb, R. Bitton, S.I. Stupp, *Soft Matter*, **2011**, *7*, 9665.

[56] A.R. Hirst, S. Roy, M. Arora, A.K. Das, N. Hodson, P. Murray, S. Marshall, N. Javid, J. Sefcik, J. Boekhoven, J.H. van Esch, S. Santabarbara, N.T. Hunt, R.V. Ulijn, *Nat. Chem.*, **2010**, *2*, 1089.

[57] E. Blanco, E.A. Bey, C. Khemtong, S.-E. Yang, J. Setti-Guthi, H. Chen, C.W. Kessinger, K.A. Carnevale, W.G. Bornmann, D.A. Boothman, J. Gao, *Cancer Res.*, **2010**, *70*, 3896.

[58] L.S. del Rosario, B. Demirdirek, A. Harmon, D. Orban, K.E. Uhrich, *Macromol. Biosci.*, **2010**, *10*, 415.

[59] C. Wu, R. Ma, H. He, L. Zhao, G. Gao, Y. An, L. Shi, *Macromol. Biosci.*, **2009**, *9*, 1185.

[60] V. Castelletto, J.E. McKendrick, I.W. Hamley, *Langmuir*, **2010**, *26*, 11624.

[61] G.J.M. Habraken, M. Peeters, P.D. Thornton, C.E. Koning, A. Heise, *Biomacromolecules*, **2011**, *12*, 3761.

[62] W. Wang, J. Ding, C. Xiao, Z. Tang, D. Li, J. Chen, X. Zhuang, X. Chen, *Biomacromolecules*, **2011**, *12*, 2466.

[63] M.A. Azagarsamy, P. Sokkalingam, S. Thayumanavan, *J. Am. Chem. Soc.*, **2009**, *131*, 14185.

[64] J.A. Amir, S. Zhong, D.J. Pochan, C.J. Hawker, *J. Am. Chem. Soc.*, **2009**, *131*, 13949.

[65] H. Kühnle, H.G. Börner, *Angew. Chem. Int. Ed.*, **2009**, *48*, 6431.

[66] P.-F. Caponi, X.-P. Qiu, F. Vilela, F.M. Winnik, R.V. Ulijn, *Polym. Chem.*, **2011**, *2*, 306.

[67] Z. Yang, B. Xu, *Chem Commun.*, **2004**, *21*, 2424.

[68] C. Wang, Q. Chen, Z. Wang, X. Zhang, *Angew. Chem. Int. Ed.*, **2010**, *49*, 8612.

[69] Y.-W. Yang, *Med. Chem. Comm.*, **2011**, *2*, 1033.

[70] a) D. Schmaljohann, *Adv. Drug Delivery Rev.*, **2006**, *58*, 1655. b) M. Vallet-Regi, F. Balas, D. Arcos, *Angew. Chem. Int. Ed.*, **2007**, *46*, 7548.

[71] N.K. Mal, M. Fujiwara, Y. Tanaka, *Nature*, **2003**, *421*, 350.

[72] a) A. Bernardos, E. Aznar, C. Coll, R. Martínez-Máñez, J.M. Barat, M.D. Marcos, F. Sancenón, J. Soto, *J. Controlled Release*, **2008**, *131*, 181. b) S. Angelos, Y.W. Yang, N.M. Khashab, J.F. Stoddart, J.I. Zink, *J. Am. Chem. Soc.*, **2009**, *131*, 11344.

[73] Q. Fu, G.V.R. Rao, L.K. Ista, Y. Wu, B.P. Andrezejewski, L.A. Sklar, T.L. Ward, G.P. López, *Adv. Mater.*, **2003**, *15*, 1262.

[74] E. Climent, A. Bernardos, R. Martínez-Máñez, A. Maquieira, M.D. Marcos, N. Pastor-Navarro, R. Puchades, F. Sancenón, J. Soto, P. Amorós, *J. Am. Chem. Soc.*, **2009**, *131*, 14075.

[75] a) K.O. Yu, C.M. Grabinski, A.M. Schrand, R.C. Murdock, W. Wang, B. Gu, J.J. Schlager, S.M. Hussain, *J. Nanopart. Res.*, **2009**, *11*, 15. b) D.B. Warheit, T.R. Webb, V.L. Colvin, K.L. Reed, C.M. Sayes, *Toxicol. Sci.*, **2007**, *95*, 270.

[76] a) G. Xie, J. Sun, G. Zhong, L. Shi, D. Zhang, *Arch. Toxicol.*, **2010**, *84*, 183. b) W. Lin, Y. Huang, X.-D. Zhou, Y. Ma, *Tox. Appl. Pharmacol.*, **2006**, *217*, 252.

[77] K. Patel, S. Angelos, W.R. Dichtel, A. Coskun, Y.-W. Yang, J.I. Zink, J.F. Stoddart, *J. Am. Chem. Soc.*, **2008**, *130*, 2382.

[78] C. Park, H. Kim, S. Kim, C. Kim, *J. Am. Chem. Soc.*, **2009**, *131*, 16614.

[79] A. Bernardos, E. Aznar, M.D. Marcos, R. Martínez-Máñez, F. Sancenón, J. Soto, J.M. Barat, P. Amorós, *Angew. Chem. Int. Ed.*, **2009**, *48*, 5884.

[80] A. Bernardos, L. Mondragón, E. Aznar, M.D. Marcos, R. Martínez-Máñez, F. Sancenón, J. Soto, J.M. Barat, E. Pérez-Payá, C. Guillem, P. Amorós, *ACS Nano*, **2010**, *4*, 6353.

[81] P.D. Thornton, A. Heise, *J. Am. Chem. Soc.*, **2010**, *132*, 2024.

[82] C. Coll, L. Mondragón, R. Martínez-Máñez, F. Sancenón, M.D. Marcos, J. Soto, P. Amorós, E. Pérez-Payá, *Angew. Chem. Int. Ed.*, **2011**, *50*, 2138.

[83] A. Schlossbauer, J. Ketch, T. Bein, *Angew. Chem. Int. Ed.*, **2009**, *48*, 3092.

[84] Y. Zhu, W. Meng, H. Gao, N. Hanagata, *J. Phys. Chem.*, **2011**, *115*, 13630.

[85] Y. Zhu, W. Meng, N. Hanagata, *Dalton Trans.*, **2011**, *40*, 10203.

[86] J. S. Mohammed, W. L. Murphy, *Adv. Mater.*, **2009**, *21*, 2361.

[87] a) R.V. Ulijn, J. *Mater. Chem.*, **2006**, *16*, 2217–2225. b) H. G. Börner, H. Kühnle, J. Hentschel, *J. Polym. Sci., Part A: Polym. Chem.*, **2010**, *48*, 1.

[88] A. S. Hoffman, P. Stayton, *Prog. Polym. Sci.*, **2007**, *32*, 922.

[89] G. A. Silva, C. Czeisler, K. L. Niece, E. Beniash, D. A. Harrington,J. A. Kessler, S. L. Stupp, *Science*, **2004**, *303*, 1352.

[90] a) C. Tang, A. M. Smith, R. F. Collins, R. V. Ulijn, A. Saiani, *Langmuir*, **2009**, *25*, 9447. b) L. Chen, S. Revel, K. Morris, L. C. Serpell, D. J. Adams, *Langmuir*, **2010**, *26*, 13466.

[91] a) Z. M. Yang, H. W. Gu, D. G. Fu, P. Gao, J. K. Lam, B. Xu, *Adv. Mater.*, **2004**, *16*, 1440. b) K. J. C. Van Bommel, M. C. A. Stuart, B. L. Feringa, J. Van Esch, *Org. Biomol. Chem.*, **2005**, *3*, 2917.

[92] a) D. Roy, J. N. Cambre, B. S. Sumerlin, *Prog. Polym. Sci.*, **2010**, *35*, 278. b) N. Suchao-In, S. Chirachanchai, S. Perrier, *Polymer*, **2009**, *50*, 4151.

[93] S. Dai, P. Ravi, K. C. Tam, *Soft Matter*, **2009**, *5*, 2513.

[94] E. E. Golub, K. Boesze-Battaglia, *Curr. Opin. Orthop.*, **2007**, *18*, 444.

[95] J. N. Andersen, P. G. Jansen, S. M. Echwald, O. H. Mortensen, T. Fukada, R. Del Vecchio, N. K. Tonks, N. P. H. Møller, *FASEB J.*, **2004**, *18*, 8.

[96] a) Z. Yang, B. Xu, *Chem. Commun.*, **2004**, 2424. b) Y. Gao, Y. Kuang, Z. F. Guo, Z. H. Guo, I. J. Krauss, B. Xu, *J. Am. Chem. Soc.*, **2009**, *131*, 13576. c) W. Wang, Y. Chau, *Soft Matter*, **2009**, *5*, 4893.

[97] a) D. Schmaljohann, *Adv. Drug Delivery Rev.*, **2006**, *58*, 1655. b) J. F. Mano, *Adv. Eng. Mater.*, **2008**, *10*, 515.

[98] N.S. Ieong, M. Hasan, D.J. Phillips, Y. Saaka, R.K. O'Reilly, M.I. Gibson, Polym. Chem., 2012, 3, 794.

[99] P. Goddard, L. E. Hutchinson, J. Brown, L. J. Brookman, *J. Controlled Release*, **1989**, *10*, 5.

[100] a) M. C. Woodle, C. M. Engbers, S. Zalipsky, *Bioconjugate Chem.*, **1994**, *5*, 493. b) S. Zalipsky, C. B. Hansen, J. M. Oaks, T. M. Allen, *J. Pharm. Sci.*, **1996**, *85*, 133.

[101] R. Hoogenboom, *Angew. Chem., Int. Ed.*, **2009**, *48*, 7978.

[102] S. Huber, N. Hutter, R. Jordan, *Colloid Polym. Sci.*, **2008**, *286*, 1653.

[103] R. Hoogenboom, F. Wiesbrock, H. Huang, M. A. A. Leenen, H. M. L. Thijs, S. F. G. M. van Nispen, M. van der Loop, C. A. Fustin, A. M. Jonas, J. F. Gohy, U. S. Schubert, *Macromolecules*, **2006**, *39*, 4719.

[104] R. Luxenhofer, R. Jordan, *Macromolecules*, **2006**, *39*, 3509.

[105] R. Hoogenboom, H. M. L. Thijs, M. J. H. C. Jochems, B. M. van Lankvelt, M. W. M. Fijten, U. S. Schubert, *Chem. Commun.*, **2008**, 5758.

[106] J. H. Gao, B. Xu, *Nano Today*, **2009**, *4*, 37.

[107] a) J. M. Zayed, N. Nouvel, U. Rauwald, O.A. Scherman, *Chem. Soc. Rev.*, **2010**, *39*, 2806. b) F. Ludlow, S. Otto, *Chem. Soc. Rev.*, **2008**, *37*, 101. c) B.A. Grzybowski, C.E. Wilmer, J.Kim, K.P. Browne, K.J.M. Bishop, *Soft Matter*, **2009**, *5*, 1110.

[108] a) D.W.P.M. Löwik, E. H. P. Leunissen, M. van den Heuvel, M. B. Hansen, J.C. M. van Hest *Chem. Soc. Rev.*, **2010**, *39*, 3394. b) C. Alexander, K.M. Shakesheff, *Adv. Mater.*, **2006**, *18*, 3321. c) M.A. Cohen Stuart, W.T.S. Huck, J. Genzer, M. Müller, C. Ober, M. Stamm, G.B. Sukhorukov, I. Szleifer, V.V. Tsukruk, M. Urban, F. Winnik, S. Zauscher, I. Luzinov, S. Minko, *Nat. Mater.*, **2010**, *9*, 101.

[109] a) R.V. Ulijn, *J. Mater. Chem.*, 2006, 16, 2217. b) M.E. Hahn, N.C. Gianneschi, *Chem. Commun.*, **2011**, *47*, 11814. c) Y.Gao, F. Zhao, Q. Wang, Y. Zhang, B. Xu *Chem. Soc. Rev.*, **2010**, *39*, 3425.

[110] T.-H. Ku, M.-P. Chen, M.P. Thompson, R.S. Sinkovits, N.H. Olson, T.S. Baker, N.C. Gianneschi, *J. Am. Chem. Soc.*, **2011**, *133*, 8392.

[111] C. Wang, Q. Chen, Z. Wang, X. Zhang, *Angew. Chem. Int. Ed.*, **2010**, *49*, 8612.

[112] M. H. Litt, A. J. Levy, T. G. Bassiri, *BE666828*, **1965**, *US3483141*.

[113] a) F. Wiesbrock, R. Hoogenboom, C. A. Abeln, U. S. Schubert, *Macromol. Rapid Commun.*, **2004**, *25*, 1895. b) F. Wiesbrock, R. Hoogenboom, M.A.M. Leenen, M.A.R. Meier, U. S. Schubert, *Macromolecules*, **2005**, *38*, 5025.

[114] R. Hoogenboom, F. Wiesbrock, H. Huang, M. A. A. Leenen, H. M. L. Thijs, S. F. G. M. van Nispen, M. van der Loop, C. A. Fustin, A. M. Jonas, J. F. Gohy, U. S. Schubert, *Macromolecules*, **2006**, *39*, 4719.

[115] a) K. Kalyanasundaram, J. K. Thomas, *J. Am. Chem. Soc.*, **1977**, *99*, 2039. b) Rengin Konuk, J. Cornelisse, S.P. McGlynn, *J. Phys. Chem.*, **1989**, *93*, 7405-7409. c) A. Chaudhuri, S. Haldar, A. Chattopadhyay, *Biochem. Biophys. Res. Commun.*, **2009**, *390*, 728.

[116] I. Yamazaki, F. M. Winnik, M. A. Winnik, S. Tazuke, *J. Phys. Chem.*, **1987**, 4213.

[117] a) P. Goddard, L. E. Hutchinson, J. Brown, L. J. Brookman, *J. Controlled Release*, **1989**, *10*, 5. b) M. C. Woodle, C. M. Engbers, S. Zalipsky, *Bioconjugate Chem.*, **1994**, *5*, 493. c) S. Zalipsky, C. B. Hansen, J. M. Oaks, T. M. Allen, *J. Pharm. Sci.*, **1996**, *85*, 133.

[118] J.R.Miller, L.J. Gut, F.M. de Lame, L.L. Stelinski, *J. Chem. Ecol.*, **2006**, *32*, 2089.

[119] Z.R. Khan, C.A.O. Midega, T.J. A. Bruce, A.M. Hooper, J.A. Pickett, *J. Exp. Botany*, **2010**, *61*, 4185.

[120] G.V.P. Reddy, A. Guerrero, *Trends Plant Sci.*, **2004**, *9*, 253.

[121] A.M. Smith, R.J. Williams, C. Tang, P. Coppo, R.F. Collins, M.L. Turner, A. Saiani, R.V. Ulijn, *Advanced Materials*, **2008**, *20*, 37.

[122] T. Bruce, J. Pickett, L. Smart, *Pesticide Outlook*, **2003**, 96.

[123] J. H. Loughrin, A. Manukian, R. R.Heath, J. H. Tumlinson, *J.Chem. Ecol.*, **1995**, *21*, 1217.

[124] K. Chamberlain, J. A. Pickett, C. M. Woodcock, *Mol. Plant Pathol.*, **2000**, *1*, 67.

[125] J.A. Pickett, M.A. Birkett, T.J.A. Bruce, K. Chamberlain, R. Gordon-Weeks, M.C. Matthes, J.A. Napier, L.E. Smart, C.M. Woodcock, *Phytochemistry*, **2007**, *68*, 2937.

[126]Y. Du, G.M. Poppy, W. Powell, J.A. Pickett, L.J. Wadhams, C.M. Woodcock, *J. Chem. Ecol.*, **1998**, *24*, 1355.

[127]M.C.B. Moraes, M.A. Birkett, R. Gordon-Weeks, L.E. Smart, J.L. Martin, B.J. Pye, R.H. Bromilow, J.A. Pickett, *Phytochemistry*, **2008**, *69*, 9.

[128] T. Iwashima, *Jpn. Soc. Biol. Sci. Science*, **2003**, *17*, 24.

[129] G. Karabourniotis, K. Papadopoulos, M. Papamarkou, Y. Manetas, *Physiol. Plant.*, **1992**, *86*, 414.

[130] V. Cody, E. Middleton Jr., J.B. Harborne, *Alan R. Liss*, New York, **1988**.

[131] L. Nandakumar, N. S. Rangaswamy, *J. Exper. Botany.*, **1985**, *36*, 1313.